UNIVERSITÀ DEGLI STUDI DI VERONA

FACOLTÀ DI MEDICINA E CHIRURGIA

Dipartimento di Scienze Neurologiche, Neuropsicologiche, Morfologiche e Motorie
Sezione Anatomia e Istologia

Scuola di dottorato di Scienze Ingegneria e Medicina

DOTTORATO DI RICERCA IN
Imaging Multimodale in Biomedicina
Ciclo XXIV

Biological impact of Quantum Dots in rodents

S.S.D. Bio/16

Coordinatore: Prof. Andrea Sbarbati

Tutor: Prof. Paolo Francesco Fabene

Dottoranda: Serena Becchi

LIST OF CONTENT

Biological impact of Quantum Dots in rodents

ABSTRACT

Quantum Dots (QDs) are fluorescent semiconductor nanocrystals that have a narrow and tunable emission wavelengths across the visible and infrared spectrum. This makes them a promising tool for *in vivo*, *in vitro* and *ex vivo* imaging (Smith et al., 2000). However, the assessment of biocompatibility and biosafety of QDs is a critical issue for further applications as diagnostic and imaging tools on humans. The work of this thesis focuses on non modified QTracker® 800 QDs, which are a commercial type of QDs with a heavy metals core of CdSeTe, specifically designed for *in vivo* vascular and tumour imaging, for their emission wavelength in the near infrared spectrum (800nm).

The biodistribution of QTracker QDs is assessed in Balb-c mice (40pM, 10µl/g) during 3 weeks following an i.v. injection. Accumulation is monitored using inductively coupled plasma mass spectroscopy, optical imaging, confocal microscopy and electron microscopy, and revealed a major accumulation of QDs in liver and spleen, specifically in the mononuclear phagocytic system. The accumulation in the brain is observed over 3 weeks, suggesting a long biological half-life, in the scale of weeks or months. It is in particularly observed around blood vessels, in different brain areas. QDs are found in neurons, glia and epithelial cells, both in cytosol and nucleus.

Animal's behaviour is investigated and novel object recognition test shows that QDs can significantly impair recognition memory at 3 weeks after treatment (with no locomotory and coordination alterations observed). Such impairment is possibly due to the alteration of physiological conditions in the anatomical regions that encode for recognition memory, such as enthorinal and perirhinal cortices, dentate gyrus and areas CA1-CA3 of hippocampus.

Therefore, an increased inflammatory response in terms of microglia and astrocytes activation is observed in all these regions. However, it do not have an effect on hippocampal plasticity, which is investigated by measuring long term potentiation (LTP) at 1 and 3 weeks after treatment.

Taken together, the data presented in this thesis suggest that due to long term accumulation, induction of neuroinflammation and behavioural changes, the application of QDs in human should be cautious.

ABSTRACT

I Quantum Dots (QDs) sono nanoparticelle fluorescenti largamente impiegate nell'*imaging in vivo*, *ex vivo* ed *in vitro*, grazie alle loro straordinarie proprietà ottiche. In particolare, i QTracker® 800 (Invitrogen) sono una tipologia commerciale di QDs con emissione nel Near-Infra-Red (800nm), disegnati appositamente per l'esecuzione di studi *in vivo* di diagnosi nell'uomo o *drug delivery* in piccoli animali da laboratorio. Uno dei principali problemi relativi a queste nanoparticelle è la presenza di metalli pesanti, fondamentali per le proprietà ottiche, che, nel caso dei QTracker®, sono CdSeTe.

Gli studi della possibile tossicità dei QDs che si trovano in letteratura sono stati effettuati principalmente *in vitro* e potrebbero non corrispondere in modo soddisfacente alla risposta scatenata *in vivo* dalle nanoparticelle.

Lo scopo di questa tesi è quindi lo studio di biodistribuzione e potenziali effetti dannosi dei QDs in sistemi viventi, con particolare attenzione al sistema nervoso centrale, prima di poter utilizzare tali nanocomposti in campo clinico.

In seguito al trattamento di topi Balb-c con QDs (con iniezione intravenosa di 10µl/g, 40pM) è stato eseguito uno studio di biodistribuzione, tramite visualizzazione *in vivo* con la tecnica di *Optical Imaging*, seguita dalla conferma con microscopia elettronica e microscopia confocale e quantificazione dei metalli pesanti mediante ICP-MS a 24h, 1, 2 e 3 settimane dopo l'iniezione.

Si è constatato che i QDs sono in grado di penetrare attraverso i vasi nei tessuti animali e di accumularsi, in particolare, nel reticolo endoteliale di fegato e milza. Inoltre i QDs sono in grado di attraversare la barriera ematoencefalica e di accumularsi intorno ai vasi sanguigni e nel parenchima in diverse aree cerebrali, soprattutto nella corteccia. L'ICP-MS ha rivelato un accumulo di metalli pesanti nel cervello immediatamente dopo l'iniezione, e significativamente elevato per tutte le 3 settimane dello studio. Nel cervello, ad una settimana dal trattamento, si trovano aggregati di alcune decine di nanoparticelle, distribuiti in neuroni, cellule epiteliali e cellule della glia, sia nel citosol che nel nucleo, talora anche a livello di sinapsi, sulle guaine mieliniche che ricoprono gli assoni neuronali e nei mitocondri.

Abbiamo quindi valutato se la presenza sporadica delle nanoparticelle possa causare anomalie comportamentali, ad esempio anomalie nell'attività locomotoria, nell'attività cogni-

tiva ecc. Dati recenti indicano che tutte le cellule cerebrali dialogano fra loro, e che l'attività dei neuroni è profondamente influenzata dall'intera orchestra cellulare. L'ipotesi di base è che se i nanocomposti, presenti a livello del parenchima, innescano una risposta infiammatoria prolungata, questo può riverberarsi in una modificazione dell'eccitabilità del neurone e conseguentemente in una modificazione del comportamento dell'animale.

La presenza di tali nanoparticelle a livello del sistema nervoso centrale ha indotto un'alterazione della memoria di riconoscimento a 3 settimane dopo il trattamento, valutata con il test del *Novel Object Recognition* (senza alterazioni delle capacità locomotorie).

La presenza di tali nanoparticelle induce una risposta infiammatoria che rimane elevata per le 3 settimane, caratterizzata da un aumento di microglia e astrociti a livello della corteccia entorinale e dell'ippocampo (giro dentato, aree CA1, CA2, CA3), che corrispondono alle aree associate alla codifica dei processi mnesici.

La *Long Term Potentiation*, un modello di plasticità sinaptica d'altra parte non ha evidenziato nessuna alterazione delle funzioni ippocampali ad 1 e 3 settimane dal trattamento.

Abbiamo valutato poi se la presenza nel parenchima cerebrale di NPs possa portare ad alterazioni del ciclo sonno/veglia e dell'attività dell'animale nell'*home cage*.

I dati ottenuti indicano che occorre una valutazione accurata degli effetti dei nanocomposti sulla salute umana, ed occorrono molti studi approfonditi sia *in vitro* che *in vivo* prima del loro utilizzo in biomedicina.

LIST OF ABBREVIATIONS

BBB = blood brain barrier

BCSF = blood cerebrospinal fluid barrier

BRET = bioluminescence resonance energy transfer

CA1/CA2/ CA3 = *Cornu Ammonis* 1/2/3

Cd = cadmium

CdSe = cadmium selenide

CdTe = cadmium telluride

CNS = central nervous system

CTR = controls

DG = dentate gyrus

GFAP = glial fibrillary acidic protein

HFS = high frequency stimulus

IBA-1 = ionised calcium-binding adaptor molecule 1

IL = interleukin

In = Indium

i.v. = intravenous

LPS = lipopolysaccharide

LTP = long term potentiation

MRI = magnetic resonance imaging

NIR = near-infra-red

NOR = novel object recognition test

NPs = nanoparticles

PEG = polyethylene glycol

PET = positron emission tomography

PL = photoluminescence

p.o. = per *os*

QDs = Quantum Dots

ROS = reactive oxygen species

s.c. = subcutaneous

Se = selenium

SPECT = single photon emission computed tomography

Te = tellurium

TEM = transmission electron microscopy

TNF-α = tumour necrosis factor alpha

TJ = tight junction

Zn = zinc

ZnS = zinc sulphide

AIM of the thesis

The aim of this thesis is to study and better understand the effects of Quantum Dots nanoparticles in an animal model of rodent.

Fig. I. Thesis organisation

First we follow the biodistribution of Quantum Dots (QDs) nanoparticles on different organs, at different time points, after a systemic administration. The systemic administration was chosen to mimic the human way of exposure. Different imaging techniques allow the study of the biodistribution both in *in vivo* and *ex vivo*. In liver, spleen and brain the accumulation is measured in terms of fluorescence emission during time, heavy metals content and ultrastructural analysis which confirms the localisation of nanoparticles inside the cells. The detection of the external coating of the nanoparticle is evaluated in order to understand their integrity of the QDs over time.

Since QDs accumulate in the brain, we study their effects on nervous system functions. Cognitive and locomotor abilities, induction of an inflammatory response and neuronal plasticity are assessed in order to understand the possible effects of QDs on central nervous system.

We also hypothesise a possible impairment on circadian rhythm after QDs treatment, and a possible development of sickness behavioural syndrome.

Moreover, during the first year of the PhD I followed some studies on silica nanoparticles toxicity, after intratracheal instillation. This part was performed in prof. Oberdorster lab, University of Rochester, NY.
Part of the experiments on Quantum Dots toxicity were performed during the third year of the PhD, in Prof. Balleine lab, Brain and Mind Research Institute, University of Sydney, NSW.

CHAPTER 1

Quantum Dots nanoparticles

The new field of nanotechnology

The prefix “nano” derives from the Greek “nanos” signifying “dwarf” and is becoming increasingly common in scientific literature. Nano is now a popular label for much of modern science, and many “nano” words recently appeared in dictionaries. Nanotechnology field in the last 20 years is receiving increasing attention as one of the leading technologies of the twenty-first century. Nanotechnology is the study of manipulating matter on atomic and molecular scale, developing materials called nanomaterials, possessing at least one dimension sized from 1 to 100 nanometers (Terminology for nanomaterials; Scientific Committee on Emerging and Newly Identified Health Risks, SCENIHR). Although nanotechnology is a relatively recent field in scientific research, the development of its central concepts born quite long time ago. It was the invention of the scanning tunnelling microscope in 1981, combined with the discovery of fullerenes few years later, that created the emergence of nanotechnology. The elucidation and popularisation of the concept of nanotechnology was introduced in 1986 in the publication of the book Engines of Creation (Drexler, 1986).

Engineered nanomaterials have been widely and increasingly used in different fields. The activities and the functions of nanoparticles depends on structure, shape (which affects the particle properties and functions), surface chemistry, and self-assembly. The small size of nanomaterials results in large surface area, giving them more reactive capacity that has generated enormous excitement and expectation regarding their application.

The journal Nature Nanotechnology in 2006 published a discussion about what is exactly nanotechnology.

While Thomas Theis (director of physical sciences at the IBM Watson Research Center) regards at nanotechnology with enthusiasm seeing it as a sparkling field that can trans-

forms medical diagnostics, energy conversion, and structural materials, and is sparking new fields such as quantum information processing and nanobiotechnology, Doug Parr (chief scientist for Greenpeace in the UK) sees the new field as an "upcoming economic, business and social phenomenon" that needs to be controlled (Theis et al., 2006).

In 2008, the Project on Emerging Nanotechnologies (http://www.nanotechproject.org/about/mission/) estimates over 800 manufacturer nano-tech products are available on the market.

The most used nanomaterials are titanium dioxide (TiO_2) and zinc oxide (ZnO_2) applied in sunscreen, cosmetics, surface coatings, and some food products (Kurtoglu et al., 2011), silver nanoparticles are used in food packaging, clothing, disinfectants and household appliances (http://www.americanelements.com/nanotech.htm).

Nanotechnology has an impact in cars, for fewer metals and less fuel to operate (http://www.nanoandme.org/nano-products/transport/) and computers for being faster and contain more memory (http://www.nanoandme.org/nano-products/computing-and-electronics/).

Many kinds of manufactured nanomaterials show promising application in biomedicine (refer to the following paragraphs). For biomedical uses, especially in *in vivo* applications, for disease diagnose and therapy, the NPs are designed to ensure that they can easily enter the cells (Yan et al., 2011). It follows that the other major concerns, regarding nanotechnology applications, is the potential risks (e.g., toxic effects) and the fate of NPs after entering normal cells.

Some internalised NPs, in fact, can interact with cellular structures and produce effects adverse to human health (Li et al., 2008; Giljohann et al., 2007; Decuzzi and Ferrari, 2007). The concern about their toxicity is due to the high ratio area/volume that provides to the NP much more area that can interact with the cell. Moreover, the small size allow easier penetration into cells of different organs and facilitate the spreading of the NPs in the body even far away from the portal of entry (Lai et al., 2007; Zhao et al., 2008; Wang et al., 2009; Nishikawa et al., 2009).

Understanding the biological fate of NPs, the mechanism of cellular uptake and accumulation is important in order to understand and prevent their toxicity.

Results in literature are mixed due to variable methods, the great variety in the types of particles studied, the different cell lines, different incubation conditions, surface functionalisations, protein adsorptions, agglomerations, and aggregations, different doses etc. (Nel

et al., 2009; Soenen and Cuyper, 2010). The great diversity and complexity of the various nanomaterials also increase the difficulty of future challenges.

In nanotechnology there are two main approaches for building engineered nanomaterials. The top-down approach starts from a bulk material and breaks it into smaller pieces using mechanical, chemical or other form of energy. The bottom-up approach synthesised materials from atomic or molecular species controlling chemical reactions and allowing for the precursor particles to grow in size. Both approaches can be done in either gas, liquid, supercritical fluids, solid states, or in vacuum. The most important part of the building engineered material is the control of the particle size, the particle shape, the size distribution, the particle composition and the degree of particle agglomeration (Rodgers, 2006).

The reaction of formation of nanoparticles are controlled by the amount of reactants (its exhaustion will terminate the reaction) or by the introduction of a chemical that block the reaction. Another method is the physical restriction of the volume available for the growth of the single nanoparticle by using templates.

Quantum Dots nanoparticles : Characteristics and synthesis

Quantum Dots composition

One of the fastest developing and most exciting fields of nanotechnology is the use of quantum dots (QDs) in biology. QDs nanoparticles were discovered at the beginning of the1980s by Luis Brus and Alexei Ekimov (Rossetti et al.,1983).

QDs are fluorescent semiconductor nanocrystals that, thanks to their narrow and tunable emission wavelengths across the visible and infrared, are a promising tool for *in vivo*, *in vitro* and *ex vivo* imaging (Smith et al., 2000). The biological targets of QDs include tumours (Akerman et al., 2002; Gao et al., 2004), vasculature in normal tissues (Larson et al., 2003), and different intracellular or extracellular targets depending on the functionalisation (Ballou et al., 2004).

QDs are colloidal nanocrystals (2–15 nm diameter) whose size and shape can be precisely controlled by the duration, temperature, and ligand molecules used in the synthesis (Alivisator, 1996). They are characterised by broad absorption band with narrow and symmetric emission band in the visible to near-infra-red (NIR) spectral range (Medintz et al., 2005;

Michalet et al., 2005; Gao et al., 2005), making them excellent probes for two-photon confocal microscopy (Larson et al., 2005).

QDs consist of a core made of heavy metal, responsible for fluorescence properties, surrounded by an external coating, generally an amphiphilic polymer, that increases solubility in a biologically compatible medium. The core/shell QDs have a layer (or "shell") of zinc sulphide (ZnS) between the core and the coating, that reduces the leaching of metals from the core, improving photo-stability (Fig. 1) (Brus et al., 2007). The most utilised materials for QDs applications are semiconducting materials: CdSe (cadmium selenide), CdTe (cadmium telluride) and CdSeTe. III/V group or ternary semiconductors such as InP and InGaP, which lack cytotoxic cadmium ions, are possible alternatives (Tab. 1). The semiconducting materials differ from a metallic conductor because the current is carried by the flow of electrons or by the flow of positively charged called "holes" in the electron structure of the material.

At present, commercial products made of CdSe or CdSeTe (from Sigma-Aldrich, Invitrogen, Evident and Plasmachem), CdTe (from Plasmachem) and InP or InGaP (from Evident) are available.

Depending on the application, the external layer can be functionalised with therapeutic and diagnostic macromolecules, receptor ligands or antibodies (Michalet et al., 2005).

Their properties depend on particle synthesis and surface modifications. Addition of the passivation shell often results in a slight red shift in absorption and emission as compared to the core alone because of tunneling of charge carriers into the shell (Daboussi et al., 1997).

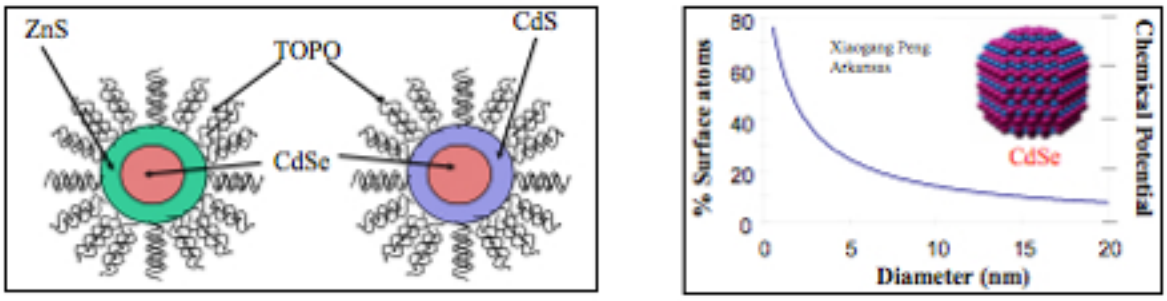

Fig. 1. On the left a schematic representation of the CdSe QDs described by Bawendi and colleagues in 1989, with ZnS shell and TOPO coating (Bawendi et al., 1989). The core of CdSe is the primary source of an optical signal. Organic molecules or "cap" are surrounding the core, preventing aggregation, oxidation and stabilising NPs in solution. They also electronically isolate the particles and passivate the surface states (Rossetti et al., 1983).
On the right image the indirect relationship between the size and the area and the chemical potential of a molecule.

Quantum Dots optical properties

One of the most attractive characteristics of QDs are their optical properties and the photostability over time.

The QDs fluorescence is associated with the transition of an electron from the conducting band to the valence band. The difference between the two energy state depends on the size of the QDs: the smaller is the QDs the higher is the energy that it requires to be excited and the higher is the energy emitted when the crystal returns to the resting state. The size depends on the core composition (Fig. 2).

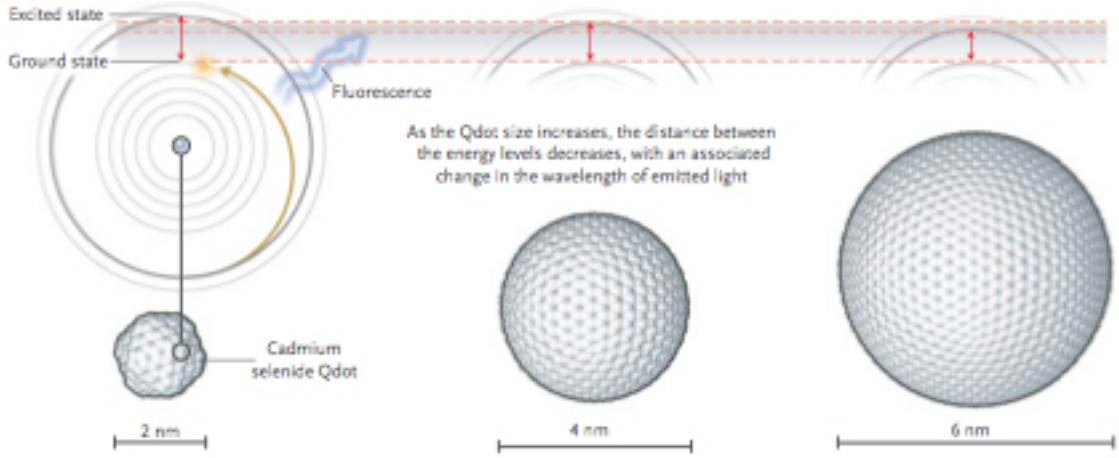

Fig. 2. Size and composition tune the optical emission of QDs. Electrons can move between energy levels in response to an external energy source. Although they move from the ground to the excited state, electrons eventually return to the ground state and emit fluorescence, the wavelength (colour) of which is determined by the distance between the two energy levels (indicated by the double arrows), which in turn is determined by the size of the nanostructure. Increasing the size of the QDs (diameter of the core) and keeping the composition constant, results in different emission wavelength in the visible region. Changing the composition of the core while the size stays constant, results in a shift of the emission wavelength. All CdSe/ZnS or CdSeTe/Zn QDs can be excited at 350nm (Kim et al., 2010).

The property of a semiconductor material was described by Pauli exclusion principle, according to which two nearby electrons can't share the same energy level. The absorption is associated with the promotion of electrons from the conduction band to the valence band. When the excitation energy exceeds that band gap energy between the two electronic bands (semiconductor band gap), the result is the formation of an electron–hole pair, called exciton. Since the QD is smaller than the Bohr exciton radius (which is a few nanometers), the energy levels are quantised, with values directly related to the QDs size (an effect called quantum confinement, hence the name "quantum dots") (Alivisatos, 1996). QDs emission is due to a radiative recombination of an exciton, which is characterised by a long lifetime (>10 ns) (Efros et al., 2000), leading to the emission of a photon in a narrow and symmetric energy band. These spectral characteristics of QD materials are different from a typical organic fluorescent molecule with red-tailed broad emission band and short fluores-

cence life-times (Resch-Genger et al., 2008). In comparison to traditional fluorescent molecules (fluorophores) or fluorescent proteins (e.g., GFP), QDs have several attractive optical features that are desirable for long-term, multi-target and highly sensitive bio-imaging applications. Some of the major optical features of QDs are:

1. Large molar extinction coefficient: QDs are highly sensitive fluorescent agents for labelling cells and tissues (Leatherdale et al., 2002), the absorption rate is approximately 10-50x faster than organic dyes and approximately 10-20x brighter than organic dyes (Dabbousi et al., 1997; Bruchez et al., 1998; Chan et al., 2008).
2. QDs are several thousand times more photostable than organic dyes (Resch-Genger et al., 2008).
3. QDs are excitable without excitation of the biological matrix and detectable with conventional instruments (So et al., 2006).
4. QDs are suitable for time-correlated lifetime imaging spectroscopy thanks to the longer excited state lifetime of QDs (Pepperkok et al., 1999; Jakobs et al., 2000).
5. Unlike in organic dyes, the excitation and emission spectra of QDs are well separated, improving the sensitivity (Gao, et al., 2004).
6. The wavelength of QD emission is size dependent allowing multiple targeting capability. This feature is particularly important in tracking a panel of disease-specific molecular biomarkers simultaneously (Gao, and Nie, 2003).

Core composition	Size range (nm)	Emission range
ZnSe	~ 4.3-6.0	UV, Visible (Size dependent)
ZnSeMn	~ 2.7-6.3	UV, Visible (Size dependent)
CdS	~ 1.0-6.0	UV, Visible (Size dependent)
CdSe / CdSeTe	~ 1.0 up to 25	Visible to NIR (Size dependent)
CdTe	~ 2.0-8.0	Visible
InP	~ 2.6-4.6	UV, Visible, NIR (Size dependent)
InAs	~ 2.8-6.0	IR
GaP	~ 2.0-3.0	UV, Visible (Size dependent)
$GaInP_2$	~ 2.5-6.5	UV, Visible (Size dependent)
PbSe	~ 3.8-12	Near/mid-IR (Size dependent)
SnTe	~ 4.5-15	Mid-IR

Tab. 1. Core composition, size range and emission wavelength ranges of QDs.

External coatings

Since QDs are insoluble in water, which limits their biological applications, a number of surface functionalisation studies have been developed to make QDs water-soluble (Kim and Bawendi, 2003).

A common approach to increase water solubility is to replace or attach to the original hydrophobic coatings water-soluble functional molecules (e.g., dithiothreitol, mercaptocarbonic acids, 2-aminoethanethiol, dihydrolipoic acid, oligomeric phosphines, peptides, and cross-linked dendrons) through the ligand exchange reactions or through the encapsulation. Because the optical properties of the inorganic core are often very sensitive to the surface, the ligand exchange process results in poorer performance, particularly in the case of QDs (Rogach et al., 2000). Other studies utilised the combinations of layers of different molecules that lead to the required colloidal stability (Matoussi et al., 2000) or developed water-based synthesis methods (Gaponik et al., 2002).

The encapsulation of QDs in an amphiphilic coating consists in attaching amphiphilic diblock copolymers, silica or polymer shells, phospolipid micelles or amphiphilic polysaccharides to the QDs core/shell structure (Chan and Nie, 1998; Bruchez et al., 1998; Dubertret et al., 2002; Kim and Bawendi, 2003; Guo et al., 2003; Pinaud et al., 2004; Osaki et al., 2004; Wu et al., 2005).

These amphiphilic molecules bind with hydrophobic ends the organic shell, protecting the core/shell structure and maintaining the original photo-physics of QDs, increases water-solubility and provides a biological interface and multiple functions (Michalet et al., 2005). The hydrophilic end groups, made of biocompatible surfactants, may not protect nanocrystals from nonspecific biomolecular interactions (Wu et al., 2009). For this reason single polymer amphiphilic chains can containing multiple hydrophobic units, are preferred. They establish numerous interactions with the organic shell on QDs, encapsulating it strongly than conventional surfactants. The range of amphiphilic polymers for creating stable and non-aggregating QDs in biological settings is relatively limited. Up to now, most of the amphiphilic polymers used are commercial and their hydrophobic/hydrophilic ratios are fixed, hence the cost is high and it is difficult to control the process of forming water-soluble QDs and optimise the forming conditions (Wu et al., 2009).

Moreover, the surfaces of QDs then can be modified with bioinert, hydrophilic molecules such as polyethylene glycol (PEG), that eliminate possible nonspecific binding, and decrease the rate of clearance from the bloodstream following intravenous injection (Fig. 3).

Water-soluble QDs also can be cross-linked to biomolecules such antibodies, oligonucleotides, or small molecule ligands that functionalise them to recognise specific biological targets (Fig. 3 Bottom). The reactivity of biomolecules generally remains stable after conju-

gation to NPs surfaces, although a decreased binding strength can occur. The optimisation of surface immobilisation of biomolecules is currently an active area of research (Lieleg et al., 2007; Pathak et al., 2007).

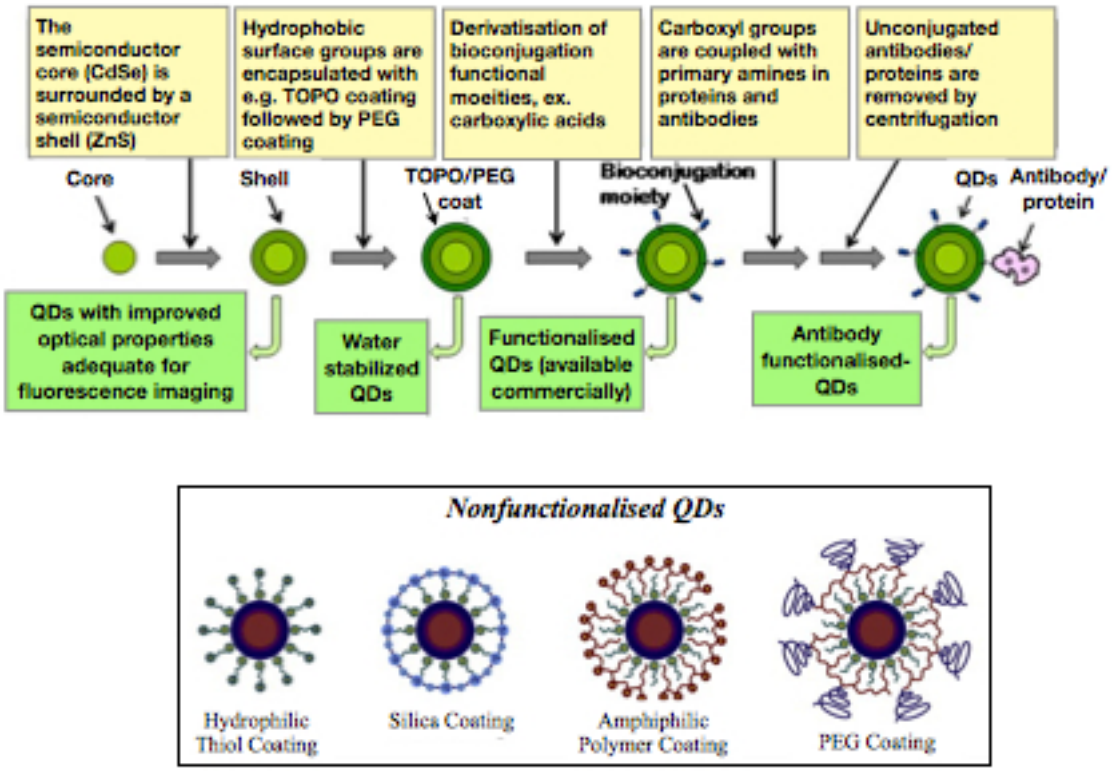

Fig. 3. Top: Schematic diagram of generation of antibody/protein-QDs conjugate (Barroso, 2011). **Bottom:** different coatings on non functionalised QDs for imaging and sensing applications (Smith et al., 2008).

Quantum Dots applications in biomedicine

Thanks to their photophysical properties and the tunable emission at different wavelengths QDs are becoming an useful tool in many biological applications.

The Tab. 2 gives an example of all the application of QDs in biology and biomedicine. The large-surface area of QDs is beneficial to covalently link to target molecules, such as peptides, antibodies, nucleic acids or small-molecule ligands for further application as fluorescent probes.

In 1998, the potential of these nanocrystals for applications involving biological labelling was first reported (Bruchez et al., 1998). Current and future applications of QDs include using fluorescent labels for cellular labelling (Bruchez et al., 1998; Kim et al., 2004), intracellular sensors (Gao et al., 2004; Liu et al., 2007), deep-tissue and tumour targeting and imaging agents (Michalet et al., 2005), nanoparticles for photodynamic therapy (Juzenas et al., 2008; Rhyner et al., 2006), vectors for gene therapy (Jiang et al., 2007; Woodle and Lu,

2005), magnetic resonance imaging (MRI) contrast agents (Nabiev et al., 2007; Lewin et al., 2000), *in situ* hybridisation and as live cell markers (Alivisator et al., 2005; Bruchez, 2005) etc.

Quantum dots applications
* Imaging: fixed cells and ICC
* Imaging: histochemistry
* FISH (*in situ* hybridisation)
* Live cell imaging
* Cell tracking and stem cell labelling
* Single molecule tracking
* *In vivo* whole animal imaging
* Flow cytometry
* Westerns blots
* Arrays and microplate assays (FRET based assays etc.)

Tab. 2. Schematic representation of QDs applications in biomedicine.

QDs for FRET- and BRET-based sensors

QDs are emerging as a new class of sensor, where beyond their application as passive labels, they transfer the electronic excitation energy to a nearby acceptor specie such as an organic fluorophore in a process called fluorescence resonance energy transfer, FRET (Tran et al., 2002; Medintz et al., 2003; Zhang et al., 2005). The rate of energy transfer depends on the distance between the donor of energy (the QDs) and the acceptor of the energy (fluorophore), their relative orientation and spectral overlap. This method allow to follow specific interactions between molecules or cleavage events (Williard et al., 2006). The first application of QDs in FRET was done in 2001 by Williard (Williard et al., 2001). For applications of QDs in FRET refer to Gill et al. (2005) and Menditz et al. (2007).

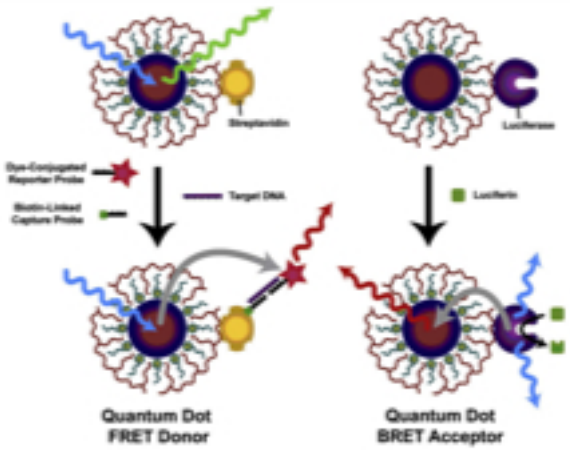

Fig. 4. Schematic representation of QD as FRET-based, BRET-based sensors

QDs can be applied also in Bioluminescence Resonance Energy Transfer (BRET) where a light emitting protein (donor) transfers energy to QDs (acceptor). With this technique QDs can emit fluorescence

without an external source of excitation, but with an enzyme is in close proximity that catalyses bioluminescent reactions (Fig. 4) (So et al., 2006).

QDs in immunohystochemistry and immunoassays

Several applications of QDs for *in vitro* bioassays (Smith and Nie, 2004; Smith et al., 2006) have been proposed e.g. labelling fixed cells (Wu et al., 2003) or tissue (Fountaines et al., 2006; Ferrara et al., 2006). The utility of QDs in immunohistochemical applications was demonstrated by Ness and colleagues (2003) who developed an immunohistochemical protocol for detection of intracellular antigens in mouse and rat brain tissue sections, showing that QDs labelling had superior sensitivity than conventional dyes (Ness et al., 2003).

The QDs staining gives molecular and morphological information at the same time (Matzumo et al., 2011). One of the earliest experiments where QDs were used to locate molecules in cells was performed by Bruchez and coworkers (1998) to stain F-actin in fixed cells with antibodies labeled with CdSe/ZnS QDs. In another experiment QD immunoconjugates showed that mortalin (heat shock protein-70) could be a reliable marker for distinguishing between normal and cancer cells (Kaul et al. 2003). For this application the possible toxic effect of QDs are less important and their multiplexing capabilities are useful in a high-throughput or multiplexed detection of biomolecules for *ex vivo* diagnosis (Fournier-Bidoz et al., 2008; Zhu et al., 2008). The use of multiple QD labels is suitable for optical bar coding of targets (Jain, 2003). The multiplexing potential of QDs can enable obtaining information on the location, abundance, and distribution of multiple proteins in living cells. It would also allow multicolour encoding of cells or beads and thus obtaining data on differential response of cell types to common stimuli. This multiplexing potential would be particularly significant for cancer diagnostics and research, where multiple cancer biomarkers can be simultaneously detected, which would help untangle the associated complex gene expression patterns (Smith et al., 2006).

QDs in Western Blot and Proteomics

QDs can be employed for detection of multiple proteins on Western blots (Bruchez et al., 2005), this would constitute a significant empowerment to the field of proteomics. Currently, kits employing QD-conjugated anti-rabbit and anti-mouse antibodies are available for use in Western blotting.

QDs in Fluorescent In Situ Hybridisation

QDs can also be used as labels for detection of multiple mRNA targets using fluorescence *in situ* hybridisation (FISH) (Chan et al., 2005). Oligonucleotide probes can be labeled with QDs or biotinylated oligonucleotide probes may be coupled to QDs coated with streptavidin.

QDs can be used for profiling of microRNA (miRNA, single-stranded RNA molecules and play a role in gene expression). In one such study, miRNAs are labeled with biotin and hybridised with complementary oligo-DNA probes immobilised on glass slides,and detected by measuring fluorescence of streptavidin-labeled QDs bound to miRNAs (Liang et al., 2005).

QDs for imaging living cells

The QDs cell internalisation has attracted many interests for diagnosis or treatment. The applications of QDs for imaging inside the cell is limited cause the difficulties in delivering QDs into the cytoplasm of living cells, since they tend to aggregate inside cells, and are often trapped in endocytotic vesicles such as endosomes and lysosomes (Lidke et al., 2004; Dahan et al., 2003 Brandenberger et al., 2010).

Nevertheless there are different pathways for delivering QDs into a cell: transfection, peptide-mediated delivery or passive uptake. It has been reported that the peptide mediated approach employed the amphiphilic peptide Pep-1, while in the transfection approach the PolyFect has been used. The QDs maintain their fluorescence, they distribute in the cytoplasm, they are passed during the mitosis to the daughter cell, escape lysosome degradation and do not inhibit cell growth (Mattheakis et al., 2004; Morris et al., 2001).

The passive uptake, on the other hand, is used to deliver non functionalised QDs into the cells through endocytosis, and depends on surface coatings. In general, the positive charge (like polyethylenimine, PEI) allows the interaction with the membrane, inducing the endocytosis. It has been shown that PEI-QDs, with the addition of the external coating PEG, show a high degree of endocytosis with reduced harmful effects.

It has been found that the efficiency of the QDs internalisation is enhanced by conjugation of the QDs to membrane receptors. For example, QDs coupled to Shiga toxin, ricin, and Tfn are all endocytosed specifically via binding to their receptors in a clathrin-mediated manner (Tekle et al. 2008). Clathrin-mediated endocytosis is the most important pathway for the intracellular delivery of peptide-conjugated QDs (Anas et al. 2009).

A new class of cell-penetrating quantum dots is based on the use of multivalent and endosome-disrupting (endosomolytic) surface coatings. The copolymer ligands PEG-grafted polyethylenimine (PEI-g-PEG), thanks to the cationic charges associated with multivalent amine groups, these QDs can penetrate cell membranes and disrupt endosomal organelles in living cells (Boussif et al., 1995; Neu et al., 2005; Pack et al., 2005; Duna and Nie, 2007).

Another positive charged QDs (2.2 nm) coated with small molecule ligands (cysteamine) spontaneously translocated to the nuclei of murine microglial cells following cellular uptake through passive endocytosis. In contrast, larger QDs (5.5 nm) and small QDs bound to albumin remained in the cytosol (Lovric et al., 2005).

QDs for single molecules tracking

The tracking of single proteins represents an important tool in many field. QD bioconjugates have been found to be powerful imaging agents for specific recognition and tracking of molecules, like plasma membrane antigens, allowing to follow the movement of single molecules in live cells for milliseconds to hours. As compared to normal fluorophores QDs are more resistant to photobleaching.

Real-time detection of single molecules antibodies is performed conjugating to different QDs that would bind to different sites of the target biomolecule. A signal is detected only if both QD-labeled antibodies bind to the target at the same time (Agrawal et al., 2006).

Some example of applications in neuroscience fields are in the study of dynamics for various receptors, like GABA, AMPA and NMDA, acetyl coline and cannabinoids receptors. One of the first experiments in this field was done in 2003, and QDs was conjugated to an antibody for detecting glycine receptor (Dahn et al., 2003). After this publication many others studies followed using QDs to monitor membrane proteins like integrins (Lieleg et al., 2007), G-protein coupled receptors (Young and Rozengurt, 2006) and for exploring the processes of synaptic vesicle fusions during neuronal stimulation.

The single molecule tracking with QDs has been also investigated for labelling molecules inside the cell. The main problem in this process is avoiding the internalisation of QDs in the cells through endocytosis, that is the most probable way of QDs uptake (Hanaki et al., 2003). By passive uptake, QDs are internalised in vesicle as aggregates and they can't reach specific intracellular targets. This is a good method to label endocytosis or cells but not single molecules. Moreover, internalised QDs it is difficult to distinguish between

bound and unbound QDs in the cells. QDs size and charge become important in order to predict the QDs behaviour inside the cell. Researchers are exploring the use of fusion tags but this application is still developing.

In vivo vascular imaging

The main applications described in literature for in vivo imaging of mice after QDs injection encompass imaging of blood vessels, lymph nodes, tumours and cell tracking.

In vivo vascular imaging

One of the most important and successful applications of QDs is the *in vivo* imaging. They are used as contrast agents for circulatory system of mammals, the cardiovascular system and the lymphatic system.

In 2003, Larson and colleagues demonstrated that red-light emitting QDs remained fluorescent and they are detectable in capillaries of adipose tissue and skin of a living mouse following intravenous injection (Larson et al., 2003).

From 2003 to nowadays, near infrared QDs have had a great application for *in vivo* imaging. They have been used to image the coronary vasculature of a rat heart (Lim et al., 2003), or blood vessels of chicken embryos (Smith et al., 2007). The conjugation of the QDs to cell adhesion molecules (CAMs) can en-light inflammation cells behaviour, like leukocytes rolling and extravasation from blood vessels (Jayagopal et al., 2007). As we reported in the previous paragraph, the advantage of QDs is that they can be detected with higher sensitivity than traditional dyes (e.g. fluorescein–dextran conjugates), and resulted in a higher uniformity in image contrast across vessel lumen.

Applications involving *in vivo* imaging must consider that haemoglobin strongly absorbs in the visible region (300–600 nm), water and lipids that are transparent in the visible region but absorb strongly in the infrared (1400–2000 nm); and autofluorescence of, for example, endogenous skin fluorophores. The latter include nicotinamide adenine dinucleotide/nicotinamide adeninine dinucleotide phosphate (em. 425 nm), flavin adenine dinucleotide (em. 520 nm), and porphyrins (em. 625 nm), with relative contributions of approximately 75%, 25%, and 2%, respectively (Nah et al., 2000).

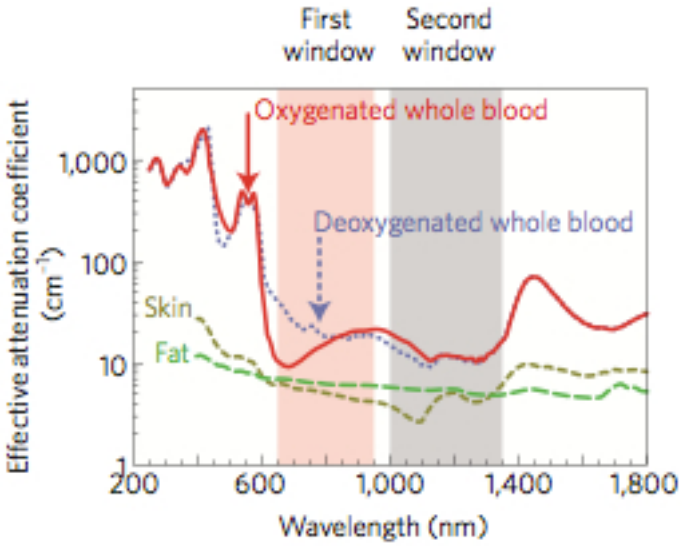

Fig. 5. The first NIR window is ideally suited for *in vivo* imaging because of minimal light absorption by haemoglobin (<650 nm) and water (>900 nm). It is called also transparency window for this reason.
The second window is also very convenient for *in vivo* imaging, but lack of adequate detection systems (from Smith et al., 2009).

Near infra-red light (700-2500 nm) can penetrate biological tissues such as skin and blood more efficiently than visible light (Smith et al., 2009). The clearer window for optical imaging *in vivo* is between 650 and 950 nm (Weissleder, 2001) (Fig. 5). At this wavelength the tissue penetration is about 1-2 cm (Smith et al., 2009) and biological components do not substantially interfere.

A different type of QDs for *in vivo* imaging have 1320 nm emission wavelength, instead of 850 (second window emission), that improves of 100 times the fluorescence of QDs (Lim et al., 2003) (Fig. 5). Other types of NPs with a second window emission have been produces for *in vivo* imaging: fluorescent single-walled carbon nanotubes, with an emission wavelength of 950-1,400 nm and plasmonic NPs, such as gold nanorods (Smith et al., 2009). The problem associated with the second window emitting NPs is the lack of the adequate system of detection, like enough sensible CCD cameras (Smith et al., 2009).

Near infra-red QDs have been used also for imaging the lymphatic system. It has been shown that intradermally injected ~ 16–19 nm near-infrared QD translocate to sentinel lymph nodes, likely due to a combination of passive flow in lymphatic vessels, and active migration of dendritic cells that engulfed the NPs (Kim et al., 2004). Only QDs with an hydrodynamic diameter smaller then 9 nm can migrate in the lymphatic system (Roberts et al., 2002). This technique could have great clinical impact due to the quick speed of lymphatic drainage and the ease of identification of lymph nodes, enabling surgeons to fluorescently identify and excise nodes draining from primary metastatic tumours (Ballou et al., 2007).

Another type of QDs designed for *in vivo* imaging are the self-illuminating QDs. Self-illuminating QDs fluorescence is based on bioluminescence resonance energy transfer, that is the conversion of chemical energy into photons energy, and has several advantages like

increased fluorescence emission and decreased autofluorescence (So et al., 2006). QDs are covalently attached to *Renilla reniformis* luciferase, which, in presence of its substrate coelenterazine, emits at 480 nm (blue light). The blue light is absorbed by QDs, giving an efficient fluorophore excitation.

This system decreases the autofluorescence since there is no excitation light but the existing formulation of QDs contains semiconductor or heavy metals with associated toxicity. Moreover, external coating, like amphiphilic molecules, are added to improve the solubility in biological fluids and secondary coating, like PEG, are added to have longer blood circulation. These external modifications increase the hydrodynamic diameter of the QDs, decreasing the possible clearance from the body (Frangioni, 2006).

In vivo tumour imaging

Imaging of tumours presents a unique challenge not only because of the urgent need for sensitive and specific imaging agents of cancer, but also because of the unique biological attributes inherent to cancerous tissue.

Recently, Doxil® (PEGylated liposomal form of doxorubicin) and Abraxane (albumin-bound Paclitaxel nanoparticle) have been approved by Food and Drug Administration for solid tumours-therapy. These NPs have a big size (about 100-130 nm) that allow to preferentially enter tumours tissues, thus reducing normal tissue toxicity. In tumours blood vessels are abnormally formed with wide endothelial pores. These pores are large enough to allow the extravasation of large macromolecules up to ~ 400 nm in size, which accumulate in the tumour microenvironment due to a lack of effective lymphatic drainage (Jain, 2001). This tumours characteristic has been called “enhanced permeability and retention” effect (EPR effect) and has inspired the development of a variety of nanotherapeutics and nanoparticulates for the treatment and imaging of cancer (Fig. 6) (Perrault et al., 2009).

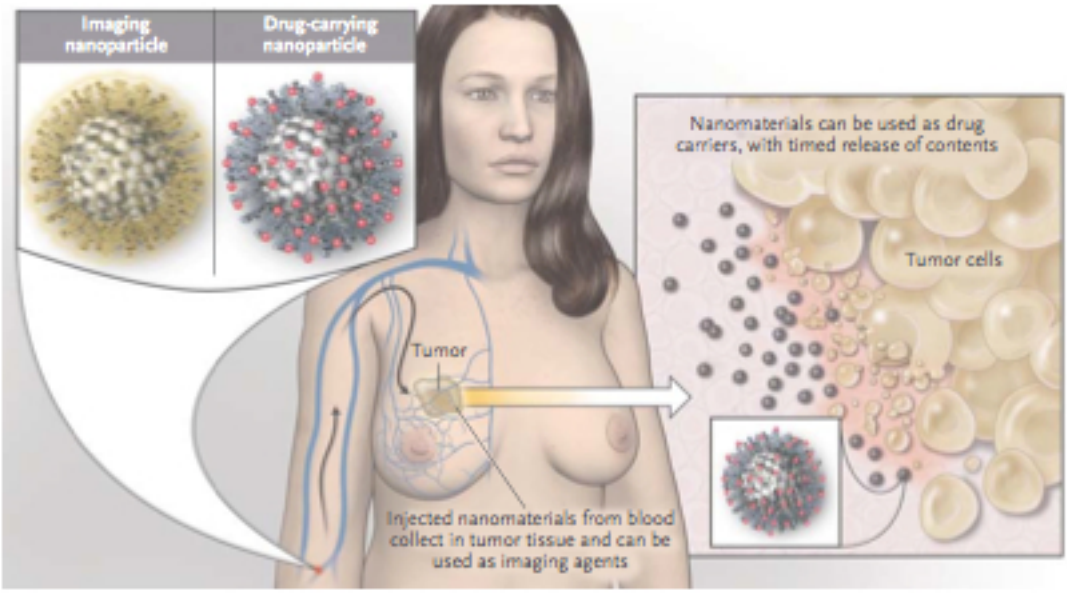

Fig. 6. Use of nanomaterials for tumour diagnosis. (Kim et al., 2010)

Cancerous cells have different surface receptors as compared to normal cells and the exposure to the bloodstream make them a good target for functionalised NPs. For this reason, active targeting of cancer antigens has become an area of tremendous interest to the field of medicine because of the potential to detect early stage cancers and their metastases.

QDs are great promise for these applications, due to their intense *in vivo* fluorescent signals and multiplexing capabilities, which could allow a high degree of sensitivity and selectivity in cancer imaging with multiple antigens.

One of the first approach for *in vivo* tumour imaging has been done in 2002 by Akerman and colleagues that conjugated QDs to peptides with affinity for various tumour cells and their vasculatures (Akerman et al., 2002). Few years later tumour targeting with QDs could generate tumour contrast in the whole-animal imaging (Gao et al., 2004). The active tumour recognition by means of QDs functionalisation with antibodies or molecules that specifically recognise tumour epitopes, results as a better tool in tumour imaging as compared to nonconjugated QDs, that by contrast, passively accumulate though the EPR effect. Conjugation with different tumoural epitopes (e.g. alpha-fetoprotein) created different type of QDs that target specifically a certain type of tumours (Yu et al., 2007). Human cancer evolves over a long time course and shows a multitude of molecular and cellular heterogeneity (Heppner and Miller, 1983). The heterogeneity is in the genetic mutations and phenotypes and in the multitude of different cells that compose the tumours (malignant cells, benign cells, fibroblasts, vascular cells, inflammatory cells etc.). At this purpose the use of multiplexed QDs-antibody conjugate with different wavelength for molecular mapping of

tumour heterogeneity on human prostate cancer tissue is an example of high throughput mapping of all the tumours variations on prostate tumours (Liu et al., 2010).

QDs can be applied for intravital microscopy techniques as a contrast agent for the imaging of tumour microenvironment (Stroh et al., 2005) or blood vessels using two-photon excitation.

Using intravital fluorescence microscopy of the tumour following systemic QD administration, it is possible to distinguish individual QDs as they circulated in the bloodstream, extravasated into the tumour, diffused in extracellular matrix, bound to their receptors on tumour cells, and then translocated into the perinuclear region of the cells (Tada et al., 2007).

The development of clinically relevant QD contrast agents for *in vivo* imaging is certain to encounter many roadblocks in the near future, however QDs can currently be used as powerful imaging agents for the study of the complex anatomy and pathophysiology of cancer in animal models.

The Tab. 3 summarises the most relevant studies using QDs for medical applications.

Application area	*Description*	*References*
Diagnosis	Detection of Her2 (hairy-related 2) on SK-BR-3 breast cancer cells by employing humanised anti-Her2 antibody, a biotinylated goat anti- human IgG, and streptavidin-coated QDs	Wu et al., 2003
	Immunofluorescence labelling of mortalin using QDs showed different staining patterns between normal and cancer cells	Kaul et al., 2003
	Detection of ovarian cancer marker CA 125 in various specimens using streptavidin-conjugated QDs	Wang et al., 2004
	Fluoroimmunoassay for the detection of prostate-specific antigen using streptavidin-coated QD	Härmä et al., 2001
	QD-based FISH labelling was used to detect specific repeats in the Y chromosome in fixed human sperm cells	Pathak et al., 2001
	Antibody-conjugated QDs were used to detect prostate cancer cell marker PSA, the QD conjugates detected the tumour site in mice transplanted with human prostate cancer cells	Gao et al., 2004
Imaging	Imaging skin and adipose tissues in mice by injection of water-soluble QDs	Larson et al., 2003
	Mapping sentinel lymph nodes at 1 cm tissue depth using oligomeric phosphine-coated QDs that emit in the near-infrared region	Kim et al., 2004
	Tracking diffusion dynamics of glycine receptors using QDs	Dahan et al., 2003
Drug delivery and therapeutics	Surface-modified CdS QDs were used as chemically removable caps to retain drug molecules and neurotransmitters inside a mesoporous silica nanosphere-based system	Lai et al., 2003
	QDs showed potential in use as photosensitisers or to excite other photosensitisers in photodynamic therapy	Samia et al., 2006
	Screening of siRNA sequences and monitoring RNAi delivery using QD–siRNA conjugates	Bakalova et al., 2005

Tab. 3. QDs-based medical approaches

Multimodal Quantum Dots

The applications of QDs described above for *in vivo* imaging, with Optical Imaging or others techniques are limited by tissue penetration depth, quantification problems, and a lack of anatomic resolution and spatial information. To overpass these limitations, it is pos-

sible to couple QD-based optical imaging with other imaging modalities (e.g. magnetic resonance imaging (MRI), positron emission tomography (PET) and single photon emission computed tomography (SPECT)) (Cai et al., 2008).

The incorporation of paramagnetic gadolinium complexes in the lipid coating layer of QDs, for example, gives the possibility of follow QDs imaging with both optical imaging and MRI (Mulder et al., 2006). *In vitro* experiments showed that labelling of cultured cells with these QDs led to significant T1 contrast enhancement with a brightening effect in MRI, as well as an easily detectable fluorescence signal from QDs.

However, the *in vivo* imaging potential of this specific dual-modality contrast agent is uncertain due to the unstable nature of the lipid coating that was used.

Another approach attaches PET-detectable radionuclide ^{64}Cu to the polymeric coating of QDs through a covalently bound chelation compound (Cai et al., 2007). This probe is used to target a subcutaneous mouse tumour model in an *in vivo* system, functionalising the QDs surface with $\alpha_v\beta_3$ integrin-binding RGD peptides (Cai et al., 2007).

The majority of these probes are still at an early stage of development. The clinical relevance of these nanoplatforms still needs further improvement in sensitivity and better integration of different imaging modalities, as well as validation of their biocompatibility and safety.

Moreover, it is possible to detect all type of QDs with TEM thanks to their electron dense core.

The synthesis of QDs containing paramagnetic dopants, such as manganese, have led to a new class of QDs that are intrinsically fluorescent and magnetic (Santra et al., 2005; wang et al., 2007). However the utility of these new probes for bioimaging application is unclear because they are currently limited to the ultraviolet and visible emission windows, they increase the amount of heavy metals and possibly the toxicity and their possibly limit the QDs stability (e.g., photochemical and colloidal) (Pradhan and Peng, 2007). All these parameters have to be investigated .

Integration of imaging and therapy

Peptide-functionalised QDs are internalised after binding to cell surface, and may thus be of value for drug delivery (Rozenzhak et al., 2005).

QDs can be utilised for controlled drug delivery via their surface modification (Alivisator et al., 2005). Surface-modified CdS QDs retain drug molecules and neurotransmitters inside mesoporous silica nanospheres. The CdS cap ensures the drug is inside the system until released by disulphide bond-reducing reagents (Lai et al., 2003).

Quantum Dots quantification techniques

Various methods are used to detect QDs *in vivo* such as fluorescent (Optical Imaging) or nuclear imaging systems (SPECT and PET). These different techniques make possible to follow QDs in a whole body over several days but give only a semi-quantitative aspect of QDs concentration *in vivo*. QD tracking methods in *ex vivo* systems are numerous and include confocal microscopy, total internal reflection microscopy, wide-field epifluorescence microscopy, and fluorometry (Bruchez et al., 1998; Chan et al., 1998; Jain, 2005; Michalet et al., 2005). The most significant techniques for measuring QDs concentration are those which detect QDs at the elementary level (Cd, Te, Se), such as Inductively Coupled Plasma - Mass Spectroscopy (ICP-MS) and Inductively Coupled Plasma - Atomic Emission Spectroscopy (ICP-AES), followed by fluorescent and radioactivity measurements which allow to quantify directly QDs. The sensitivity of ICP-MS is an enormous asset to identify trace levels that are undetectable by optical methods. However, these four last techniques can only be used *ex vivo* after resection and specific preparations of biological samples. Nevertheless, despite numerous techniques for the detection of QDs, biodistribution studies *in vivo* are sparse.

ICP-MS

The ICP-MS is one of the most utilised technique in nanotoxicology because of its sensitivity. The instrument employs a plasma (ICP) as the ionisation source and a mass spectrometer (MS) analyser to detect the ions produced (Fig. 7). It can simultaneously measure most elements in the periodic table and determine analyte concentration down to the sub nanogram-per-liter (ng/l) or part-per trillion (ppt) level. It can perform qualitative, semiquantitative, and quantitative analysis, and since it employs a mass analyser, it can also measure isotopic ratios.

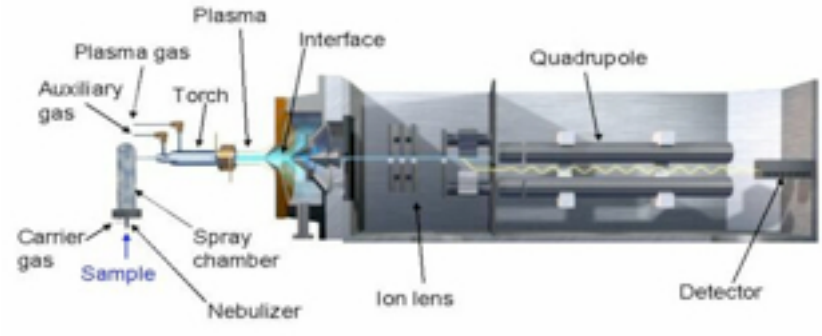

Fig. 7. ICP-MS schematic representation.

In general, samples are introduced by a peristaltic pump, to the nebuliser where the sample aerosol is formed. Argon (Ar) gas is introduced through a series of concentric quartz tubes which form the ICP. The torch is located in the centre of an radio frequency coil, through which radio frequency energy is passed. A radio frequency potential applied to the coil produces an electromagnetic field that causes collisions between the Ar atoms, generating a high-energy plasma. The sample aerosol is instantaneously decomposed in the plasma (plasma temperature is in the order of 6000 - 10000 K) to form analyte atoms which are simultaneously ionised. The ions produced are extracted from the plasma into the mass spectrometer region which is held at high vacuum (typically 10-4 Pa). The vacuum is maintained by differential pumping: the analyte ions are extracted through a pair of orifices, known as the sampling and skimmer cones.

The analyte ions are then focused by a series of ion lenses into a quadrupole mass analyser, which separates the ions based on their mass/charge ratio. The term quadrupole is used since the mass analyser is essentially consists of four parallel stainless steel rods to which a combination of radio frequency and DC voltages are applied. The combination of these voltages allows the analyser to transmit only ions of a specific mass/charge ratio. Finally, the ions are measured using an electron multiplier, and are collected by a counter for each mass number.

CHAPTER 2

Biodistribution of Quantum Dots after i.v. administration

INTRODUCTION

Safety issues of nanoparticles

The small size of NPs corresponds to a large surface area. In fact, the ratio of the surface atoms to total atoms of the molecule increases with a decreasing molecule size. This property is important when NPs interact with biological systems: the large surface area increases the reactivity of NPs as compared to normal molecules, representing an important property for many biomedical and industrial applications. The same properties which make NPs so attractive for nanomedicine and for specific industrial processes can also be deleterious when NPs interact with cells, causing potential adverse effects or environmental contamination. NPs biological activity can have a positive and desirable effect (e.g. drug delivery, penetration of cell barriers, interactions with cells and reactions), but they can provoke also negative effects (e.g., toxicity, induction of oxidative stress or of cellular dysfunction), or a mix of both (Holsapple et al., 2005).

Industrial and academic researchers are more interested in discovering new NPs for biomedical and industrial applications rather than evaluating the potential risk that NPs can have on human health and environment. The exposure to NPs can occur for medicinal purposes, or after unintentional exposure, during manufacture or processing for industrial applications. Many nanomaterials have been demonstrated to have adverse effect to human health and cell cultures, resulting for example in increased reactive oxygen species production, inflammatory response, mitochondria perturbation, protein denaturation and degrada-

tion, nuclear uptake, blood clotting and cell death (Oberdorster et al., 2005; Nel et al., 2006).

The term "nanotoxicology" first showed up in 2004 and it is defined as the "science of engineered nanodevices and nanostructures that deals with their effects in living organisms" (Oberdorster et al., 2005). Nanotoxicology research not only will provide data for safety evaluation of engineered nanostructures but also will help to advance the field of nanomedicine by providing informations about their undesirable properties and means to avoid them. United States Environmental Protection Agency and the Food and Drug Administration in U.S. and the Health and Consumer protection Directorate of the European Commission, have started dealing with the potential risks posed by nanoparticles, but still nanomaterials or materials containing nanoparticles, are not subjected to any special regulation regarding production, handling or labelling.

Most of the toxicity research on NPs *in vivo* has been carried out in mammalian systems. The exposure routes of NPs are: skin, respiratory tract and gastrointestinal tract (Fig. 9). They need to be considered as potential portals of entry. Portal-of-entry-specific defence mechanisms protect the mammalian organism from harmful materials. However, these defences may not always be as effective for NPs. In biomedicine, humans can be also exposed to NPs trough a systemic or subcutaneous administration.

The number of publications on the topic of nanomaterials has increased at an exponential rate since the 2000 to the 2011, reaching about 20 000 in the year 2011. The large number of publications on nanomaterials can be explained by the fact that nanoscience and nanotechnology are developing in a wide range of fields, including chemistry, physics, materials engineering, biology, medicine, and electronics. There is also a notable rise in the number of publications discussing the toxicity, of nanomaterials. The total number of papers on toxicity, however, remains low compared to the total number of publications on nanomaterials, with only around 500 publications in the year 2011.

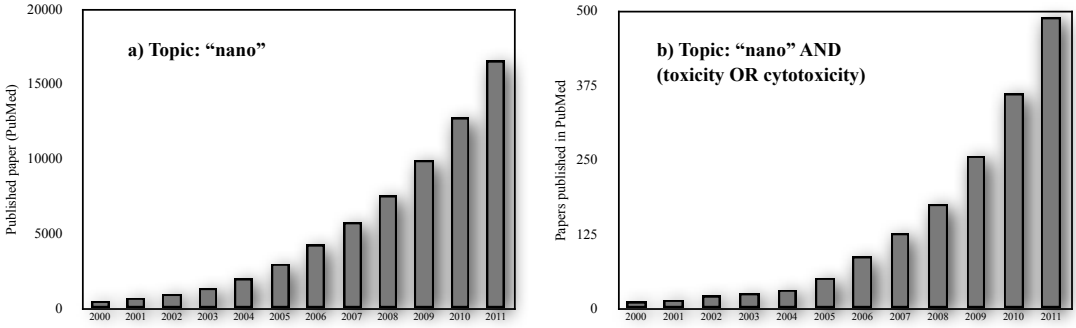

Fig. 8. Statistics on scientific articles published on a) nanomaterials and b) their toxicity.

The possible adverse health effects associated with inhalation, ingestion, and contact with nanoparticles depends on various factors, including size, aggregation, composition, crystallinity, surface functionalisation, etc (Harman, 2006). In addition, the toxicity of any nanoparticle to an organism depends on the individual's genetic background (Buzea et al., 2007).

NPs have a similar size as viruses but even if they do not replicate and do not take the control of cell cycle, they can interfere with the cell functions and cause diseases or increase the gravity or the chance to be affected by a disease. Multiple sclerosis, stroke, and Parkinson's disease are all increased in people exposed to these pollution particles, especially the ultrafine particles, that are the NPs with a size smaller than 100nm (Genc et al., 2012). In fact, ultrafine nanoparticles cause much greater inflammation and microglial activation than larger particles and the involvement of systemic inflammation even if it regards the body and not the brain, can lead to the inflammation of the brain and the subsequent degeneration (Genc et al., 2012). Nanoparticles in the gastrointestinal tract have been linked to Crohn's disease and colon cancer. Nanoparticles that enter the circulatory system are related to occurrence of arteriosclerosis, blood clots, arrhythmia, heart diseases, and ultimately cardiac death. Translocation to other organs, such as liver, spleen, etc., may lead to diseases of these organs as well. Exposure to some nanoparticles is associated with the occurrence of autoimmune diseases, such as systemic lupus erythematosus, scleroderma, and rheumatoid arthritis (Fig. 9) (Buzea et al., 2007).

The issue of QD toxicity is a serious obstacle to a full exploration of their *in vivo* usage in biomedical imaging. The toxicity arises primarily from two sources: **1**. the semiconductor materials that commonly constitute the QDs core (and sometimes the overcoating shell) which can leach under certain circumstances (Derfus et al., 2004), and **2**. the generation of reactive and free radical species during excitation (Bakalova et al., 2004a, 2004b). The toxicity of metals such as Cd and Se is well documented (Colvin, 2003; Hoet et al., 2004; Hardman, 2006; Nel et al., 2006). These heavy metals can cross the blood-brain barrier, can accumulate in adipose tissue with biological excretion half-lives greater than ten years. They are primarily toxic to the liver and kidneys, and are considered possible teratogens and probable carcinogens (Colvin, 2003; Hoet et al., 2004; Hardman, 2006; Nel et al., 2006). Today almost all synthetic precursor materials used to make semiconductor QDs are toxic.

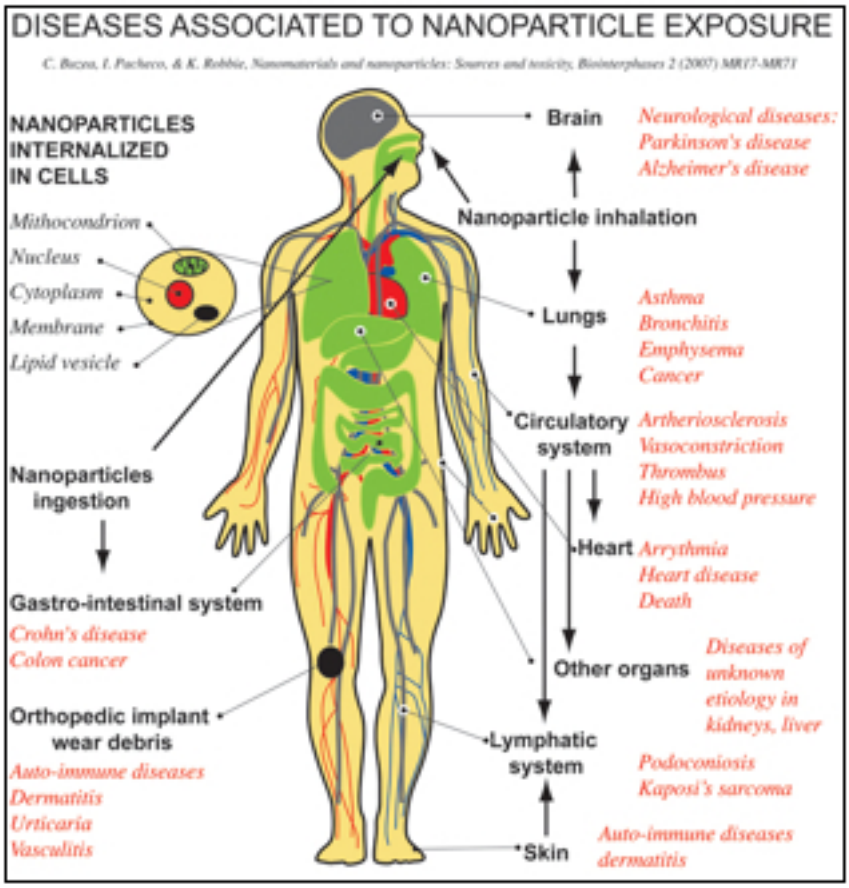

Fig. 9. Schematic representation of human body biodistribution of nanoparticles after inhalation, ingestion or penetration trough the skin and the possible diseases they can induce (Buzea et al., 2007).

However, before QDs can enter the market they will be subjected to some form of regulatory scrutiny, but which type of scrutiny is still undetermined. In the world there isn't a jurisdiction that defines specific safety-related data for nanomaterials or declare when and if such requirements can be expected (Pelley and Saner, 2009).

This type of regulation should consider the toxicity and the biological fate of substances, including adsorption, distribution, metabolism and excretion (ADME) within a body and the transportation and transformation within the natural environment (Pelley et al., 2009).

Biodistribution and biological effect of different type of QDs

The vast majority of scientific papers reporting on the toxicity of QDs have limited their investigation to cytotoxic effects observed in short-term, cell culture-based assay systems. Only in the last few years the literature is exploring the *in vivo* effect, viability, reproductive capacity and biological fate over long term period in rodents or other species. The number of studies on QDs toxicity is increasing, but the final interpretation of the cy-

totoxic effects is further complicated because of the diversity of QDs being tested, as each individual type of QD possesses its own physicochemical properties, and due to the diversity of test systems used. The dosage of QDs used and exposure times also vary widely in the literature. Furthermore, it is often unclear how the experimental dosages relate to concentrations associated with real-world commercial applications of QDs. Moreover, it is difficult to extrapolate the results of such studies in order to form any conclusions regarding the health and safety of QDs.

In 2006 a review summarising the toxicology data of QDs concluded that the toxicity of QDs was dependent upon their physicochemical properties as well as environmental factors (Hardman, 2006). Three years later Pelley and collaborators adapted and extended Hardman's table to summarise the studies that have been published.
Here we combine the data reported by both authors and we include all data from december 2008 to january 2012 (refer to Appendix, Tab. X and XX).

Quantum Dots biodistribution in the body

In his review of 2006, Hardman claimed that some studies, both *in vitro* and *in vivo*, did not find enough evidence to prove that QDs induce toxicity.
The first studies with QDs, *in vivo,* after injection into mouse tail veins appeared around 2003/2004 for *in vivo* imaging (Larson et al. 2003; Ballou et al. 2004). The CdSe QDs used by the authors immediately distribute in the circulatory system, but within an hour the particles are mainly cleared from the blood unless a large PEG polymer is used on the surface (Larson et al., 2003). CdSe/ZnS QDs capped with an amphiphilic polymer and mercaptoacetic acid/peptides respectively show a decreased fluorescence during time in animal studies (Akerman et al., 2002; Gao et al., 2004), suggesting a possible degradation of the surface coatings *in vivo*, that causes surface defects and loss of fluorescence. The QDs that are coated with a high molecular weight polymer have greater *in vivo* stability than those of a lower molecular weight (Gao et al., 2004). Moreover, the surface chemistry, the size and and the surface modifications determine the half life of the NPs in the blood, before entering in the organs and direct the fate of the nanoparticle in terms of excretion and accumulation. The distribution, accumulation and clearance of CdSe/ZnS QDs in rats in a short term study (up to 10 days) with different coatings: MUA (MUA–QDs) or BSA (BSA–QDs), and hydrodynamic radii of 25 nm and 80 nm respectively, reveals that QDs accumulate in the liver rather than the spleen, although the uptake is from both organs (Fisher, 2006). In par-

ticular, the main portion of the two types of QDs accumulates in liver at the edges of the liver sinusoid, in Kupffer cells and that there is a significant quantitative difference in tissue distribution between both QDs in liver, spleen, lung and kidney (Fischer, 2006). After 10 days there isn't any sign of degradation of the inorganic core/shell part, or excretion of the QDs: the sequestered QDs remain in the RES cells (Fischer et al. 2006).

It has been reported that QDs accumulate also in lymphoid organs. QDs accumulate in cells of the red pulp of the spleen, in cells within the subcapsular sinus in the lymph nodes and in the vascular sinus periphery in the bone marrow. MUA-QDs are found in higher quantities than BSA-QDs in both the lung and kidney.

They show a lack of cadmium ions in the faeces and urine, but other studies have confirmed the presence of fluorescence within the bladder and kidneys. A possible explanation is that these QDs are too large for excretion by the kidneys (Fischer et al. 2006).

An important aspect of the QDs toxicity is the need of excretion of administered NPs in a relatively short time.

Longer term studies with commercial CdSe QDs coated with methoxy PEG-5000 (emitting at 705 nm) show that, even if plasma half life of the NPs is short (18,5h), there is not excretion after 28 days from the systemic administration. The QDs continue to accumulate in the spleen, liver and kidneys during the time of the investigation (Yang et al., 2007). Similarly, another type of QDs, the CdSe/ZnS QDs coated with mPEG 5000 and emitting at 655 nm, immediately after injection accumulate in various organs, including liver, spleen, lymph and bone marrow. Within five days, the fluorescence decreases in the liver, but it takes up to six months for the emission in the bone marrow to fade. The lymph nodes maintain the emission for up to two years, and although the amount of material retained within the animal varies, the locations does not. Interestingly, the QDs show a blue-shifted signal (up to 40 nm) at two years from the injection as compared to the beginning. The phenomenon isn't observed in the animals sacrificed soon after injection, or in tissue that had been sacrificed early and frozen for up to two years. The effect could be due to a slow breakdown of the QDs, resulting in the release of toxic heavy metal ions. However, no acute toxicity was observed and the particles remained fluorescent for up to 2 years (Fitzpatrick et al., 2009). Moreover, commercially available QTacker 705 nontargeted QDs (QD705) injected intravenously into mice accumulate primarily within the liver, spleen, and kidney (Li et al., 2008). Also these type of PEGylated QDs don't show any evidence of excretion or metabolism within 28 days following dosing. After 6 months these NPs cause

significative renal toxicity in the treated but not control mice. Treated mice showed evidence of proximal tubular degeneration, with pronounced changes in mitochondria in the proximal convoluted tubules. In contrast, other studies have demonstrated efficient excretion of QDs in mice (Lin et al., 2008). In contrast to the results described above (Lin et al., 2008) the biodistribution and excretion paths of water-soluble hydroxyl group-modified silica coated CdSeS QDs, intravenously injected in mice is rapid via both faeces and urine, within 5 days following injection (Chen et al., 2008).

On the base of the data in literature it is possible to reach a generalisation regarding the preference of QDs for accumulation in certain target organs, like liver and spleen and in a minor quantity in kidneys, lungs, lymph nodes, bone marrow. In a very small amount as compared to the injected dose QDs are detected also in the brain (Yang et al., 2007). The migration to the liver and spleen is due to the clearance of QDs by phagocytic cells of the reticuloendothelial (RE) system, which suggest that QDs residing in organs have already been internalised by cells (Kennel in 2008).

When QDs are injected either subcutaneously (Zimmer et al., 2006; Robe et al., 2008), intradermally (Gopee et al., 2007) or directly into animal tumour tissues (Ballou et al., 2007), the pattern of organ deposition is different. Also the size of QDs can determine the biological fate: QDs with a size above a certain limit, have limited ability to migrate further into the lymphatic system or to extravasate from the vasculature (Zimmer in 2006).

Quantum Dots biodistribution in the brain

ICP-MS studies reveal that QDs after both systemic or intraperitoneal administration can enter in the brain (Akerman et al., 2002; Yang et al., 2007, Kato et al., 2010, Yeh et al., 2011). The biodistribution of QDs 636 nm with a captopropil cap in the brain is investigated by means of ICP-MS (Kato et al., 2010).

The brain is a challenging organ for molecules to enter because of the blood brain barrier (BBB), functioning as a controller, avoiding the entrance of exogenous substances. Six hours after intraperitoneal administration, 15% of the Cd remain in various organs including liver, spleen, kidney, brain and blood. In the brain, QDs are detected in the parenchyma and in the blood vessels. The relatively high concentration of Cd in the thalamus and brainstem as compared to the other regions might reflect the anatomical lack of BBB characteristic of these areas. Even if in a minor quantity, QDs accumulate also in olfactory bulbs, hippocampus and cortex .

There are different strategies for the NPs to cross the BBB. Small size QDs may be transferred through a space of 20 nm that separate the capillary endothelium to the astrocytes or interact with the receptors located at the BBB (Sigh and Nalwa, 2007). Another suggested route of entry into the brain is the retrograde axonal transport, which has been reported for the pathogenic mechanism of prion disease (Sigh and Nalwa, 2007).

When injected into the brain, QDs are taken up primarily and with high efficiency by microglia, whereas a small fraction (0.5%) can be found in neurons. In particular the QDs accumulate in lysosomes in the microglia and don't affect mitochondria. The presence of PEG coating decreases the activation of glial cell marker GFAP as compared to CdTe QDs (Maysinger et al, 2007). A recent publication used mixed primary cortical cultures to assess the internalisation pathway followed by QDs. The uptake of QDs by microglia cells is decreased by inhibitors of clathrin-dependent endocytosis, implicating the endosomal pathway as the major route of entry for QDs into microglia (Minami et al., 2012). Furthermore, the inhibition of mannose receptors and macrophage scavenger receptors blocked the uptake of QDs by microglia, indicating that QD uptake occurs also through microglia-specific receptor endocytosis. Moreover, QDs conjugated to the toxin saporin depleted microglia in mixed primary cortical cultures, protect neurons in this culture against amyloid beta-induced neurotoxicity (Minami et al., 2012).

Quantum Dots in the cell

ASTI is an efficient peptide for delivering QDs in living mammalian cells and shows functional and sequence similarity to G-protein-coupled galanin receptors in mammals. Functionalised QDs with ASTI mostly enter the cell by the enzyme phosphoinositide 3-kinase (PI3K) which is involved in the formation of clathrin-coated vesicles. The clathrin-mediated endocytosis is confirmed by colocalisation of QD560-labeled clathrin heavy-chain antibody and QD605-AST1. For a 10% the endocytosis was also galanin receptor-mediated (Anas et al., 2009).

QDs can induce acute and chronic toxicity to cells and organisms. Most of the studies relate the toxicity to the presence in the tissue of free heavy metals, like Cadmium and Selenium, that directly induce reactive oxygen species (ROS) production by mitochondria (Turrens JF, 2003; Lovric et al., 2005a; Ipe et al., 2005; Lovric et al., 2005b; Cho et al., 2007). In fact QDs affect mitochondrial membrane properties Li et al., 2011) and mitochondrial network fragmentation and disruption of mitochondrial membrane potential (Yan

et al., 2011). Moreover QDs alteration of miRNAs in NIH/3T3 cells with apoptosis-like death and increased p53 protein levels and its post-translational modification by phosphorylation at Ser-15 (Li et al., 2011), DNA damage and generation of DNA adduct, after *per os* administration in mice (Khalil et al., 2011) and in human umbilical vein endothelial cells, in a dose-dependent manner (Zhang et al., 2010).

Once they enter the cell via diffusion throughout plasma membrane or internalisation, they can interact with cellular structures, homeostasis, signal transduction, DNA repair, apoptosis and oxidative mechanism (Fig. 10). CdSe QDs induce a significant reduction in the rates of oocyte maturation, fertilisation, and *in vitro* embryo development (Hsieh et al., 2009). CdSe/CdS capped with 3-mercaptopropionic acid or polyethylene glycol or SiO2 may be transferred from female mice to their foetuses across the placental barrier. The smaller QDs are more easily transferred across the placenta than larger QDs and the number of QDs transferred increases with increasing dosage (Chu et al., 2010). At doses of 3,600 and 720 pmol/mouse, QDs caused marked vascular thrombosis in the pulmonary circulation, most likely by activating the coagulation cascade via contact activation. Moreover, carboxyl-QDs and amine-QDs enhanced adenosine-5′-diphosphate–induced platelet aggregation (Geys et al., 2008).

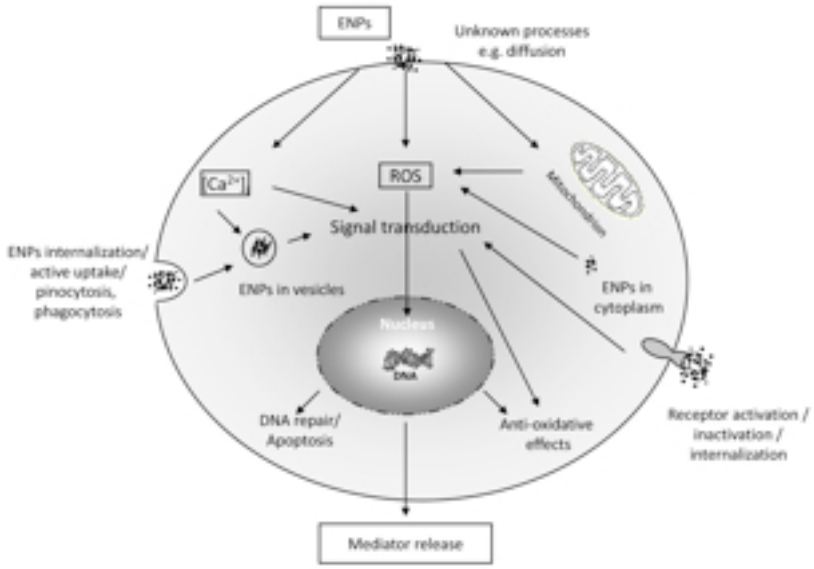

Fig. 10. Various way for uptake of ENPs to mammalian cells and the effect nanopaticles can have on intracellular processes (Simkò and Mattsson, 2010).

The toxicity of QDs and the capping materials is an issue that has to be considered before any application in biomedicine. Several groups in capping materials such as mercaptoacetic acid and tri-*n*-octylphosphine oxide (TOPO) are reactive to the cell and can produce toxicity to cells (Smith et al., 2008).

At the moment all the data don't show any Cadmium based QDs with a possible clinical application. New generation of fluorescent NPs without heavy metals and with coating adapted for the excretion can be the alternative. To reduce the cytotoxicity of QDs, replacement of the cadmium by nontoxic or less-toxic metals such as Indium (In), or encapsulation of the core with a biocompatibile shell or designing them as small as possible, thus facilitating their clearance from the body(Smith et al., 2008) should be considered. In-based semiconducting dots contain Arsenic, have an acceptably low cytotoxicity.

Phagocytosis and uptake of nanoparticles

After systemic administration, or inhalation, NPs are sequestered by RE system by means of phagocytic mechanism. The organs where NPs mostly accumulate are liver, spleen and lung (refer to the follow paragraph) where the macrophages have different names according to the organs where they are: alveolar macrophages (lung), splenic macrophages (spleen) and Kupfer cells (liver).

The phagocytosis of a molecule is a process where a molecule is internalised, by means of engulfment in vesicles, into a macrophage or a non professional phagocyte. The phagocytosis mechanism involves the interaction between macrophages membrane receptors and specific "presenting" ligands that recognise the NPs and, by a mechanism called opsonisation, they label the exogenous molecule as non-self, facilitating the particles internalisation in the macrophages (Aderem and Underhill, 1999). The opsonisation molecules are antibodies or complement molecules (e.g. complement protein 5a and IgM). Hydrophobic or charged molecules are quickly recognised by opsonisation molecules and internalised (Kelf et al., 2010), while the presence of hydrophilic coatings like PEG diminishing the opsonisation process, decreasing the possibility of phagocytosis from macrophages and other non specialised cells (Palecanda and Kobzik, 2000, Kelf et al., 2010).

The opsonisation mechanism is initialised by different mechanisms involving the complement protein 5a that act as a chemotactic molecule (Oberdorster et al., 2005), the electric charge of the NPs (Kobzik, 1995) or the toll-like receptor that recognise non-self molecules and organisms (Inoue et al., 2006). After the interaction between macrophages and opsonising ligands, the particle is internalised by the formation of a phagocyte vesicle or phagosome (Park, 2003), than successively, becomes a phagolysosomes, internalising digestive enzymes. The presence of PEG on the particle surface reduces the internalisation

(Kelf et al., 2010) while the absence of PEG and the charge on the surface promote the internalisation into the cells (Kelf et al., 2010).

The inflammatory response is increased by the release of chemical messengers for the recruitment of other inflammatory cells by macrophages. The digestive process in the phagolysosomes involves proteases, nicotinamine adenine dinucleotide phospate (NADPH) oxidase that produces oxygen radicals (Park, 2003). After digestion the residues are removed by exocytosis. The phagocytosis process, generally, lasts several hours. In the case of NPs, thanks to their small size and the presence of heavy metals, it is difficult for a macrophage to stop and digest particles of few nanometers (Takenaka et al., 2001). The efficiency of macrophages is higher with a cell size material (13-20um) than NPs, and the clearance is much quicker. In fact, the administration of high doses of NPs result in a better clearance from macrophages in the lungs and other organs than low doses. The reason is the final size: when the concentration is high, the NPs tend to form aggregates that results in a bigger size as compared to the single NP. Macrophages can stop easier aggregate of NP, while the single NP accumulates for longer period in organs and circulatory system. The NP that can not be digested results in a longer inflammatory response. When the phagolysosome can not digest the NPs, the continuing production of ROS damage the phagosome membranes, that release the reactive species in the cytosol of the macrophage. The ROS lead to impairment of cell motility and functions, and subsequently, cell death. The death of the macrophage releases the reactive species outside, recruiting other macrophages that can't digest the NPs as well. These inflammatory response create a source of reactive species and macrophages debris accumulation that can induce a long term inflammation (Oberdorster et al., 1994). In the brain the increase of oxidative stress caused by this mechanism can be associated with diseases like neurodegerative deseases (Bondy, 2011).

This can be the reason why in the brain it is difficult to see an immediate inflammatory response after systemic injection. The concentration is too low to be seen by microglia. Only after intracortical injection there is an immediate inflammatory response in terms of GFAP induction and microglia activation (Maysinger et al., 2007).

Non stopped NPs that stay in the circulatory system are more likely to enter non phagocytic cells, like endothelial cells, epithelial cells (Hopwood et al., 1995), red blood cells, platelets (Nemmer et al., 2002) and nervous cells (Oberdorster et al., 2002).

The entrance does not produce any vesicle, and the NPs can accumulate both in the cytoplasm, or nucleus and interact with different structures of the cell. The uptake of the cell is assumed to be a passive uptake or adhesive interaction (Geiser et al., 2005).

RESULTS AND DISCUSSION

Qtracker® 800 QDs characterisation

The QDs tested in our experiments are the Qtracker® 800 non targeted QDs from Invitrogen (QDs 800) (Cat. Q21071MP). Their core is made up of a few hundred to a few thousand atoms of a semiconductor material (CaSeTe). The ICP-MS analysis of a QDs 800 solution reveals that for 33 atoms of Cadmium (Cd) there are 11,43 atoms of Selenium (Se) and 1 atom of Tellurium (Te). The core is surrounded by a semiconductor shell of Zinc sulfide (ZnS) which stabilises the core, improving both the optical and physical properties of the material. An amphiphilic polymer encases the core and the shell, providing an hydrophilic surface and a substrate for functionalisation with peptides and antibodies to create targeting QDs 800 nanocrystals.

This amphiphilic inner coating is covalently modified with a polyethylene glycol (PEG) outer coating that, in our case, is not functionalised (Fig. 11 Bottom). The PEG surface improves signal-to-noise ratios and provides a clearer resolution of cell populations and cellular morphology. Moreover, it reduces opsonisation, extending the circulation time of the NPs in the blood (Peracchia et al., 1999). PEG has been approved from FDA and has a lot of applications in the polymer based drug delivery (Knop et al., 2010).

The composition of the core is important for the emission wavelength. They are the biggest type of QDs produced by Invitrogen, with NIR emission wavelength, 750-800nm. Non targeted QDs 800 are designed for *in vivo* imaging, for studying vascular structure after injection. These nanocrystals exhibit intense fluorescence, red-shifted emission that permits to increase tissue penetration, and the PEG surface coating minimises any immune response by the tissue, and the cell uptake. The PEG surface coating is not modified with reactive functional groups, permitting the QDs 800 to be retained in circulation for at least 3 h and to be imaged for up to 3 months without additional injections (Invitrogen data sheet).

We analyse the particle size and morphology by TEM. The particle size in water suspension is 8,27 ± 1,27 nm.

The hydrodynamic size, measured with Malvern Nano Zs instrument with a 633 nm laser diode, is 36nm (Rampazzo et al., 2011). The morphology of the NPs is shown in Fig. 11 Top.

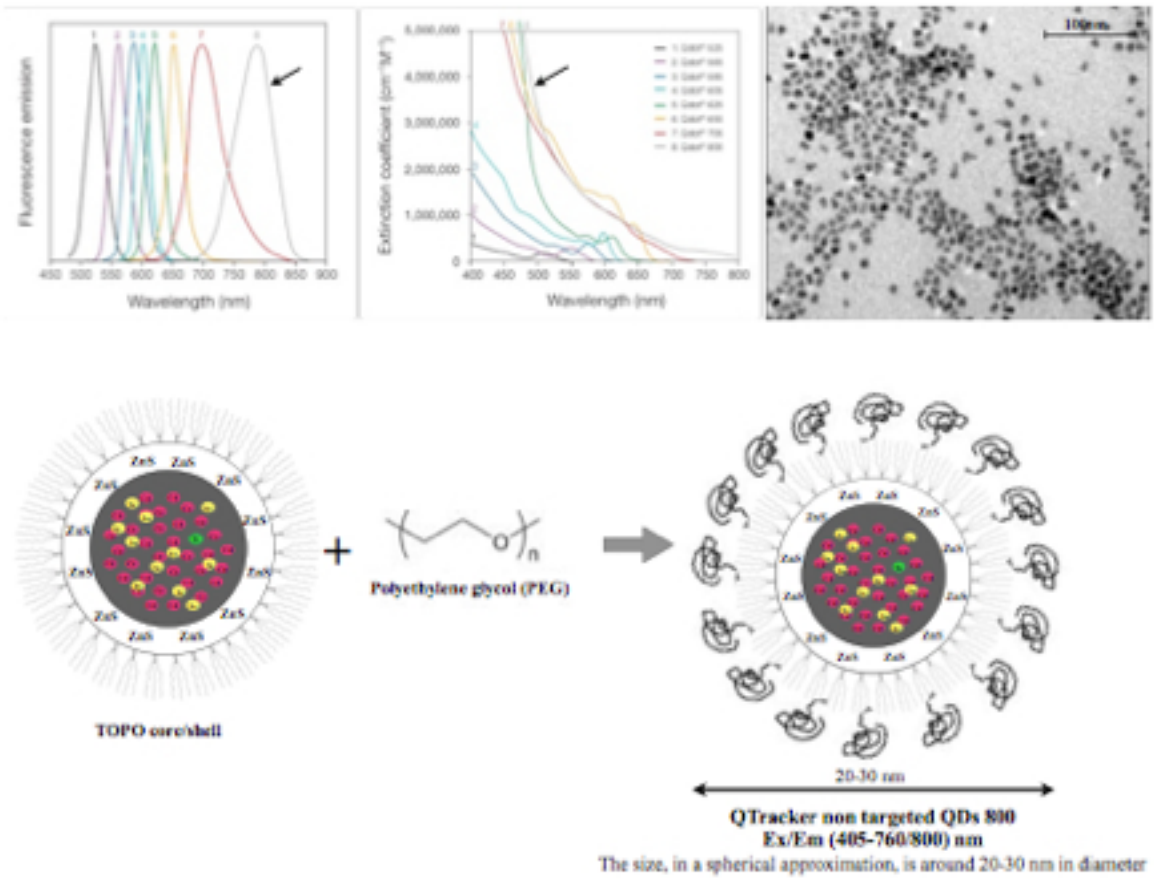

Fig. 11. Top: Characteristics of QDs® 800: the two graphs on the left indicate the absorption and emission spectra of different type of QDs. We excited the QDs® 800 at 405nm and the emission wavelength was collected at 750-850nm. On the right hand side a TEM image of QDs® 800 morphology and the measure of the electron dense part of the NPs (nm). **Bottom**: Schematic representation of non target QDs® 800.

Comparative body retentions and tissue distributions of QTracker® 800 QDs in mice

The biodistribution analysis of QDs 800 in mice, after i.v. injection, is performed using different imaging techniques (e.g. optical imaging, electron microscopy, confocal microscopy etc). The systemic administration mimics the human route of exposure.

The optical imager allows to detect NIR fluorescence in *in vivo* and *ex vivo* systems. The QDs 800 excitation and emission wavelengths can penetrate in the tissue within 1 cm depth, giving higher fluorescence intensity and more specific QDs localisation in small animals. The instrument is equipped with different filters which discriminate the NIR

emission. At 800 nm there are no interference from water or haemoglobin of the tissue, maximising the signal/background in the experimental animals (Weissleder, 2001).

Firstly we follow the kinetic of biodistribution of QDs 800 *in vivo* for 3h after the injection. *In vivo* images just after the injection reveal a significative increase of signal as compared to background, measured in the pre-injection images. Region Of Interest (ROI) are traced manually on the planar images where fluorescence builds up: in the anatomical regions of lung, liver and spleen and brain (Fig. 14A). The average efficiency (fraction of fluorescent photons relative to the number of incident excitation photons) of the ROIs is represented with the standard error mean (SEM) in Fig. 12.

Measurements of the total flux (p/s) emitted from the extracted organs after perfusion with PBS with SEM are reported in Fig. 13. Using Cy5.5 filter, QDs 800 show a significantly higher ($p<0,05$, paired Student's *t*-test) fluorescent signal as compared to controls in all organs analysed at 3 h. The fluorescence is particularly high in the liver.

The data are confirmed with ICP-MS analysis that quantifies the amount of heavy metals (Cd, Se and Te) in the organs and tissues and electron microscopy that discriminates the cells and structures of accumulation.

Cd is the major core material of QDs and is not detectable in physiological conditions keeping the background noise virtually to zero. We estimate QDs quantity on the basis of the amount of Cd measured in the organs.

The QDs800 biodistribution is investigated at 24h after the i.v. injection, where the acute response occurs, and at longer time points, 1, 2 and 3 weeks.

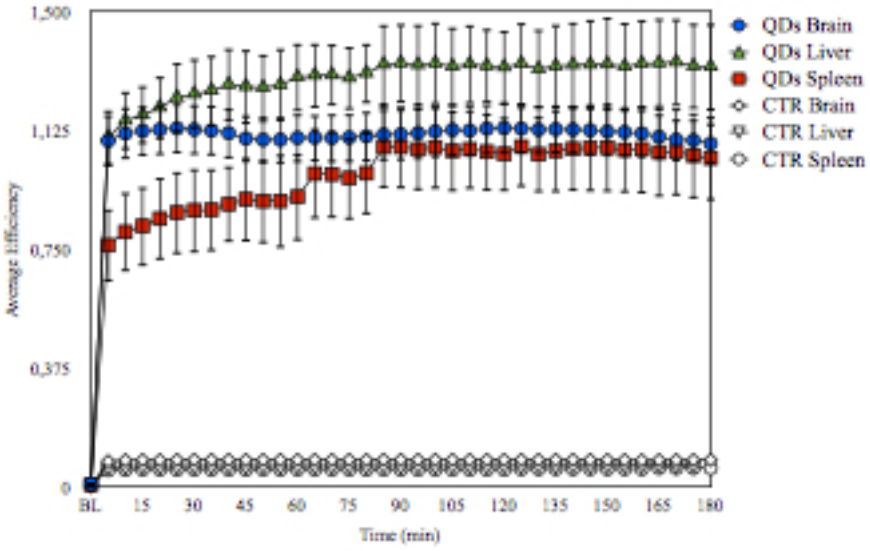

Fig. 12. Kinetic of biodistribution of fluorescence during 3 h after the injection. The average efficiency for ROIs is measured in different regions before and after the injection. The black triangles, circles and squares are the pre and post treatment of controls animals while the coloured triangles , circles and squares are respectively the pre and post treatment of QDs 800 animals.

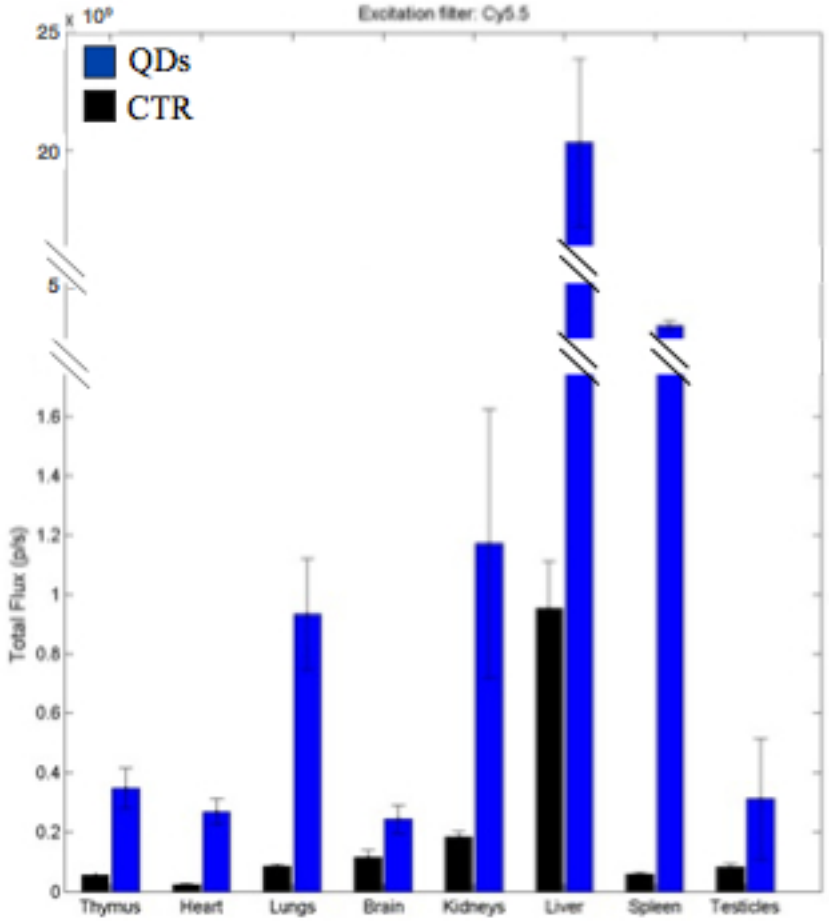

Fig. 13. Quantification of the fluorescence signal (in photon counts/second) from QDs in various extracted organs of animals treated with QDs and saline and imaged with Cy5.5 filter. The bars represent averages ± SEM (N = 3).

The serum clearance, assessed with ICP-MS at 1, 2 and 3 weeks reveals Cd concentrations (± SEM) of 0,2435 ± 0,068; 0,0075 ± 0,0005 and 0,013 ± 0,0019 µg/ml at 1, 2, 3 weeks respectively. Cd concentration decreases after 1 week, as reported also for other type of QDs (Yang et al., 2007; Lin et al., 2008), but doesn't reach the control levels at longer time points. The Cd concentrations in treated animals are statistically different at all time points as compared to controls ($p<0,001$, two ways ANOVA test). Non specific binding of QDs to cellular blood components (e.g. erythrocytes) is detected with TEM analysis.

Red blood cell do not have phagocytic ability, and the uptake of QDs depends only on the small size of the NPs (Peters et al., 2006). The charge, instead, determines the uptake by platelets. NPs influence the formation of blood clot (Nemmar et al., 2002): QDs 800 interact with plasmic proteins and in particular with fibrinogen (Pozzi-Mucelli et al., 2009).

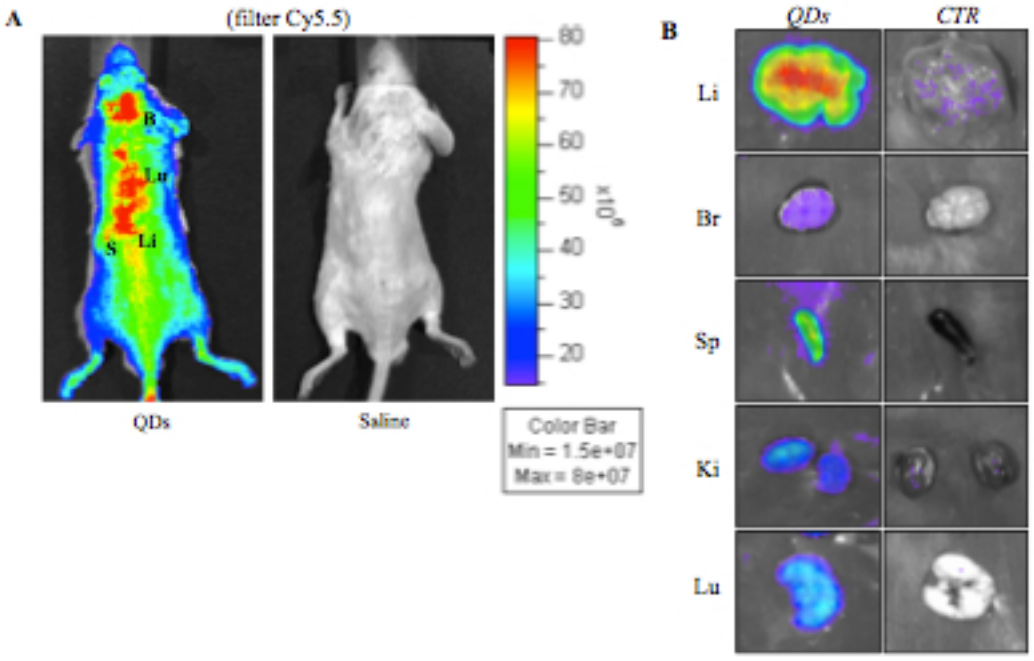

Fig. 14. A) *In vivo* average efficiency at 3h after injection in treated and control animals. B=brain; Li=liver; Lu=lungs; S=spleen. **B)** *ex vivo* images after PBS perfusion, imaged with Cy5.5 filter. Li=liver; Br=brain; Sp=spleen; Ki=kidneys; Lu=lungs.

The levels of Cd in all organs are significantly higher than controls, at all time points analysed ($p<0,001$ two ways ANOVA test) (Tab. 4).

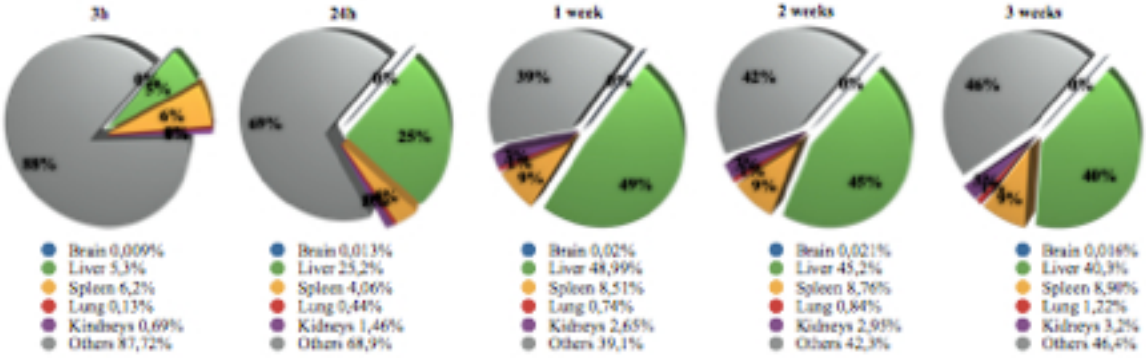

Fig. 15. Amount of Cd in different organs expressed as percentage of the injected dose at 3h, 24 h, 1, 2 and 3 weeks after the iv injection.

Cd concentrations (ng Cd/mg organ wet weight)					
Time points/ Organs	**Liver**	**Spleen**	**Lung**	**Kidneys**	**Brain**
Baseline / Controls	n.d.	n.d.	n.d.	n.d.	n.d.
3h	2,384 ± 0,81	32,443 ± 7,36	0,329 ± 0,05	0,848 ± 0,26	0,011 ± 0,002
24h	11,314 ±1,415	21,431 ± 1,206	1,096 ± 0,336	1,799 ± 0,035	0,015 ± 0,001
1 week	22,036 ± 1,165	44,877 ± 2,784	1,847 ± 0,152	3,272 ± 0,214	0,023 ± 0,004
2 weeks	20,311 ± 1,699	46,183 ± 5,882	2,101 ± 0,433	3,649 ± 0,331	0,024 ± 0,004
3 weeks	18,106 ± 2,686	46,913 ± 7,657	3,05 ± 0,809	4,002 ± 0,552	0,019 ± 0,003

Tab. 4. Concentration of Cd in each organ (ng of Cd / mg organ wet weight). Data represent QDs treated animal organs before (baseline) and after i.v. injection. Average ± St.Dev.

Already at 3 h, part of the QDs leave the bloodstream and accumulate respectively 6% of the injected dose in the spleen, and 5% in the liver. The 0,1% is found in the lung, the 0,7% in the kidneys while only the 0,01% of the injected dose is found in the brain (Fig. 15). No changes in organ weights are revealed during the 3 weeks of exposure ($p>0,05$ two ways ANOVA test). The Cd levels detected in tissues from control mice are negligible, below 0,001 ng Cd/mg wet tissue. This is expected, as Cd has no known biological function, and laboratory mice are not exposed to typical sources of Cd. We compare the QDs treated animals to saline animals because the vehicle controls, which consisted of suspension buffer with the QDs removed, yielded insignificant levels of Cd and behave similarly to saline group.

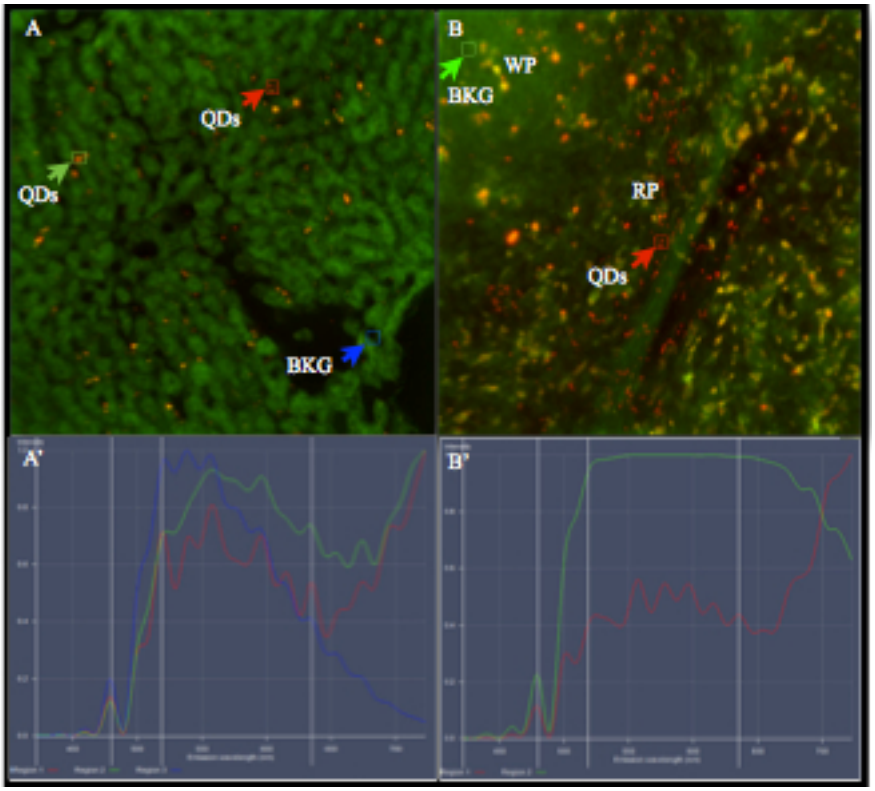

Fig. 16. Fluorescence images of QDs at 3 weeks after injection with simultaneously analysed emission spectra profile in liver **A)** and **A')** and spleen **B)** and **B')** (20x magnification lens). In the images, ROI are placed on the particles (red and green arrows in A' and red arrow in B') and on the background (blu arrow in A' and green arrow in B').

The organ with the highest Cd concentration is the spleen (and therefore the maximum QDs accumulation). In terms of percentage of the injected dose, principally QDs accumulate in the liver, since it is a bigger organ. The spleen is the most probable cause of the presence of Cd in the blood after 2 and 3 weeks. We believe that the spleen behaves like a "sponge", absorbing blood full of QDs immediately after the injection and continuing to release the NPs in time, e.g. by inflammatory cells, red blood cells and platelets as carriers.

It is also possible that inflammatory cells transport QDs from the spleen to the brain, increasing the Cd concentration in the brain over time. The amount of NPs accumulated in each organ reflects the different absorption properties. Heavy metals concentration is high in all organs throughout all time points, suggesting a biological half-life in the scale of weeks or months for QDs in rodents and possibly humans.

The fluorescence microscopy is used as an additional method for detecting QDs. It confirms the presence of fluorescence at 3 weeks in liver and spleen. A closer analysis of the fluorescence images shows localisation of QDs at the edges of the liver sinusoid. Lambda scan reveals the typical peak of emission of QDs, which differs from the background (Fig. 16).

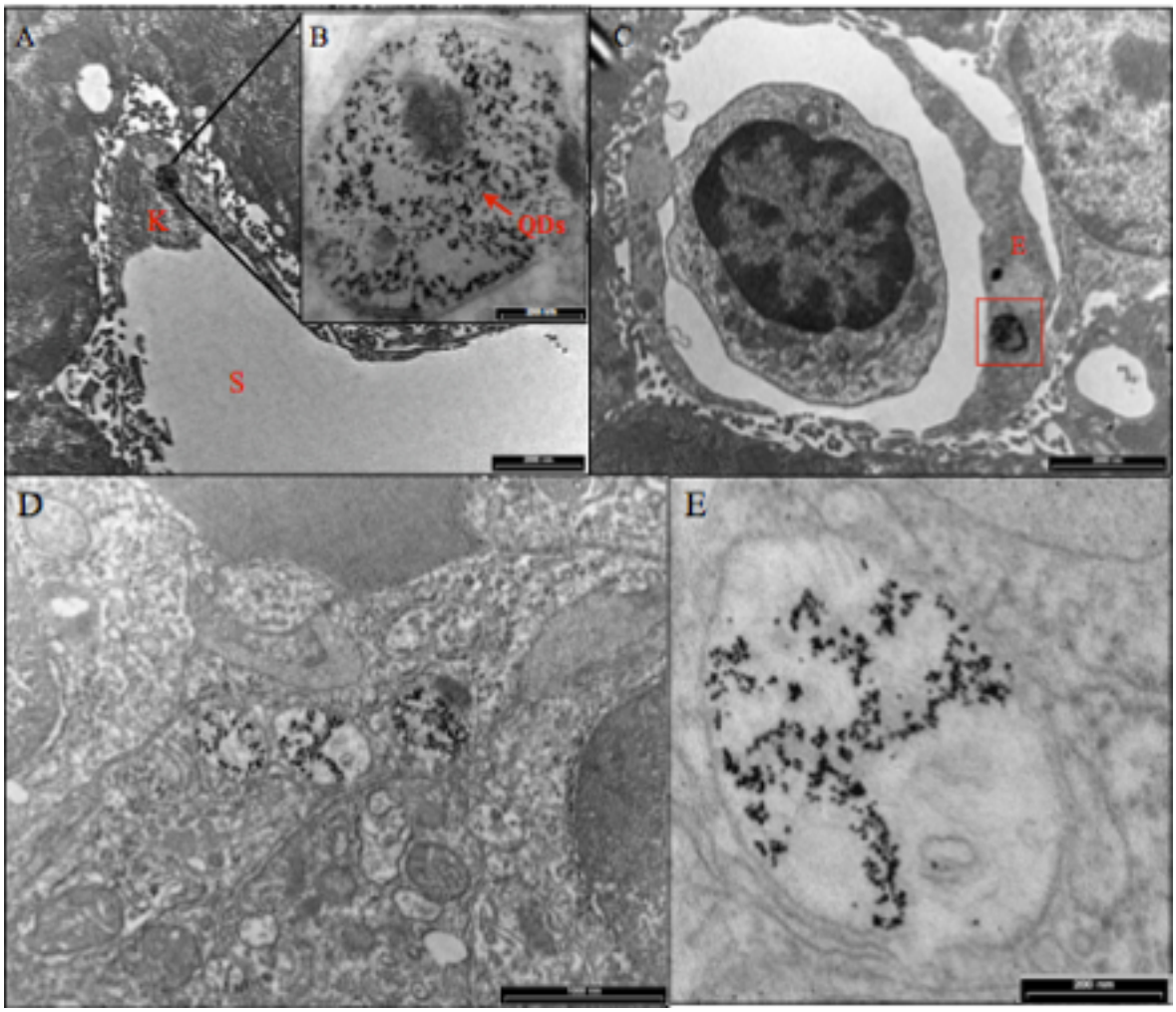

Fig. 17. TEM images. **A** and **B)** QDs in Kupffer cell (K) at the boundary of the hepatic sinusoid (S) and sequestration in phagolysosome. **C)** QDs are sequestrated in vesicles in endothelial cells (E). **D)** and **E)** QDs in a histiocytes and sequestration in lysosomes in the red pulp.

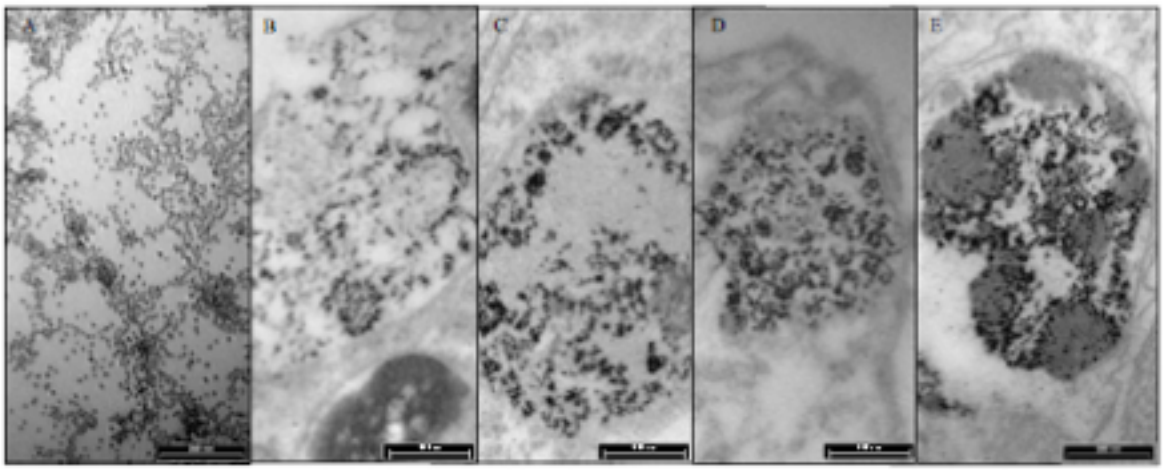

Fig. 18. QDs at the different time points. A) QDs on a grid before being injected, from B) to E) at 24h, 1 week, 2 weeks and 3 weeks.

The electron microscopy images show that at all time points spleen and liver macrophages (histiocytes and Kupffer cells) and endothelial cells take up the QDs. The QDs seem to enter the cells via phagocytic process and endocytosis. In fact they are entrapped in phagolysosomes in both Kupffer cells and histiocytes (Fig. 17). The Kupffer cell can be identified by its active phagocytic morphology, with many phagolysosomes in the cytosol, and location within the sinusoid. No QDs are found in the hepatocytes. In the spleen, QDs are mostly sequestered in phagosomes in the macrophages of the red pulp (Fig. 17 D and E). The morphology of QDs changes depending on the accumulation site: in the lysosomes they are smaller and less defined as compared to the vesicles in the endothelial cells. The digestive chemicals of phagocytic cells, hydrochloride acid and hydrogen peroxide, can cause considerable QDs degradation after 1week of incubation, and zinc leaches early in the phagocytic degradation process since it is located in the external shell of the QDs (Mancini et al., 2008).

This hypothesis is confirmed by the fact that the diameter of the QDs, measured with TEM, becomes smaller over the time: 8,2 ± 1,87 nm (mean ± SEM, on the grid), 7,96 ± 2,17 nm (mean ± SEM, after 24 h), 6,71 ± 1,39 (mean ± SEM, after 1 week).

An increasing amount of Cd in the kidneys after 2 and 3 weeks is detected with ICP-MS (Tab. 4). The liver is detoxifying the body, digesting and biotransforming QDs in order to excrete them thought the kidneys. As reported in literature, QDs, are not likely to be digested and excreted by kidneys: after 6 months they are still accumulated in the kidneys causing proximal tubular degeneration with changes in mitochondria in many convoluted tubules (Lin et al., 2008, with QDs similar to the QDs 800 used in our experiments). We can expect a similar renal toxicity. Choi and colleagues in 2007 demonstrated that QDs

can't be renally cleared unless they are less than 5.5 nm in diameter. The QDs used in these experiments have an organic coating that increases hydrodynamic diameter to 36 nm, possibly preventing renal excretion. Further experiments are needed to elucidate the effect and accumulation of QDs over longer time on kidneys.

The ratios between the elements Cd, Se and Te over time compared to the ratios in the injected solution is different (data not shown). One possible explanation for the difference in heavy metal ratios is the leaching of Cd, Se, Te and Zn ions from the NPs, an evidence already reported in literature (Lovric et al., 2004; Kirchner et al., 2005; Maysinger et al., 2007).

PEGylated QDs, BSA coated QDs and polymer QDs behave quite similarly (Hauck et al., 2010).

PEG immunohistochemistry reveals the persistence of the external coating on the QDs over time. The Fig. 19 shows the amount of PEG staining in liver and spleen over time. Considering the difference in staining amount over the background, it seems that there is a reduction of PEG at 2 and 3 weeks as compared to 24h in both liver and spleen. The staining quantification with light microscopy is still on going.

and location within the sinusoid. No QDs are found in the hepatocytes.

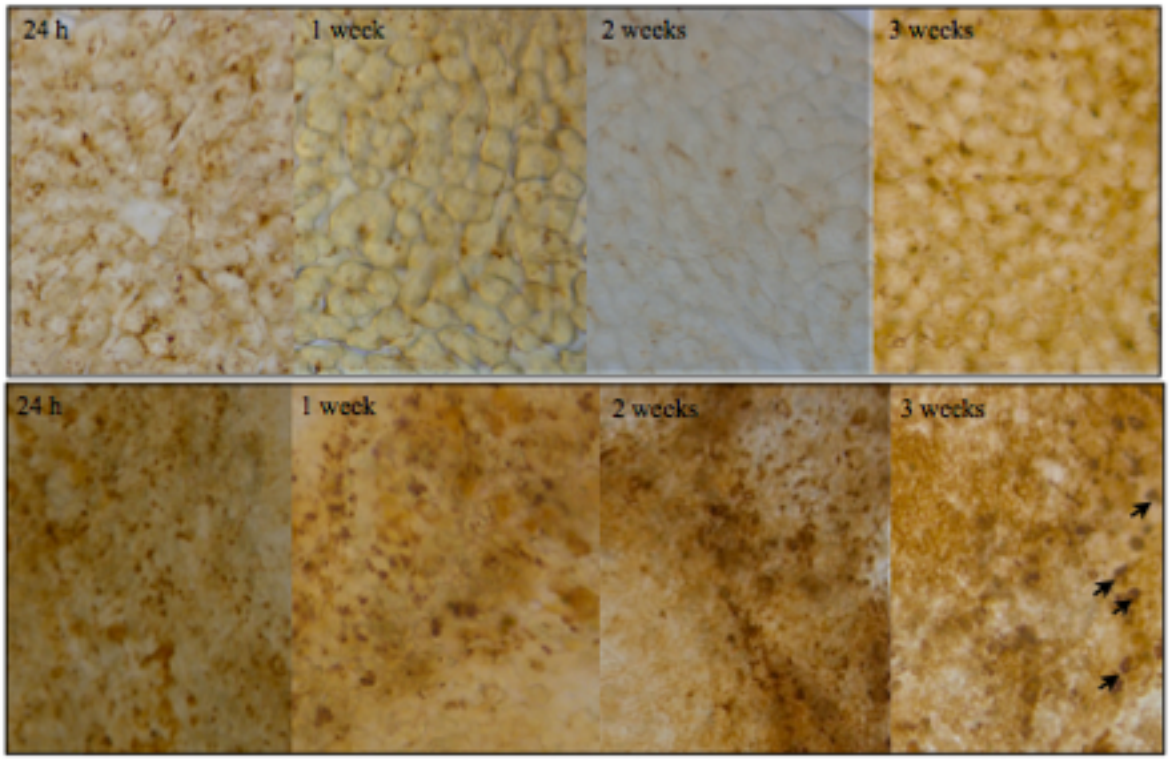

Fig. 19. PEG staining. **Top:** Liver at different time points and acquisition with a 20x magnification. **Bottom:** Spleen with 20x and 10x magnification lenses at all time points. The arrows indicate the unspecific signal given by mast cells in the spleen.

Referring to the brain, the contents of Cd, illustrated in Tab. 4, is significative higher as compared to controls ($p < 0,01$, two ways ANOVA test) at all time points

The electron microscopy reveals the presence of the nanoparticles in the somatosensory cortex in epithelial cells, neurons and glia, accumulated both in cytosol and nucleus. The NPs are not sequestrated by specific structures, but they form small aggregates that interact with cell structures like mitochondria, myelin sheath, synapses, chromatin etc. (Fig. 20). In hippocampus and thalamus no QDs aggregates are found, probably due to the lower concentration of QDs in these specific regions and to the technique, the electron microscopy, which allows to look only at a very small area.

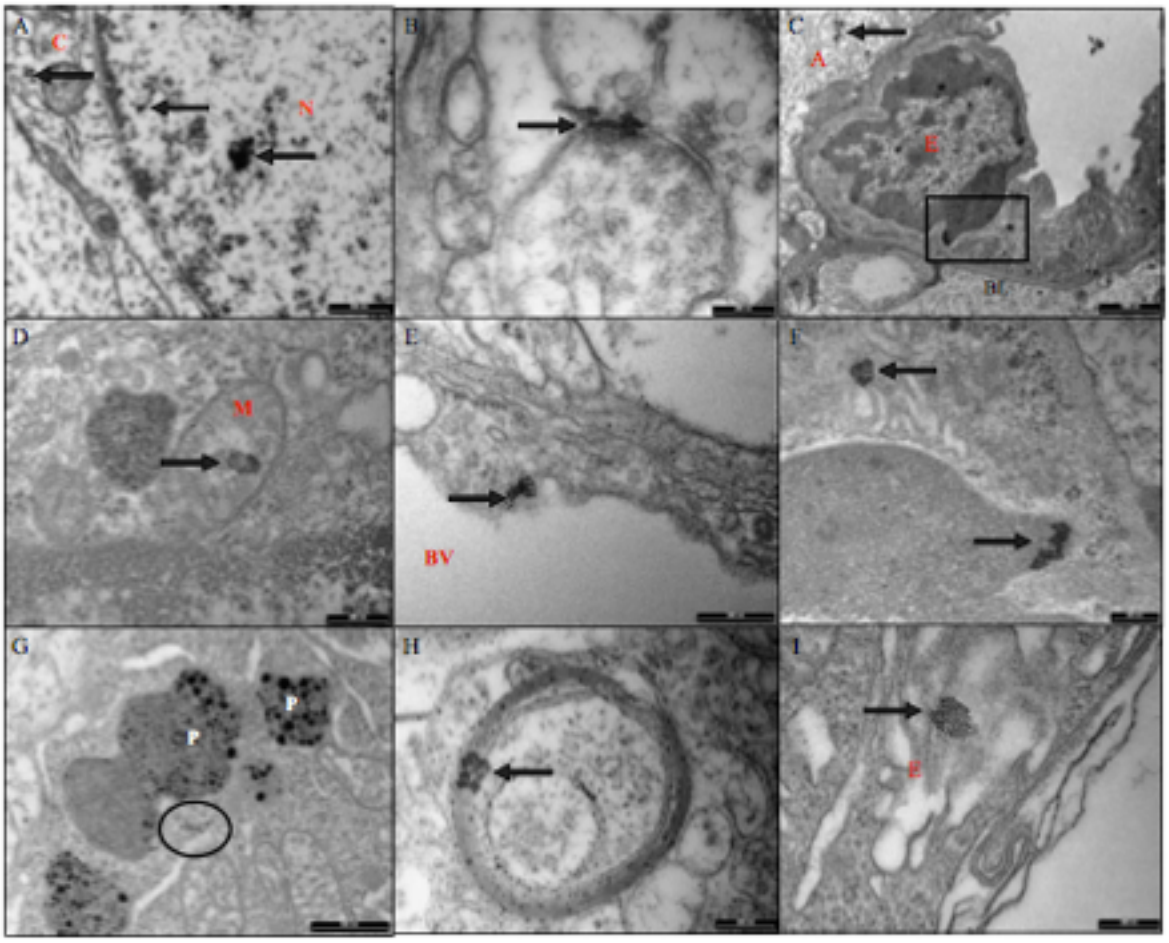

Fig. 20. TEM images of cerebral cortex slices at 1 week. **A)** QDs in the nucleus (N) and cytosol (C) of a neuron. **B)** QDs in a synaptic bouton. **C)** QDs are sequestered by endothelial cells (E) and are localised in the nucleus and in the cytosol. An aggregate is localised outside the endothelial cell probably in the cytosol of an astrocyte (A), BL=basal lamina. **D)** QDs in a mitochondria (M). **E)** QDs are crossing BBB, BV=blood vessel. **F)** Enlargement of image C). **G)** QDs in the cytosol of a microglial cell, indicated by the circle. Lysosomes (P) containing ingested materials and some QDs. **H)** QDs on myelin sheath. **I)** QDs in an epithelial cell. Arrows indicates the aggregates of QDs.

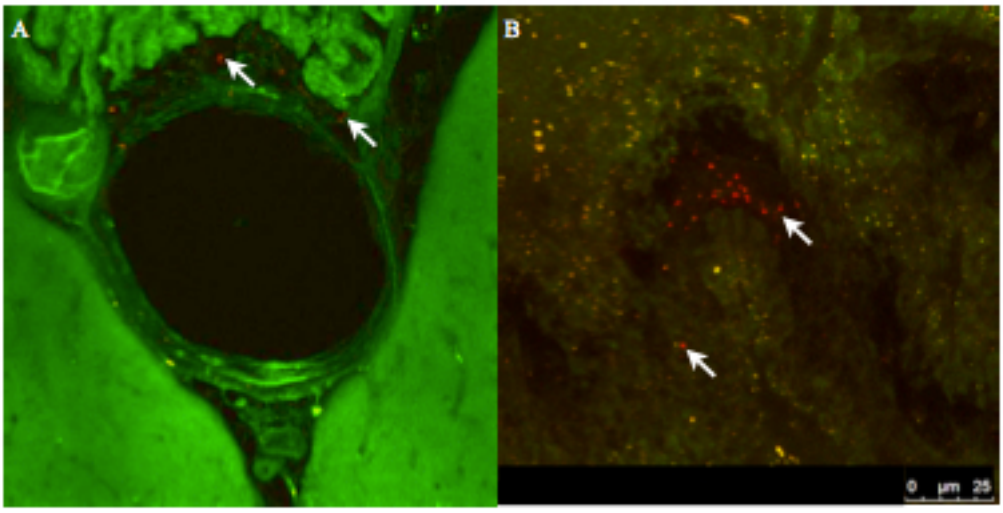

Fig. 21. Confocal images of central (A) and lateral (B) ventricles at 3 weeks after treatment with QDs. The red dots indicated by the arrows are the 800nm emitting QDs. Acquisition with 20x magnification lens.

At 3 weeks after the treatment the nanoparticles are only found in the ventricles (Fig. 21). At the same time point the PEG is detected around blood vessels and in the parenchyma, in the anatomical structures around the ventricles (Fig. 22).

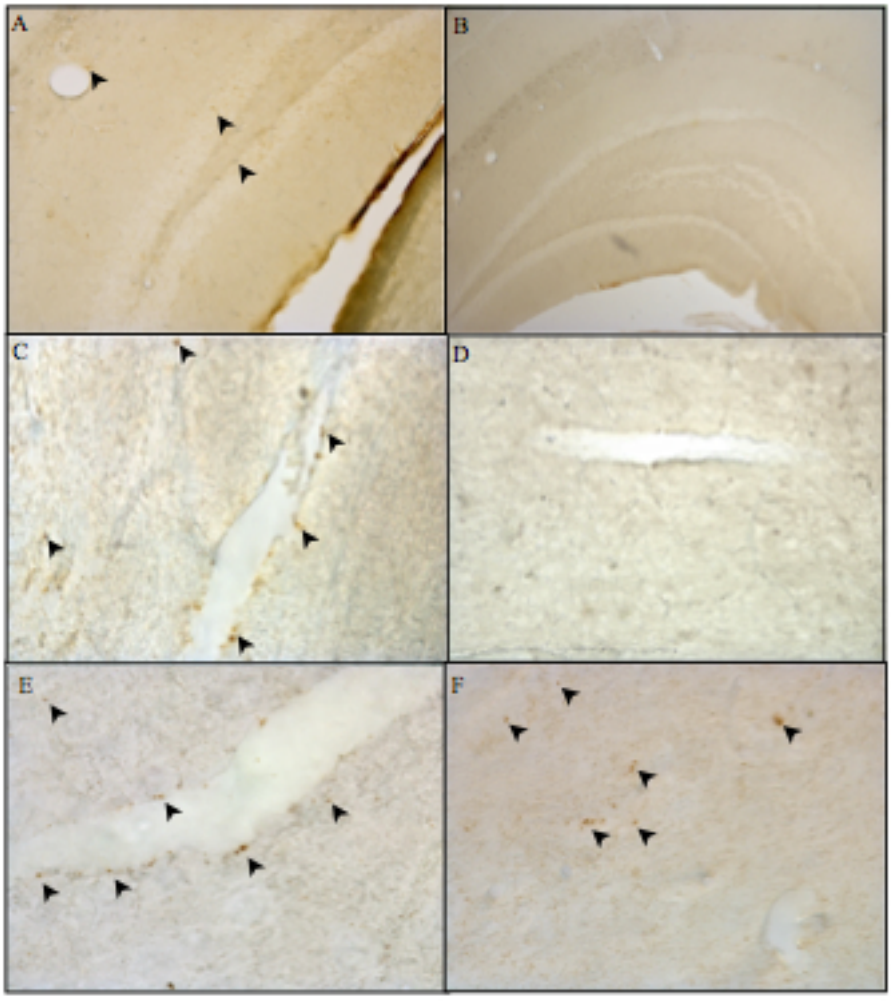

Fig. 22. PEG staining of different brain areas. **A)** Hippocampal section from a treated animal sacrificed after 2 weeks from injection. The staining is on and around dentate gyrus cellular layer (4x magnification lens). **B)** Hippocampal section from a control animal sacrificed after 2 weeks (4x magnification lens). **C)** Section of somatosensory cortex of a treated animal after 2 weeks from the injection (60x magnification lens). **D)** Section of cortex of a control animal (20x magnification lens). **E)** Cortex of a treated animal at 1 week (60x magnification lens). **F)** Cortex of treated animal at 3 weeks (60x magnification lens).

Discussion

Our observations have the following implications: **a)** the visualisation of red fluorescence (Fig. 16 and 21) suggests aggregation of a large number of QDs nanocrystals *in situ* because fluorescence from only a few particles would be undetectable; **b)** a major mechanism of distribution of QDs involves mononuclear phagocytic system in many organs; **c)** at low concentration QDs enter the brain, and after 1 week they are not stooped and sequestered by microglia. An early inflammatory response is elicited only after intracortical injection (Maysinger et al., 2007).

The lack of an immediate inflammatory response in the brain is probably due to:

a) after systemic injection, a lower amount of nanoparticles reaches the brain as compared to the amount after an intracortical injection, and they are not immediately seen by the immune system, or **b)** the PEG coating decreases the opsonisation process and minimises the recognition by the mononuclear phagocytic system in the brain (Akerman et al., 2002), or **c)** the size of the QDs is too small to be phagocytized in the first instance by microglia (Oberdorster et al., 1994).

Our results of biodistribution are confirmed by literature (Yang et al., 2007; Lin et al., 2008, Tiwari et al., 2011, Sui et al., 2011, Yeh et al., 2011).

Even if the amount in the single organs is different, which may reflect differences in the type of QDs used and in the dose and the analysed time course, we confirm that the highest Cd concentration is in the spleen, followed by the liver and the kidneys. The reticuloendothelial system in liver and spleen is the major cleanup site of nanoparticles via uptake by mononuclear phagocytes, Kupffer cells in liver and histiocytes in the spleen. Macrophages are diffused in the connective tissue and in liver (Kupffer cells), spleen and lymph nodes (sinus histiocytes), lungs (alveolar macrophages), and central nervous system (microglia). In the spleen macrophages remove senescent erythrocytes, leukocytes, and megakaryocytes by phagocytosis and digestion. It is possible that QDs accumulate in a significant amount in lymph node as well, since they represent the organ of the immune system. All these data haven't been confirmed yet.

Commercial QDs 705 from Invitrogen show a plasma clearance in about a week with a return to background level at longer time points (Yang et al., 2007). QDs 800 behave differently, decreasing after one week but still continuing to circulate in the blood stream at 2 and 3 weeks after the injection. These two types of QDs are very similar, and the difference

is only in emission wavelength and core composition. Among the possibilities, a different sensitivity of the ICP-MS instruments, can be the explanation of the different results.

About 0.1% of the QDs in the body, accumulate in the brain, after both i.v. and i.p. administration (Yang et al., 2007; Kato et al., 2010). The blood brain barrier (BBB) plays an important role in the homeostasis and as a defencing mechanism. The endothelial cells and the tight junctions form a physical barrier for exogenous compounds.

There are many hypothesis of how QDs and in general NPs cross the BBB. QDs can cross BBB through the 20nm gap between astrocytic foot processes and the capillary endothelium, or through receptors located at the BBB (Kato et al., 2010). Another possibility is that QDs induce inflammatory response which increases the permeability of the BBB facilitating their entrance. ROS production is another well known effect after QDs treatment (Tang et al., 2010; Kim et al., 2011; Liu et al., 2011; Yan et al., 2011).

We find QDs 800 at 3 weeks from the injection in the ependymal cells of the choroid plexus. Other PEGylated NPs after 24h from systemic injection are found in choroid plexus and in the epithelial cell of the pial surface (Calvo et al., 2001) and the authors attribute the retention of the particles by the choroid plexuses as “the logical consequence of the function of this tissue as a producer of cerebrospinal fluid”. The possible mechanisms of entrance of NPs in the CSF crossing blood-CSF barrier, are diffusion and active transport (Bhaskar et al., 2010).

Colloidal polymer particles, coated with polysorbate 80, are found in the brain parenchyma as well, supporting the view that many type of NPs can cross BBB (Kreuter et al., 1995).

The presence of Cd and Se in the brain can induce directly ROS production that increases BBB permeability. It seems that also mitochondria are the major sources of ROS production in most mammalian cells (Turrens et al., 2003), and their ROS production increases in many pathological conditions and is associated with mitochondrial dysfunction (Newsholme et al., 2007; Swerdlow, 2007). A mitochondrial toxin, the 3-nitropropionic acid (3-NP), disrupts the mitochondrial electron transport chain, causing an elevation of ROS generation, thereby triggering events such as MMP-9 induction that eventually leads to BBB opening (Kim et al., 2003). Another study shows QDs toxicity on mitochondria in human umbilical vein endothelial cells: CdTe QDs elicited significant oxidative stress, mitochondrial network fragmentation, as well as disruption of mitochondrial membrane potential. The effect is reversed with ROS scavenger (Yan et al., 2011). Also Vieira and col-

leagues in 2011 report mitochondria toxicity in a T. Cruzi protozoa model. The mitochondria impairment can affect BBB permeability by ROS production as well as cell energy production.

An increase in oxidative stress leads to elevated oxidative damage to biomolecules such as proteins and lipids. A decrease of Na^+/K^+ ATPase is closely correlated to the induction of oxidative stress, suggesting that elevated ROS levels damage the ATPase, thereby leading to BBB dysfunction by allowing excessive and inappropriate influx of Ca^{2+} into cells (Huang et al., 2008). Future experiments regarding the energy production and the BBB permeability after QDs treatment are necessary.

The tight junctions are also present in other organs; e.g in the liver. In healthy liver the endothelium is fenestrated with pores up to 100nm, while, in the presence of inflammation, the permeability is increased.

All the studies reported in literature are performed in healthy animals. It is important to understand that not only the chemistry of QDs but also the the tissue/organ conditions strongly determine their uptake and toxicity. The impact of NPs in pathophysiological conditions is still unknown. The QDs effect has been investigated only on the vasculature and on the inflammatory reactions in postischemic skeletal and heart muscle (Reheberg et al., 2012). Amine-modified QDs are strongly associated with the vessel walls of postcapillary venules and they amplify ischemia-reperfusion-elicited leukocyte transmigration (Reheberg et al., 2012). Moreover, the postischemic myocardium shows a strong association of amine-QDs with microvessel walls.

An increasing number of studies report biodistribution of QDs at long time points, but still there is a little knowledge about the effect of NPs on organs such liver, spleen, kidneys, brain etc. As long as they accumulate for long term period, potentially, they can induce adverse effects and cytotoxicity.

The majority of the published papers regarding QDs toxicity shows no relevant effects on cell viability at the concentration used for imaging applications. *In vivo* experiments, on the other hand, show many possible adverse effects. Literature lack of *in vivo* toxicological studies, for long term periods and with a deep analysis of the effects on single organs. *In vitro* models, with cell viability assays, represents only a good screening and point of start for a toxicological evaluation.

The Fig. 22 is a schematic summary of QDs biodistribution in the body, based on our results and literature.

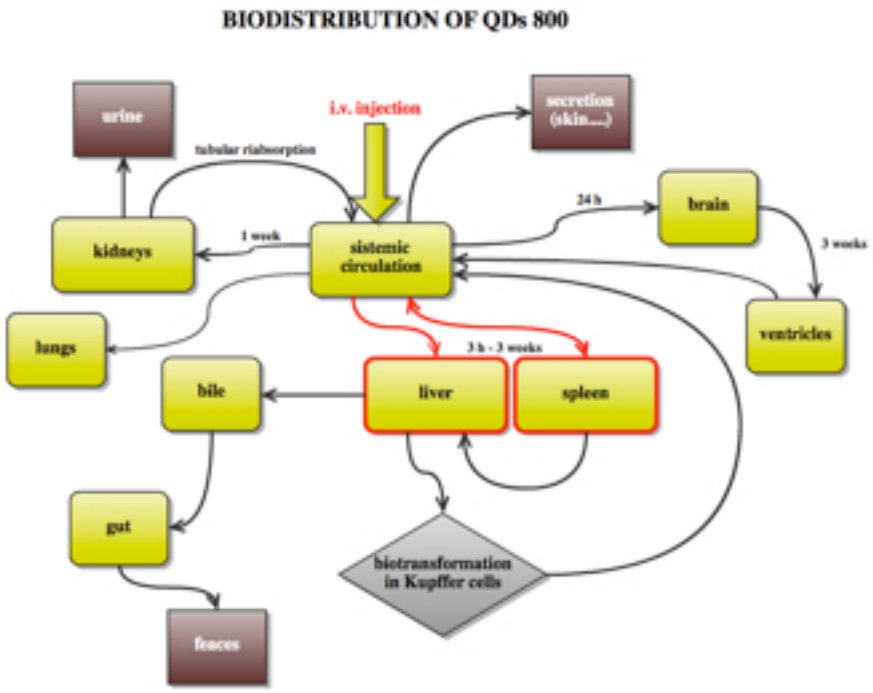

Fig. 22. Schematic representation of the QDs biodistribution fate after systemic administration.

CHAPTER 3

Learning and Memory abilities after Quantum Dots administration

INTRODUCTION

Nanoparticles and blood-brain-barrier

Anatomy of the blood brain barrier

Nanoparticles have the potential to revolutionise medicine because they can reach and affect target organs and tissues at the molecular and cellular levels.

It has been reported that neuronal cells can uptake NPs via the olfactory nerves, in the case they have been inhaled (Driscoll et al., 1996, Oberdorster et al., 2009) or via the blood-brain barrier (Peters et al., 2206).

The blood-brain barrier (BBB) protects the central nervous system (CNS) from potentially harmful xenobiotics and endogenous molecules (Bhaskar et al., 2010), but it represents also an insurmountable obstacle for a large number of drugs, like antibiotics, antineoplastic agents etc.

The BBB is composed by a monolayer of specialised endothelial cells linked by tight junctions (TJ), which restrict the movement of small polar molecules and macromolecules between the blood and the brain parenchyma. TJ possess transmembrane proteins (e.g. junctional adhesion molecule-1, occludin, claudins) and cytoplasmic proteins (e.g. zonula occludens-1 and -2, cingulin etc.) which act as physiological barrier (Fig. 23). The endothelial barrier is supplemented with capillary pericytes. The basement membrane (or basal lamina) is interposed between endothelial cells and astrocytic end-feet. The astrocytic end-

feet are linked by gap junctions and express a variety of receptors, ion channels, and water-transporting proteins, that transport substances across the BBB.

Hydrophobic molecules (e.g. O2, CO2, hormones, etc) enter the brain trough the transcellular lipophilic pathway, while hydrophilic molecules use the paracellular aqueous pathway, the transport proteins, the receptor-mediated transcytosis, and the adsorptive-mediated transcytosis (Abbott et al., 2006). The diffusion of drugs from the blood into the brain depends upon the ability of the molecule to traverse the lipid membranes (Roney et al., 2005). Some drugs are structurally modified to mimic endogenous molecules to take advantage of transport proteins on the membranes.

In addition to BBB, the Blood-CerebroSpinal Fluid barrier (BCSF) is formed by epithelial cells of the choroid plexus and controls the exchange of molecules between blood and CSF (Fig. 23).

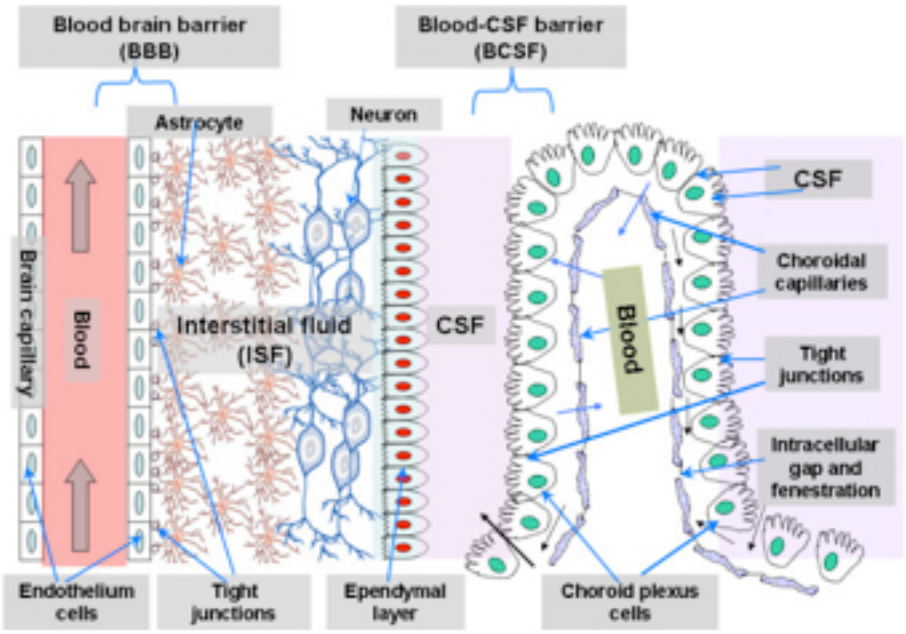

Fig. 23. BBB and BCSF representation. CSF = cerebrospinal fluid. (from Bhaskar et al., 2010)

Surface modifications and functionalisation for crossing the blood brain barrier

The uptake and the dynamic of the NPs in the CNS are very complex.

Surface modifications of NPs are intensely studied for medical applications like diagnosis and therapy aiming to influence the behaviour of the NPs and to improve the brain permeability.

Coating the NPs means absorbing specific proteins or polymers onto their surface. The coatings prolong their circulation in the blood, increase the interactions with endothelial

transport receptors and augment the possibility of crossing the barrier. In fact, the longer blood circulation of NPs influences endothelial cell membrane permeability (Chen et al., 2008), and induce vesicular transport to gain access into the CNS. Moreover, the solid polymeric matrix, which covers the NPs, protects the incorporated drugs against degradation (Garcia et al., 2005).

Several molecules like lectin and polysorbate-80 (Gao et al., 2006), apolipoprotein E (Kreuter et al., 2002), transferrin (Mishra et al., 2006), and peptides (Krauzewicz et al., 2000) have been used for targeting brain endothelial cell membranes and can facilitate the transport across BBB.

It has been reported that circulating NPs cause the generation of free radicals that can disrupt or increase the permeability of the BBB, augmenting the NPs adsorption in the brain.

An important factor for crossing BBB is electrostatic charge of NPs. Since BBB is negatively charged, cationic charged molecules are more likely to interact with the endothelium (Nagy et al., 1983) and increase cell permeability (Hardebo and Kahstrom, 1985). An *in vitro* study reveals that cationised NPs translocate more readily to the brain than anionic or neutral NPs (Fenart et al., 1999). However, neutral NPs and low concentrations anionic NPs do not affect BBB integrity, while high concentrations of anionic NPs or cationic NPs disrupt the BBB structure. Cationic NPs, in particular, have a greater toxic effect and immediately open the BBB (Lockman et al., 2004). An example is polysorbate 80-coated polybutylcyanoacrylate (P80-PBCA) (Kreuter et al., 2002; Calvo et al., 2011). Poloxamine 908-coated NPs, on the other hand, do not cross BBB efficiently because of their incapacity to interact with the endothelial cells of the BBB (Calvo et al., 2001).

So far, for medical applications of drug delivery, low concentration of neutral and negatively charged NPs should preferentially be used (Koziara et al., 2006).

PEGylated nanoparticles are neutral and have shown good stability in the blood stream and to efficiently avoid mononuclear phagocyte system (Kelf et al., 2010). PEG also increases the possibility of receptor-mediated transport through the brain capillary endothelium (Oliver, 2005). Moreover, while other NPs coatings (e.g. poloxamine 908) are easily lost after *in vivo* administration, the PEG chain is covalently attached to the NPs hydophobic core and its release over time takes much longer (Calvo et al., 2001). PEGylated NPs are much more effective carrier to improve nanoparticle brain concentration as compared to uncoated NPs, especially for the deeper regions of the brain like striatum, hippocampus,

hypothalamus and thalamus, without any BBB permeability modification. PEGylated NPs are found in choroid plexus after 24h from i.v. injection (Calvo et al., 2001).

Other *in vivo* studies have shown that the NPs coated with both PEG and the poly(hexadecylcyanoacrylate) PHDCA-hydrophobic chain are able to penetrate the healthy rat brain and brain glioma (Brigger et al., 2001; Calvo et al., 2002).

NPs coated with PLA, PLGA or PEG surface modifications, or the combinations of all, seem to be promising for drug delivery to the brain. They are neutral, biocompatible and they can pass the BBB. Nevertheless, the safety profile of most PEGylated NPs is still unclear (Plard and Didier, 1999; Olivier, 2005).

Not only the charge but also the size of the NP is important for drug delivery: small size and lipophilicity allow molecules to passively diffuse and cross BBB (Sahagun et al., 1990; Fischer et al., 1998).

Another possible route for the uptake of NPs is the endocytosis by endothelial cells of the BBB via low-density lipoprotein receptor (LDLR) family. NPs functionalised with Apoliprotein E (ApoE) and B (ApoB) can act as Trojan Horse lipoprotein-like particles (Kreuter et al., 2002). ApoE protein mimics low density lipoprotein (LDL) causing the particles to be transported across the blood brain barrier via the LDL receptors. The cellular uptake of PEG-PHDCA NPs by endothelial cells, in an *in vitro* model, is via endocytosis, with an intracellular endo/lysosmal localisation (Kim et al., 2007). The clathrin is the mediator of the small invaginations in the cell membrane. The formation of clathrin mediated vesicles is generally linked to the action of proteins from the LDLR gene family (Kim et al., 2007).

Nanoparticles functionalised with a thiamine surface ligand (Lockman et al., 2003), with an average diameter of 67 nm, are able to associate with the blood brain barrier thiamine transporters and thereby increase the unidirectional transfer coefficient for the particles into the brain.

QDs are sequestered by microglia through clathrin-dependant endocytosis (Anas et al., 2009). Carboxyl-QDs naturally incapsulate in vesicles in a Ca^{2+}- and clathrin-dependent manner (Zhang and Tsien, 200) and are used to study the synaptic vesicles release.

Nanoparticles effects in the brain

The study of the effects of NPs in the brain is becoming an increasingly hot topic in literature. The number of publications regarding NPs biodistribution in the brain (Kato et al., 2010) and their effect on neuronal cells, both *in vivo* and *ex vivo*, are steadily increasing (Maysinger et al., 2007, Tang et al., 2009).

While the reticuloendothelial system is the major cleanup sites of nanoparticles in liver and spleen, via uptake by mononuclear phagocytes, unrecognised NPs may have a long circulation half-life and relocate to other target organs, like the brain (De Jong and Borm, 2008).

Once NPs accumulate in the brain, they can induce oxidative stress (Tang et al., 2009). Due to their surface coatings, NPs can be internalized by macrophages, which in turn induces oxidative stress by generating free radicals. Both *in vivo* and *ex vivo* studies show that different type of NPs (e.g. fullerenes, QDs, nanotubes etc.) induce reactive oxygen species (ROS) (Oberdorster et al., 2005), leading to damage of cell functions, DNA, cell membranes, proteins etc (Brown et al., 2004). ROS are generated directly by the NPs, by the heavy metals that constitute the NPs core (Risom et al., 2005), by mitochondria dysfunction (Sioutas et al., 2005), or by inflammatory cells like neutrophils and macrophages (Long et al., 2004).

Some type of non-PEGylated and PEGylated QDs induce inflammatory response and possibly gliosis after injection in the brain (Maysinger et al., 2007). This inflammatory state can lead to dysfunctions, depending on the duration of this oxidative stress within the CNS and on the sensibility of the brain area to the inflammatory changes.

For example, injection of CdSe QDs and streptavidin-QDs in the hippocampus affect synaptic transmission and plasticity. Pair-pulse relation and long-term potentiation are significantly decreased after treatments, and oxidative stress is induced: SOD activity, GSH content and MDA levels are all increased in the animals treated with QDs. The authors attribute the cause of toxic effects to Cd, which is released from the NPs (Tang et al., 2009). Moreover, an *in vitro* study shows that unmodified CdSe QDs induce intracellular Ca^{2+} concentration involving both extracellular and intracellular Ca^{2+}. Cytoplasmic Ca^{2+} is involved in many cellular pathways and in the development of ROS (Trump and Berezesky, 1995). Extracellular Ca^{2+} in-fluxes mainly through sodium channels, and partially through N-type Ca^{2+} channels. The intracellular component involves Ca^{2+} release from mitochon-

dria through mitochondrial Na^+– Ca^{2+} exchangers (MNCX), that further induced more Ca^{2+} release from endoplasmic reticulum through ryanodine receptors (Tang et al., 2007).

Recently, it has been shown that CdSe QDs can activate voltage gated ion channels in cortical neurons cell culture. When stimulated, QDs can produce a photo-generated dipole that perturbs the cell membrane potential, hyperpolarizing and depolarizing both K^+ and Na^{2+} channels and generating action potentials. This is a new application of QDs that can represent a new frontier for treatment of neurodegenerative diseases (Lugo et al., 2012).

The heavy metals, that compose the QDs core, can be deleterious to the brain functions. Neuro-2A cells exposed to Zn-O NPs change morphology, increasing the size and displaying cellular shrinkage, and increase in apoptosis. Moreover, Zn-O NPs increase the amplitude of sodium currents (I_{Na}), enhancing Na^+ influx and accumulating intracellular Ca^{2+}, and increase the excitability of neurons in hippocampal *cornus ammonis* (CA) pyramidal neurons. This effect results on *in vivo* enhanced Long Term Potentiation (LTP), barely influencing depotentiation in the Dentate Gyrus (DG) region of the hippocampus while the escape latency in Morris Water Maze is prolonged (Han et al., 2011).

Exposure to Cd *in utero* and in infancy is associated with risk of impaired cognitive development (Hu, 2000). *In vivo* and *in vitro* studies have revealed that exposure to Cd induce oxidative stress in astrocytes and accumulates ROS that induce astrocytic death (Yang et al., 2008). Se and Te are also well know to be toxic to humans, causing hepatic, renal and neurologic toxicity. All these toxic effects are mediated by the direct interaction of heavy metals with neuronal cells as well as by the activation of the glial cells that change the environment and physiological condition of the neuron.

Immune cells in the brain

The brain functions depend on an integrated system of interactions between neurons, glial cells, epithelial cells and white blood cells. In the classical view, the inflammation is an accumulation of mobile innate and/or adaptive immune cells in the tissue, recruited via the bloodstream or proliferating locally (Jenkins et al., 2011). The innate immune system in the CNS includes microglia and perivascular macrophages (termed also ‘‘perivascular cells’’) that serve as the first line of defence of the CNS.

All these cells maintain the homeostasis of the brain’s microenvironment. Consequently, an alterations of the communication between neurons, glial cells, epithelial cells

and white blood cells can lead to dysfunctions and diseases (e.g. multiple sclerosis and neurodegenerative diseases).

Glial cells are very active even in the absence of pathological insults and their processes periodically contact dendritic spines and axon terminals *in vivo* (Nimmerjahn et al., 2005; Davalos et al., 2005). Recently, MHC class I antigens have been implicated in synaptic plasticity and memory function (Shatz, 2009). Moreover, microglia regulate perisynaptic extracellular spaces, remodel dendritic spines, and phagocyte axon terminals and dendritic spines (Tremblay and Majewska, 2011). Fourgeaud and Boulang described a role for immune molecules in the establishment and plasticity of glutamatergic synapses (Fourgeaud and Boulang, 2010).

Astrocytes also have different roles in physiological conditions: they control synaptogenesis (Christopherson et al., 2005) and synaptic transmission (Newman, 2003) while microglia has been demonstrated to be important in neurogenesis in the DG (Ziv et al., 2006) and in neuroprotection (Streit, 2002).

At this point the classical concept of "neuroinflammation" has to be revisited, since inflammation is not the only role that all these components exert in the brain (Graeber et al., 2011).

A change in the "inflammatory state" after an insult involves a change in the role and activity of these cell types (microglia, astrocytes, immunity-related blood cells, endothelial cells) as well as of the pro-inflammatory mediators, like cytokines and chemokines, that are released by immune cells and can interfere with normal innate immunity functions. Tissue damage and classic inflammation can lead to changes in synaptic plasticity and memory function via dysregulation of MHC class I expression (Shatz, 2009), as well as a peripheral inflammatory challenge (like lipopolysaccharide) results in the parallel activation of microglia and alterations in dendritic spine dynamics (Kondo et al., 2011).

Cytokines and chemokines are small molecules released by immune cells, with pro- and anti-inflammatory roles (Lok et al., 2007). In physiological condition they regulate the communication between the cells of neurovascular unit, contributing to the maintenance of the brain structure and functions, and modulate neuronal excitability and energy demands imposed by neuronal activity (Abbott et al., 2006; Rostene et al., 2007; Willis and Davis, 2008). Cytokines are synthesised *de novo* in the CNS by neurons (Merz et al., 1998) and glia (Garden and Moller, 2006).

The immune system also modulates sleep and wakefulness and some cytokines are involved in sleep regulation under physiological conditions (Imeri and Opp, 2009).

During an inflammatory response chemokines and cytokines induce chemotaxis in nearby responsive cells. The inflammatory reaction in the brain must be highly regulated to minimise neuronal damage because neurons have a high sensitivity to inflammatory stimuli (Northrup et al., 2011).

For these reasons, prolonged imbalances in the chemokines and cytokines levels and in the innate immune system can lead to neuronal dysfunction.

The presence of free heavy metals released by QDs in the brain parenchyma or in neuronal cells, can directly induce ROS production and inflammatory response. The inability of the immune system to detect and phagocyte NPs in the brain can have potentially dangerous consequences, since it can lead to a long term inflammatory state.

Moreover, activated microglia induces the expression of pro-inflammatory mediators like TNF-α and Egr-1 and the increased ROS levels contribute to BBB dysfunction and may alter its integrity (Lynch et al., 2004; Shiu et al., 2007). Microglia also express inducible nitric oxide synthase (iNOS), that generates significant and possibly damaging levels of nitric oxide (NO) (Marques et al., 2008).

Neuronal plasticity and inflammation

In the last years it has been established that microglia can express ‘‘immune molecules’’, which can have CNS-specific roles independent of their roles in the immune or inflammatory response (Graeber, 2010). An example is MHC class I antigens that have been implicated in synaptic plasticity and memory function (Shatz, 2009) and, consequently, tissue damage and classic inflammation can change synaptic plasticity and memory function via dysregulation of MHC class I expression (Shatz, 2009). Ullian and colleagues (2001) demonstrated that glia cells induce the formation of new functional synapses and they release cytokines, like TNF-α, which has an important role in synaptic strength (Ullian et al., 2001; Beattie et al., 2002).

Moreover, glial cells not only modify neuronal plasticity, but they are themselves also plastic and can change in response to neuronal activity (Oliet et al., 2001; Piet et al., 2004).

The consequence that an inflammatory reaction can lead in the brain are dangerous and they must be very highly regulated to minimise neuronal damage. If an insult changes glial

structure for long period, it alters both the immediate synaptic environment as well as the surrounding extracellular space. These changes could have profound effects on synaptic function and plasticity. In fact a peripheral inflammatory challenge (lipopolysaccharide injection) results in the parallel activation of microglia and alterations in dendritic spine dynamics (Kondo et al., 2011). The change in inflammatory state can induce alterations in the electrical activity of neurons as well as in the expression and/or functions of all major categories of ion channels like sodium, chloride, calcium, potassium channels (Eisenhut and Wallace, 2010).

One of the most utilised animals model for studying learning and memory functions, that identifies the changes in plasticity in synaptic connections, is LTP.

Even if it is not yet clear whether the changes that underlie LTP also underlie memory consolidation, it shares many features with memory and learning mechanisms.

The first description of LTP was done by Bliss and Lomo in 1973 where they reported that trains of high-frequency stimulation to the rabbit perforant path caused a sustained increase in efficiency of synaptic transmission in the granule cells of the DG (Bliss and Lomo, 1973).

LTP underlies some aspect of plasticity and memory storage:

a. consolidation of memory requires some forms of synaptic remodelling, that is at the basis of LTP formation;
b. LTP shares many features with long-term memory like cooperactivity, associativity, input specificity and durability (Abraham et al., 1995);
c. Similar cellular/molecular mechanisms are responsible for some type of learning (like spatial learning);
d. the rhythmic bursts of activity that induce LTP mimic the occurring theta rhythm that takes place in the hippocampus during exploratory behaviour (Diamond et al., 1988);
e. some forms of memory are inhibited by agents that also inhibits LTP (Lynch, 2004).

However, it has be considered that LTP recording are made from specific populations of cells in response to a specific inputs from a specific collection of fibers, while the consolidation of memory involves activation of numerous pathways and several brain areas.

LTP is most easily demonstrable in the hippocampus, which is a fundamental area in memory acquisition (Cooke and Bliss, 2006), but several other pathways support LTP (e.g.

entorinhal cortex to DG (Lomo and Bliss in 1973), Schaffer collateral to CA1, Hippicampus (CA1) to subiculum, hippocampus (CA1) to prefrontal cortex, thalamus to layer IV cortex, cortex to cortical pathways, cortex to striatum, auditory thalamus to amygdala etc).

During LTP two neurons, one pre synaptic and the other post synaptic communicate across a synapse. This communication is predominantly carried out by improving the postsynaptic cell's sensitivity to excitatory neurotransmitter (glutamate) received from the presynaptic cell, by increasing the the number of neurotransmitter receptors (NMDA receptors) on the postsynaptic cell surface. The binding of glutamate or D-serine (released by astrocytes) to NMDA receptors facilitate the diffusion of Ca^{2+} ions across plasma membrane of the synapse and act as intracellular messenger if the same postsynaptic cell has been simultaneously depolarised by other synapses. The influx of Ca^{2+} activates the enzyme Ca^{2+}-calmodulin-dependent kinase II (CaMKII) that phosphorilates another glutamate receptor, the AMPA receptor, which increases the permeability of Na^{+}, depolarising the cell and making it more sensible to incoming impulse.

The change is about 50% increase in the amplitude of the response and can last for at least ten hours in an anaesthetised animal or up to 16 weeks in the unanaesthetised animals, following a series of tetanic stimuli.

A negative correlation exists between LTP and oxidative stress (Lynch, 2002) and between LTP and inflammation. ROS have a negative effect on synaptic plasticity, and they impair LTP in CA1 *in vitro* (Pellmar and Lepinski, 1993) and DG *in vivo* (Lynch, 2002).

The injection of LPS in hippocampus, that increases the concentration of IL-1β, a pro-inflammatory cytokine, decreases the LTP (Nolan et al., 2002).

IL-1β impairs LTP through the augmentation of the enzyme superoxide dismutase (SOD) that decreases the level of ROS (Vereker et al., 2001). The augmentation of IL-1β is correlated to inflammation, ageing (Murphy and Segal, 1997) and stress (Murray and Lynch, 1998). On the other hand, chronic treatment of aged rats with aspirin, which combats inflammation, improves the performance in spatial learning task in aged rats (Smith et al., 2002), restoring the normal LTP signal.

Novel object recognition test for cognitive abilities

QDs have been proposed for diagnosis and imaging but before any clinical applications, an investigation on the potential undesirable effects on physiological functions is re-

quired (Guideline for Safety Pharmacology Studies). To study potential adverse effects of QDs on the CNS, an important function to take in consideration is learning and memory. The potential impact of any new chemical entity on memory function has to be evaluated because the major users of drugs are old people, who are increasingly affected by neurodegenerative disorders like Parkinson's and Alzheimer diseases, as compared to young people.

The NOR, novel object recognition test (or one trial object recognition) is a well documented task that provides the basis for the study of a wide range of cognitive abilities in rats and mice. NOR test is used to assess recognition memory that is part of the declarative memory. Declarative memory is defined as the conscious memory for facts and events and is divided in episodic memory (memory for personal events) and semantic memory (memory for general information) (Winters et al., 2008). In contrast to non-declarative memory, such as procedural memory (in habits or skills), which often requires an extensive acquisition phase, declarative memory is associated with shorter learning phase.

NOR test, initially described in rodents by Ennaceur and Delacour in 1988, is based on the natural exploratory ability of rats and mice. The difference in exploration between a previously seen object called familiar object and a novel object is taken as an index of memory performance. An healthy animal in NOR test recognises the familiar object as already seen and spends more time exploring the novel object. The test is not stressful, is repeatable and, with the appropriate set up, it can be performed in the animal home cage, thus decreasing anxiety related behaviour (that can mask or interfere with the result).

Some scholars consider the object recognition test a model of short-term episodic memory (Mathiansen and DiCamillo, 2010). Since short term memory, or primary memory, has a limited duration, from a few seconds to a maximum of a minute, we prefer to define the NOR test as a model of long term memory that by contrast, has a greater capacity and duration. The difference is based on the duration of retention, i.e. the capacity of storing information, and on different anatomical circuits and neural mechanisms underlying each storage system.

Different anatomical regions of the brain are implicated in NOR task. Lesions in the perirhinal cortex (PRh) disrupt object recognition (Buckley and Gaffan, 1998; Gaffan et al., 2000; Gutierraz et al., 2004; Winters ate al., 2010). The PRh is part of the parahippocampal region and is located dorsally to the hippocampal formation. Inactivation of PRh cortex show normal one-trial object recognition at short delays up to 10 minutes (Norman

and Eacott, 2005) and impairment at longer delays (Ennaceur et al., 1996, 1997; Mumby et al., 2002; Hannesson et al., 2005; Norman and Eacott, 2005) suggesting an involvement of this structure in the maintenance of object memory during time. PRh and postrhinal corteces are important for processing complex visual stimuli. The PRh cortex has both direct and indirect connections with the hippocampus via the entorhinal cortex (Ent) (Witter et al., 1986). Both structures are part of the medial temporal lobe system (Buffalo et al., 2000).

The hippocampus is another region involved in NOR task. It is anatomically connected with the PRh and prefrontal cortices (Jay and Witter, 1991; Burwell et al., 1995). The role of the hippocampus in recognition memory is controversial. While a number of studies show that hippocampal or fornix lesions produce no effect in object recognition (Bussey et al., 2000; Mumby et al., 2002; Winters et al., 2004; Forwood et al., 2005; Good et al., 2007; Langston and Wood, 2010), other studies report significant impairments (Clark et al., 2000, 2001). The informations we can obtain from these works are: the rodent hippocampus is not required for the encoding or retrieval of object information after short retention intervals (up to 5 min), but becomes important when object information has to be maintained over longer delays (from 15 min to 24 hours). Moreover, deficits are only evident after near complete hippocampus lesions: only the lesion of the 75–100% of total hippocampal tissue impairs NOR task, while damages of only 50–75% of the hippocampal don't impair the one-trial object recognition after a 3 h retention delay (Broadbent et al., 2004).

RESULTS AND DISCUSSION

Behavioural changes induced by administration of QTracker® 800 Quantum Dots

QTracker® 800 Quantum Dots impair Novel Object Recognition test

All details of the experiments are described in Materials and Methods.

Our data indicate that one single administration of QDs can elicit biological and behavioural effects. The Fig. 24 illustrates the discrimination difference of NOR test. The discrimination difference is a parameter indicating the amount of time spent investigating the novel object relative to total object-investigation time, during the test trial (Gaskin et al., 2003). The object recognition is reflected by a discrimination ratio above 50%. At 3 weeks after treatment, the discrimination difference of treated animals is 53%, meaning that animals spend a similar amount of time exploring novel and familiar objects as compared to controls and indicating the evidence of an impairment in NOR test ($p<0,02$, two ways ANOVA for repeated measures). The position of novel and familiar objects are counterbalanced between groups and time points. All objects are tested for intrinsic preference before the test.

The training trials show no preference for object position at all time points (data not shown).

The impairment in object recognition after 1h delay time, is probably caused by alteration of different regions of the brain. It is still difficult to understand what are exactly the anatomical regions coding for recognition memory in NOR test, and the results in literature are confusing (Dere et al., 2007). Moreover, QDs are not localised in a specific brain area.

In order to exclude that the decreased novel object exploration is due to an impairment of locomotory functions, immediately after NOR test the animals are tested with rotarod, grip strength meter tests and we measure the distance moved during NOR test.

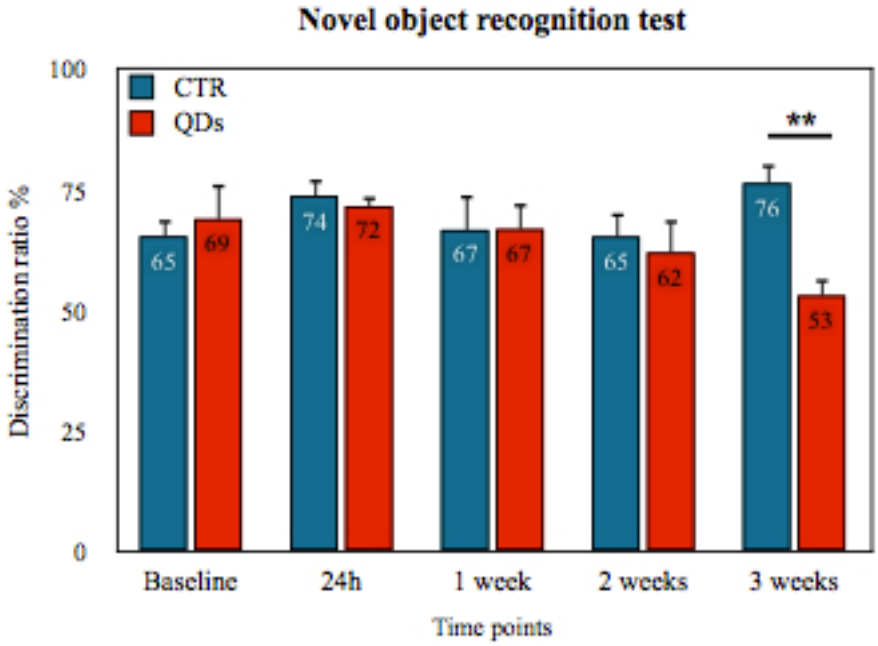

Fig. 24. Novel object recognition test results. The graph represents the discrimination ratio of QDs=treated animals (red bars) vs CTR=control animals (blu bars) at all time point. Data represent average ±SEM.

Grip strength meter is a measure of the forelimb grip force in grams, while rotarod measures the duration of riding time (seconds) of the animals on a rotating cylinder suspended above a cage floor. Rodents naturally try to stay on the rotating cylinder (rotarod), and avoid falling to the ground. We measured the length of time that a given animal stays on this rotating rod as a measure of their balance, coordination, physical condition, and motor-planning, during the time points.

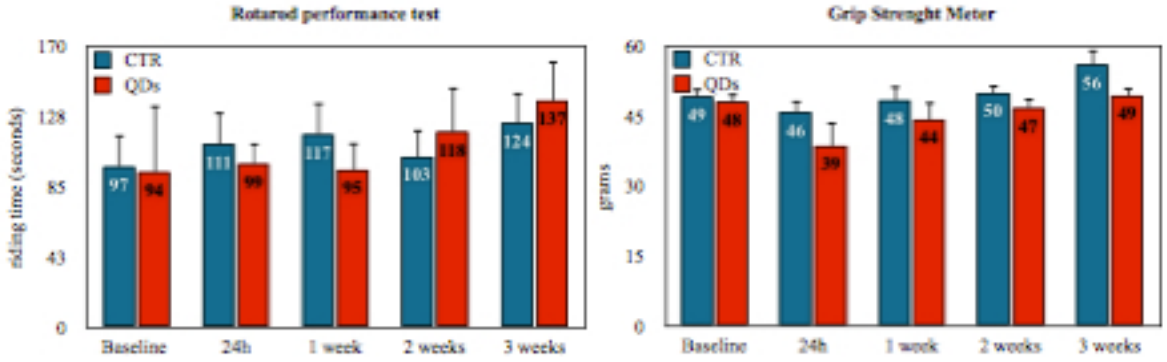

Fig. 25. Locomotor activity tests. **Left:** Rotarod. **Right:** Grip Strength Meter. QDs=treated animals (red bars) CTR=control animals (blu bars) at all time points. Data represent average ±SEM.

No statistical differences are found between controls (CTR) and treated mice (QDs) ($p>0,05$ two-way ANOVA for repeated measures) in all the three tests (Fig. 25 and 26).

The survival and mean body weights of treated mice are similar to controls for all the 3 weeks of the study.

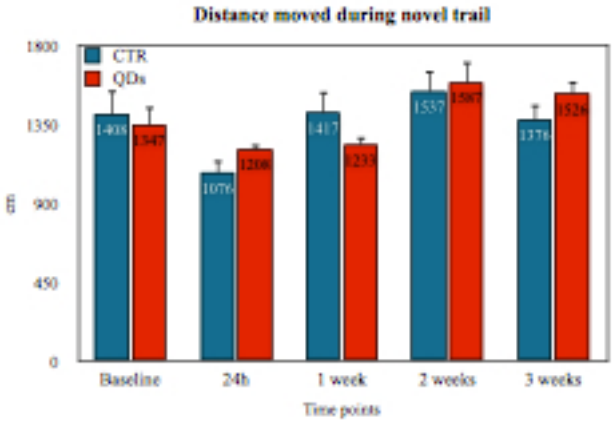

Fig. 26. Distance moved during test trial in the NOR test. No differences between the two groups. QDs=treated animals (red bars) vs CTR=control animals (blu bars) at all time points. Data represent average ±SEM.

Discussion

Balb-c mice are associated with a higher level of anxiety as compared to others strains (Brooks et al., 2005). Animal anxiety may cause inhibition of exploration of a novel object (Tang and Sanford, 2005). During the past 30 years NOR test has been performed in a novel environment, giving to the animal a period of environment habituation before running the test.

A decrease in object interaction during training and test trials may be due to a too short habituation period (Lukaszewska and Radulska, 1994), influencing novelty approach (Sheldon, 1968). The use of the home cage as testing environment has been proposed to meet some of the concerns of interpretation and reproducibility of behavioural data (Gerlai, 2002; Wurber, 2002 Kas & Van Ree, 2004; Tecott & Nestler, 2004; Spuijt & DeVisser, 2006).

In our experiments, the animals perform the tasks in their home cage, showing a higher object exploration as compared to other studies in literature (Dellu et al. in 2000; Sik et al., 2003; Brooks et al., 2005).

The exposure to NPs induces less novel exploration during time, with an impairment at 3 weeks, which can be caused by the presence of exogenous compound, the presence of heavy metals, the increased inflammatory response or the combination of the three.

One feature of the one-trial object recognition paradigm is that the effects of lesions or drugs on attention, sensory–motor functions or the motivation to explore novel objects can potentially affect the results (Dere et al., 2007). On the other hand, NOR test is less stressful than the other cognitive tasks, short in time, and optimal for repeated measures.

In our experiment we exclude the impairment in motor performance as verified by locomotory tests.

NOR test is performed during dark period, with the use of red light. Mice have neither red nor infrared vision so they can be considered blind under the infrared illumination. Objects are cleaned with ethanol and water in order to eliminate odours as much as possible. In these conditions we don't exclude a contribution of somatosensory cortex for the exploration and recognition of objects. Somatosensory cortex is an area where inputs from the thalamus, carrying information from whiskers, terminate. Rodents, in fact, explore their local environment by actively whisking their mystacial vibrissae to localise objects and identify them, based on their shape, texture etc. (Moreno et al., 2010).

Thus, as compared to other cognitive tasks, NOR test can be affected by a strong cortical components, that is required to explore and encode objects. This cortical component can be affected by the presence of QDs as well. Moreover, NPs in most cases, reach the blood flow. The cortices are areas in the brain with a high level of vascularisation, and, potentially, could be one of the main accumulation areas. For these reasons, future experiments will explore somatosensory cortex functions.

QDs toxicology studies mostly lack of the behavioural studies component. Some papers report behavioural alteration induced by aluminium, TiO2 , Zinc oxide, diesel, Manganese, gold NPs.

The behavioural tests that have been used in literature, such as Morris water maze (Win-Shwe et al., 2008), passive avoidance (Chen et al., 2010) and Y-maze (Hu et al., 2010) are referred to hippocampal spatial memory functions.

It has also been shown that, even if NPs do not cross BBB, they can induce behavioural impairments.

The effect that NPs exposure can have on the behaviour of animals and of the human population is an important point to take in consideration and to analyse further.

Inflammatory response induced by QTracker® 800 Quantum Dots administration

Microglia and astrocytes response

The inflammation in the brain leads to microglia and astrocyte activation. Microglia and astrocytes are sensitive to the changes in the microenvironment of the CNS and rapidly activate in all conditions that affect normal neuronal functions.

The presence of QDs in the brain elicit an inflammatory response, that changes the morphology and the number of glial cells. Different areas of the brain react differently to the inflammatory response and the presence of pro-inflammatory cytokines. Herrera and colleagues in 2000, for example, reported that substantia nigra is far more sensitive than the striatum to the inflammatory stimulus.

In our experiments the level of inflammation at 3 weeks after exposure to QDs is evaluated in terms of astrocytes (GFAP expression) and microglia (Iba-1 expression) response. GFAP is an established marker of astrocyte maturation and reactivity (Gomes et al., 1999). Iba-1, ionized calcium-binding adaptor molecule 1, is located in the cytosol of all microglia and infiltrating monocytes, regardless of activation state, although its expression increases with activation.

In the treated samples there is no evidence of colocalisation of QDs and astrocytes at 3 weeks after treatment. This is in line to the fact that QDs fluorescence, at this time point, is observed only in ventricles.

Interestingly, we find traces of PEG staining in the hippocampus, localised in the pyramidal cell layers in CA1, CA2 and CA3, in the *stratum radiatum* and in the *stratum lacunosum-molecolare*. In the DG, PEG is localised in the granular cell layer, in the hilus and in the enclosed blade of the DG. The double staining with GFAP and PEG antibodies reveals no specific colocalisation of PEG and astrocytes in hippocampus at 3 weeks. In literature it is shown that different type of PEGylated QDs are sequestered in microglia lysosomes within 7 days, after intracortical injection (Maysinger et al., 2007).

In our case, the systemic injection provides a lower amount of QDs that reach the brain as compared to an intracortical injection and possibly the amount of QDs is not enough to induce an immediate inflammatory response.

The density of GFAP staining and the number of Iba-1^{+} cells and their morphology in different regions of the brain are evaluated to assess the inflammatory state.

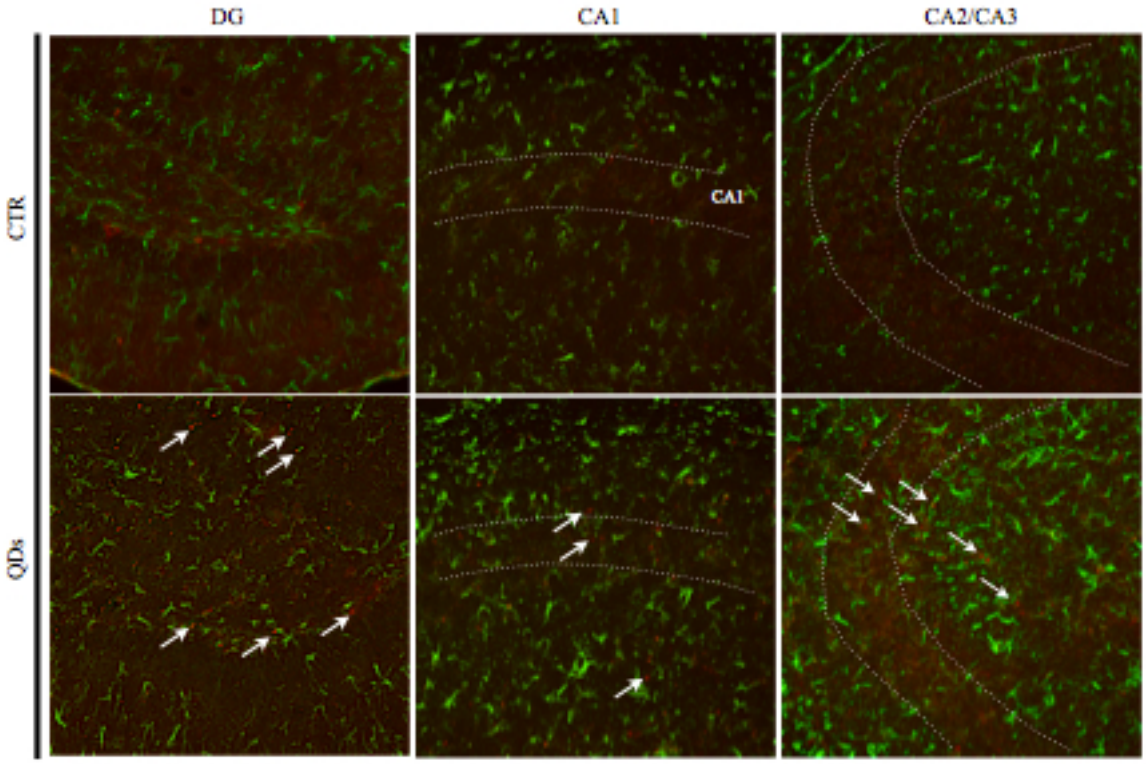

Fig. 27. Immunofluorescence of astrocytes (green) and PEG (red) in the hippocampus. From the left to the right: dentate gyrus (DG), CA1 area and CA2/CA3 area. The pictures represents controls animals (top), and QDs animals (bottom). Images are acquired with 20x magnification lens.

A single injection of QDs 800 induce an increase in a astrocytes activation in the hippocampus (Fig. 27). The quantification of GFAP is performed with a western blot which shows a significative increase in astrocytes expression in the hippocampus after 3 weeks from the treatment (P<0,05 Student's *t* test) (Fig. 28). A quantification with light microscopy is still on going.

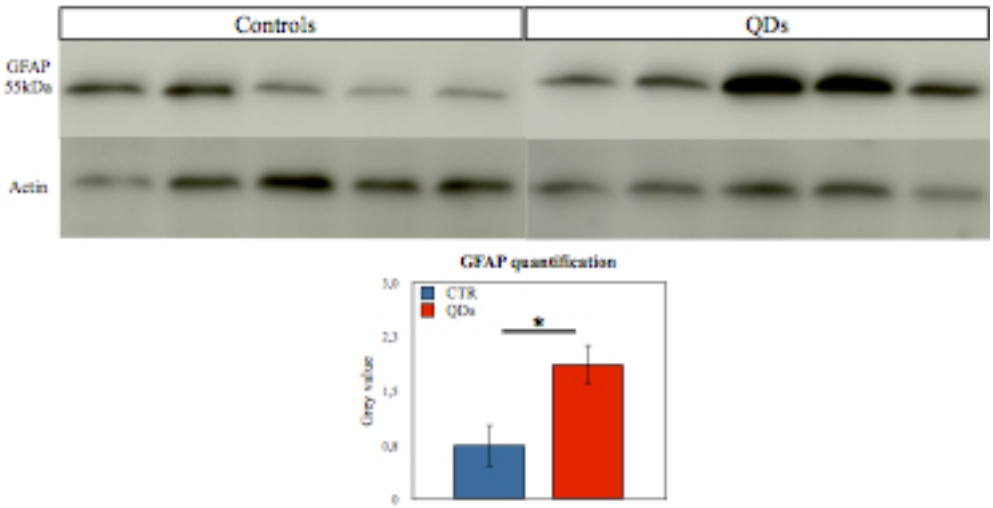

Fig. 28. Western blot of GFAP in the hippocampus. Data show average ±SEM.

Hippocampus, PRh and LEnt are involved in novel recognition test (Dere et al. 2007). In particular the PRh-to-LEnt-to-hippocampal formation pathway conveys non-spatial information about external stimuli (Naber et al., 1997).

All these areas show an increased microglia response at 3 weeks after QDs treatment ($p<0.02$ Student'*t* test), while somatosensory cortex (S1Tr) shows no differences ($p>0.05$) (Fig. 30).

Microglia are activated in response to brain injuries and immunological stimuli (Streit et al., 1999; Liu and Hong, 2003) to undergo dramatic alterations in morphology, changing from resting, ramified microglia into activated, amoeboid microglia (Kreutzberg, 1996). The ameboid microglia is thought to favour phagocytosis and mobility.

Photomicrographs in Fig. 29 show the distribution and appearance of microglia in the hippocampus, PRh and LEnt. Qualitative examination reveals that most of the Iba-1^+ cells exhibits a ramified morphology with larger-diameter processes, characteristic of moderately activated microglia (Ladeby et al., 2005) and that large, macrophage-like cells are rare.

The quantitative evaluation is described in Materials and Methods section.

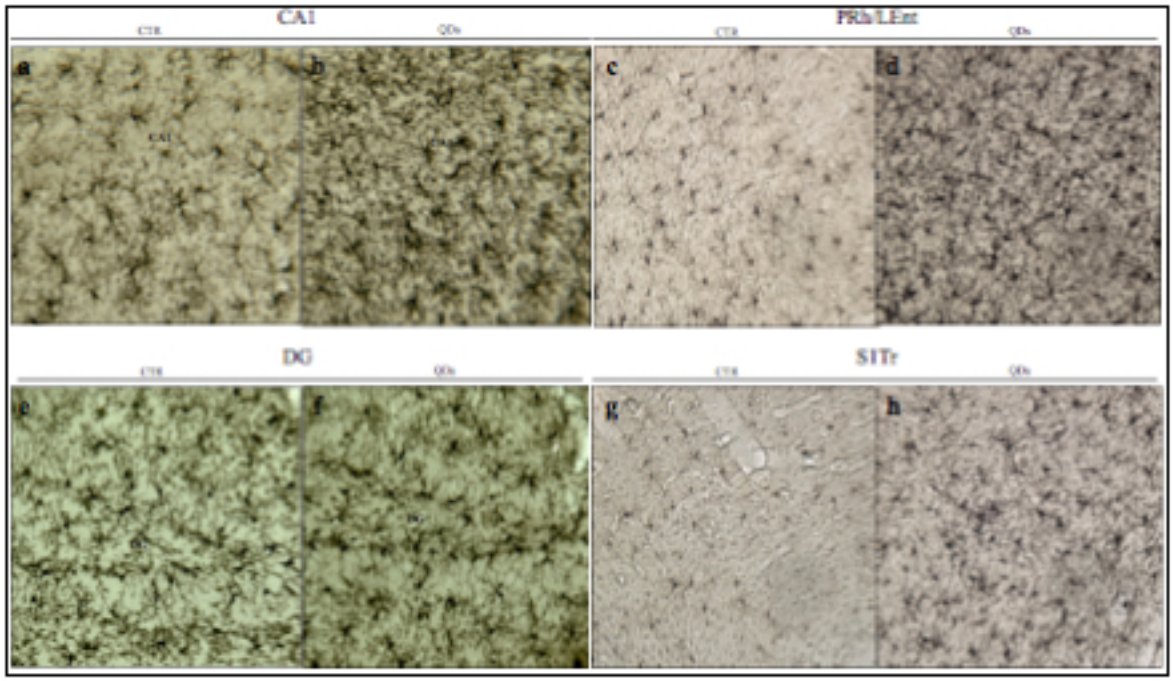

Fig. 29. Microglia (Iba-1) immunohistochemistry of CA1 area (a, b); DG (e, f); Perirhinal cortex (PRh) and Entorhinal cortex (LEnt) (c, d) and primary somatosensory cortex (S1Tr) (g, h). The pictures represent control animals (left) and QDs animals (right). Images are acquired with 40x magnification lens.

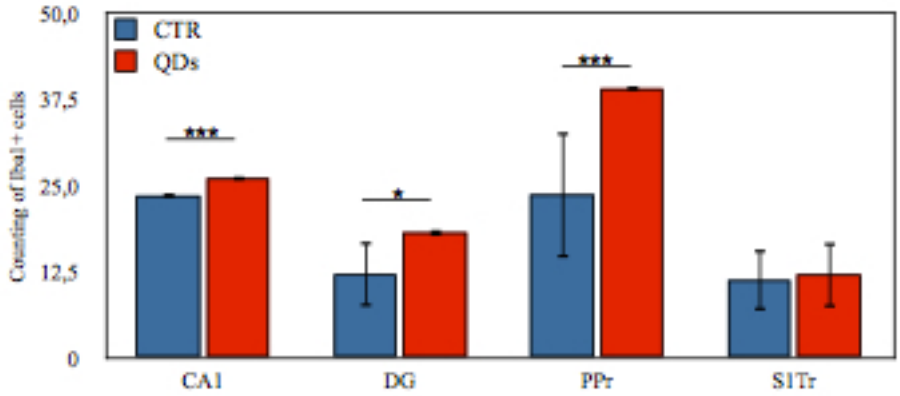

Fig. 30. The graphs represent the number of Iba-1$^+$ cells in the analysed areas. A significative difference is detected in CA1, DG and PPr areas between treated and controls ($p<0,05$, Student's *t*-test). PRH=perirhinal cortex, LEnt=lateral entorhinal cortex, S1Tr=primary somatosensory cortex trunk region. Data represent average ± SEM.

Discussion

Our data demonstrate that QDs800 induce an inflammatory response characterised by an augmentation of glial cells in different part of the brain at 3 weeks after QDs.

The brain is more sensitive to immune reactions and takes longer to return to basal level as compared to other organs (Streit, 2006; Frank et al., 2010).

The activation of microglia generally leads to an augmentation of cytokines like interleukins IL-1, IL-6 and IL-8, which results in a cytotoxic effect. In fact, when their production is prolonged in the time, they recruit and activate macrophages that produce high concentration of ROS (Bondy, 2011).

As demonstrated by immunohistochemistry results, the presence of QDs within and around neurons activate glial mechanism for at least 3 weeks. TEM analysis reveals an unspecific localisation of QDs within neurons and glial cells in the brain after 1 week, while in liver and spleen they are immediately recognised as non self and sequestered in in vesicles and lysosomes for digestion and excretion. It seems that the brain fails in the first instance in phagocyting activity, delaying the response as compared to liver and spleen.

Many neurodegenerative diseases are associated with the extended presence of structures (like amyloid plaques, Lewy bodies etc.), that are not readily guided into degradation by a proteolytic processes (Salminen et al., 2009). The prolonged phagocytic activity leads to their identification as non-self, and causes prolonged activation of inflammatory system (Golde and Miller, 2009) that results in an increased production of nitric oxide (Sugama et al., 2009).

QDs effect in the brain seems to be in part similar to neurodegenerative diseases inflammatory component. If the stimulus remains unsolved the inflammatory response, that has a beneficial value in the short term, can have deleterious consequences (Bondy, 2011). Longer exposure times are needed to evaluate the duration of inflammatory response and the consequent effects.

Example of mineral or nanoparticles (e.g. titanium dioxide, silver, iron oxide, manganese oxide) that cause prolonged immune response are shown in literature (Mohor et al., 1991; Wang et al., 2008; Antonini et al., 2009; Shin et al., 2010).

Moreover, the exposure of NPs on a pathological state, like LPS-induced inflammatory state, increases the inflammatory response (Wang et al., 2008). An inflammatory state induced near cerebral blood vessels can increase the permeability of capillary endothelium and disrupt normal function of the BBB (Trickler et al., 2010).

Chemokines and cytokines quantification

The activated microglia may release some cytotoxic factors, such as cytokines, that might cause neurotoxicity. Cytokines and chemokines control, with positive and negative feed-back mechanisms, the inflammatory response in the brain.

We find that the exposure to QDs 800 does not significantly increase the levels of pro-inflammatory cytokines in brain and serum. Only IL12p40, TNF-α and IL-1β levels show an increasing trend in the brain at 1 week after treatment ($p>0,05$ two way ANOVA) (Fig. 31). All other measured cytokines are not detectable.

The cytokine amounts are associated with high variability per animal: for this reason a number of 3 animals per group is not enough to have a robust data, but it should be increased to 6 animals per group. The data are used in a pilot study as an indication of cytokines behaviour during time.

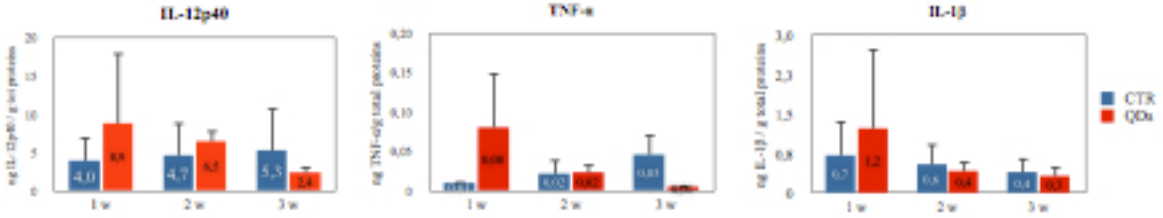

Fig. 31. Cytokines quantification in the brain (N=3). The data represent the average ±SEM.

IL12p40, TNF-α and IL-1β are pro-inflammatory cytokines that stimulate leukocyte proliferation, cytotoxicity, release of proteolytic enzymes, synthesis of prostaglandins and others

cytokines (Cannon, 2000; Bao et al., 2002). Cytokine measurements after treatment show that QDs cause negligible or limited cytokines reaction *in vitro* (Nguyen et al., 2012), but they increase TNF-α and IL-6 levels in the liver at 16 weeks after exposure (Lin et al., 2011). Intratracheal instillation of PEGylated QDs705-COOH results in acute neutrophils infiltration in the lung, followed by interstitial lymphocyte infiltration and a granulomatous reaction on days 17 and 90. The NPs also induce gene expression of cytokines, chemokines and metalloproteinase 12 in lung tissues (Ho et al., 2011).

Neuronal plasticity after QTracker® 800 Quantum Dots administration

Consistent with the classical view, CA1 synaptic plasticity is related to learning and memory (Neves et al., 2008).

The QDs 800 induce an inflammatory response with an increase of microglia and astrocyte expression in the CNS simultaneously with an impairment in NOR test at 3 weeks after injection. As verified in the previous paragraph, the inflammatory response is particularly evident in the anatomical regions associated with recognition memory: Ent, DG, areas CA1-CA3, PRh of the limbic system.

Rodent learning and memory performance has been linked to NMDA-receptor-dependent forms of synaptic plasticity.

NMDA-receptor-mediated LTP. The genetic inactivation of the critical NR1 subunit of the NMDA-receptor, selectively in pyramidal cells of the CA1 region, impairs one-trial object recognition in mice at delays ranging from 30 min to 24 h (Rampon et al., 2000).

To explore if QDs treatment could impair long-term synaptic plasticity in CA1 area, LTP is induced by a high frequency stimulus (HFS).

Our results show no difference in LTP at 1 and 3 weeks after treatment between QDs and controls animals ($p>0.05$ Student's *t* test) (Fig. 32). At 3 weeks controls and treated animals behave very similarly, while at 1 week after treatment there is a decreasing trend of QDs animals as compared to controls after the HFS. More animals are needed in order to confirm the data.

The NMDA receptors activation initiates a cascade of cellular reactions that is thought to lead to maintenance of LTP, via the increase of intracellular Ca^{2+} concentration.

Studies show that acute application of CdSe QDs is capable of elevating intracellular Ca^{2+} concentrations in the primary cultures of hippocampal neurons (Tang et al., 2008a; Tang et al., 2008b). The increased intracellular Ca^{2+} levels could enhance certain presynaptic neurotransmitter release and boost postsynaptic response (Berridge, 1998; Augustine et al., 2003).

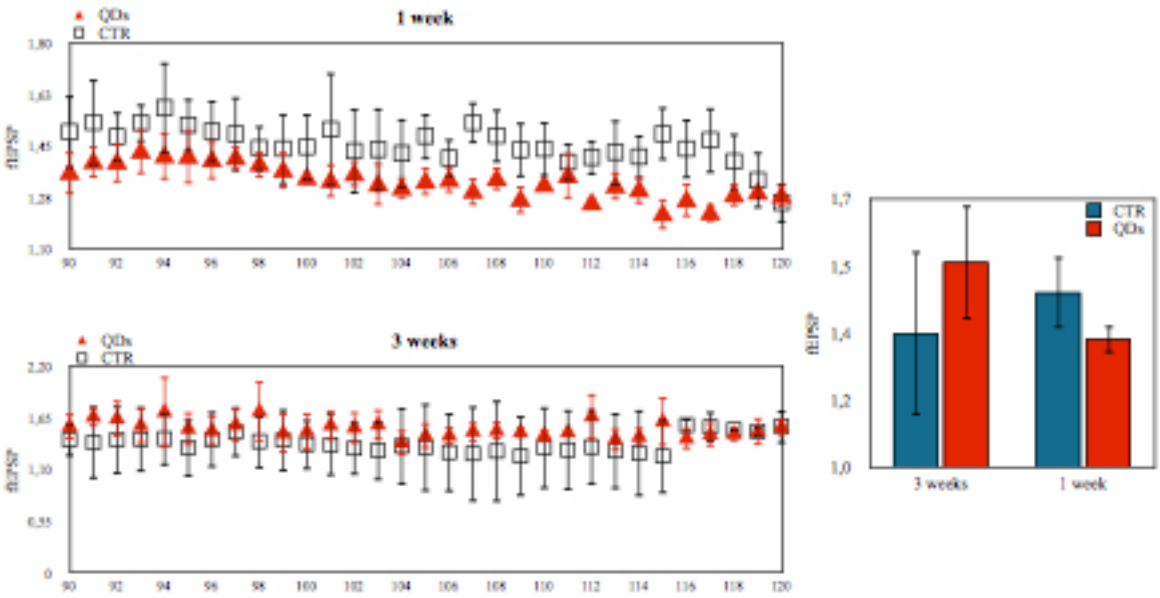

Fig. 32. Effect of QDs 800 on LTP of fEPSP in CA1 area. The data show the LTP signals after 60minutes after the high frequency stimulus (HFS) is applied. The graph on the right represents the averages of the time-course ± SEM.

Acute exposure to either streptavidin-CdSe/ZnS QDs or unmodified CdSe QDs significantly increases the Input/Output functions (a measure that reflects the level of presynaptic neurotransmitter release and the postsynaptic receptor response), indicating that QDs enhance the basal synaptic transmission and plasticity in DG area, and increase the baseline of both fEPSP slope and population spike (PS) amplitude, suggesting that QDs enhanced synaptic efficiency in this area. It has also reported that LTP of both fEPSP slope and population spike amplitude are significantly depressed under QDs insult (Tang et al., 2009). Considering the complexity of mechanisms underlying the LTP, it is very hard to figure out how QDs impair the LTP. The authors attribute the responsibility to the increase of free Cd^{2+} (QD core degradation), free radical formation and interaction of QDs with intracellular components at 20minutes after hippocampal injection.

Moreover, QDs administration can significantly increase the malondialdehyde (MDA) concentration which is considered as index of lipid peroxidation (Tang et al., 2009).

The lipid peroxidation, caused by ROS, results in a decreased membrane concentration of polyunsatured fatty acids and alteration of membrane composition and fluidity (Murray et al., 1997; Lynch, 2002). A change in membrane composition and fluidity impacts on receptor functions: an example is the age related decrease in NMDA receptor caused by ROS production and lipid peroxidation increase, that lead to binding and signalling changes (Tamaru et al., 1991).

Astrocytes play an important role in LTP (McCall et al., 1996), with a direct participation of GFAP in the change in arborization of astrocytic process during LTP (Wenzel et al., 1991). It is reasonable that an impairment in GFAP expression interfere in the necessary signalling between astrocytes and neurons or synapses.

It has been shown that a metal mixture of As, Cd and Pb, affects neurobehavioral parameters and reduces the expression of GFAP, an important protein component of BBB (McCall et al., 1996), accompanied by increased apoptotic and morphologically changed GFAP-expressing astrocytes. The apoptotic effect on astrocytes involves the increase in intracellular Ca^{2+} release and ROS generation (Rai et al., 2010).

The fact that there is no alteration of LTP function at 3 weeks while we observe an impairment in recognition memory (novel object recognition test data), is probably caused by a stronger correlation between spatial memory and LTP rather that recognition memory and LTP.

A possible impairment in hippocampal function caused by the presence of QDs can occur earlier. At 3 weeks in fact, we don't find any QDs in the brain parenchyma, while at one week after injection electron microscopy reveals their presence in different cell types in the somatosensory cortex.

The impairment in LTP and NMDA receptors, associated with an impairment in recognition memory and with an increase in inflammatory markers like GFAP astrocytes, has been found in other animals models like the genetic rat model of depression, the Flinders Sensitive Line (Gómez-Galán et al., 2012).

CHAPTER 4

Sleep/wake period and QDs 800

INTRODUCTION

The sickness behaviour hypothesis

Some studies establish that systemic administration of cytokines leads to a wide variety of side effects, developing a condition known as the systemic inflammatory response syndrome (SIRS).

Pro-inflammatory cytokines act in the brain to induce fever and profound psychological and behavioural changes, like decreased locomotory activity, decreased social investigation, sleep changes, decreased food intake (D'Mello and Swain, 2011). These changes are generally called ''sickness behaviour'' (Kent et al.1992).

The sickness behaviour syndrome serves as an adaptive purpose during systemic infections and consequently inflammation, and one of its consequences is an impairment in sleep-wakefulness cycle. Cytokines, like TNF-α and IL-1β play a role in the physiological control of sleep-wake cycle and contribute to daytime sleepiness observed in patients with peripheral disease (Vgontzas et al., 1997; Imeri and Opp, 2009).

The presence of cytokines and inflammatory response in the brain has been associated with a communication between brain and other organs like liver, after a peripheral inflammation stress. The liver communicates with the brain through TNF-α, IL-1β and IL-6 and the result is the increase in pro-inflammatory cytokines and glia activation also in the brain, even if the insult is not related to brain. Circulating TNF-α and IL-1β, released by Kupffer cells, communicate with brain via many pathways, as described by D'Mello and Swain, 2011.

TNF-α has been linked with sleep abnormalities, fatigue, and mood disorders (Aouizerat et al., 2009). The correlation between inflammation and sleep abnormalities has been studied both in humans and animals models.

Sickness behaviour is associated with many behavioural alterations that can be screened using different behavioural tests like plus maze, light dark box, elevated T maze, open field and ultrasound vocalisation (Bassi et al., 2011). Locomotor activity measurements have been used for many years to evaluate chemical-induced changes in the CNS (Reiter, 1978). Measures of activity has been established as an indicator of internal state or motivation level (Maestripieri et al., 1992).

For specific research questions all these behavioural tests are the appropriate assays. However, automated home cage observations offer the possibility to study long-term behaviour with a high temporal and spatial resolution in undisturbed mice under both novelty-induced and baseline conditions. The automated home cage can represent a potential good model of behavioural screening for NPs exposure effect, thanks to the long time period assessment without stress for the animal.

Automated home cage activity has been proposed as a good tool for the characterisation of inbred mice (De Visser et al., 2006). It represents a quantitative characterisation of behavioural organisation in freely acting mice and provides a powerful approach for assessing the impact of chemical exposure, nervous system alteration and environmental manipulations on whole animal physiology and behaviour (e.g. energy balance, thermal status, osmotic/volume status, sleep). It can en-light differences in locomotor activity, circadian rhythmicity and activity between different strains and experimental conditions. Animal behaviour can be divided into two major discrete states: active and inactive (Goulding et al., 2008). During the active states, animals forage and control the external environment, traversing the home range. During inactive states the animals return to a refuge (nest or the home base) and rest or sleep (Adam and Davis, 1967). Motor activity has been suggested for the routine preliminary assessment (screening) of the neurotoxic potential of chemicals for its noninvasive nature, ease of testing, availability of automated test equipment, and objectivity of the data (Mac Phail et al., 1989). The automatic home cage has been used for example, for discriminating the effect of gene mutation (Wade et al., 2008).

Ganea and colleagues used the home cage locomotor activity to find changes in circadian rhythm, novelty-induced locomotor activity as well as alterations in locomotion due to pharmacological interventions (Ganea et al., 2007). Tang and colleagues described signifi-

cant correlations of home cage activity with the activity in other behavioural tests (open field, emergence and novelty object) conducted in an open field (Tang and Sanford, 2005).

RESULTS AND DISCUSSION

Basal activity

In our experiment the animals are housed in Phenotyper® cages (Noldus) for all the period of the study and their activity is automatically recorded with video-tracking software, EthoVision XT® (Noldus), that permits to score the basal activity (e.g. distance moved and velocity) during 24h. We hypothesise that the inflammatory response induced by the long term presence of QDs 800 in the brain, leads to a sickness behaviour syndrome, affecting sleep-wake cycle.

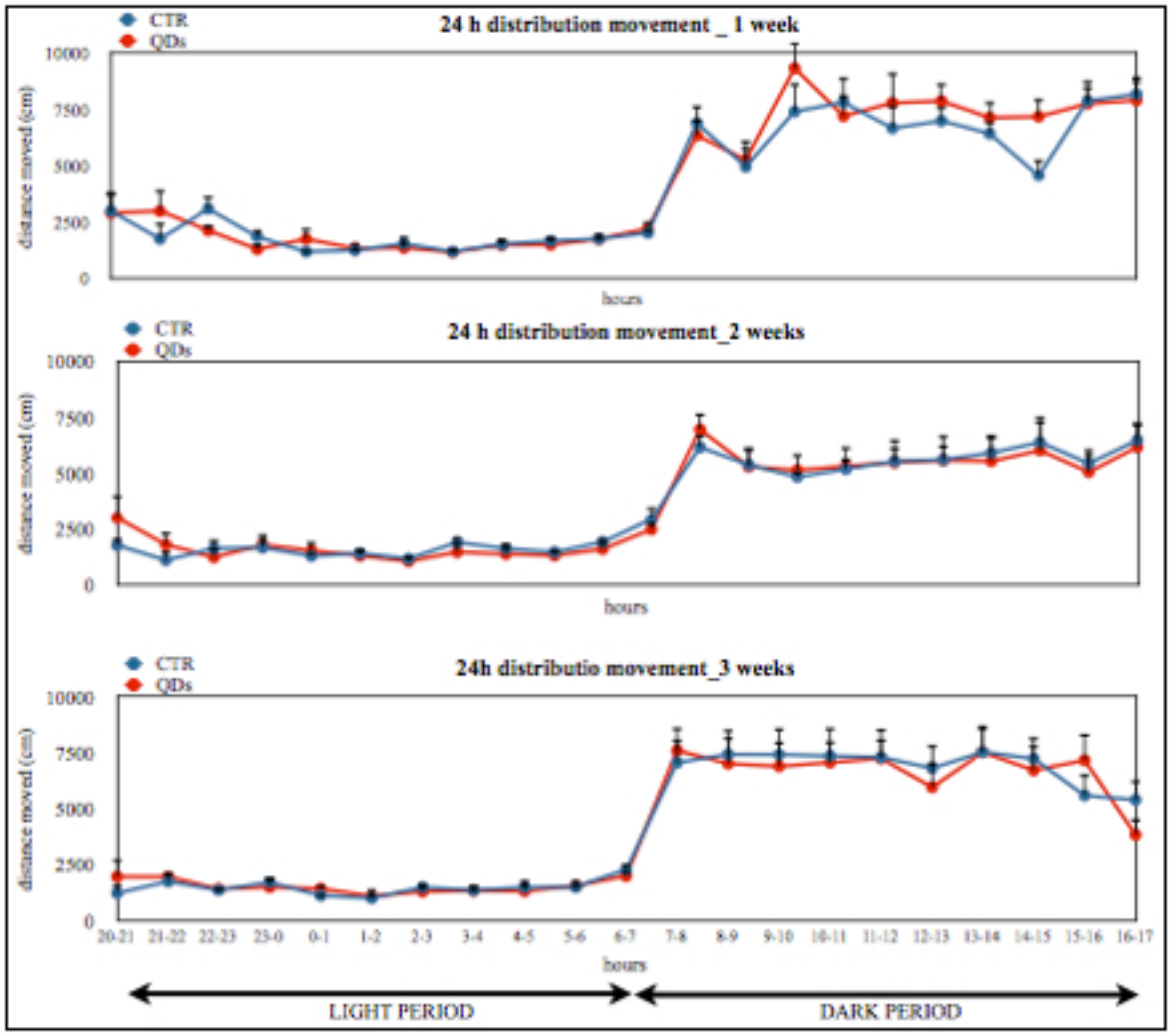

Fig. 33. Animal basal activity in the home cage during 24h. Data represent average ±SEM.

Different parameters can be used for the description of basal or novelty-induced behaviour in rodents: “duration of movement” and “distance moved” are considered as indexes of the level of activity, that is an indication of how animals interact with the surrounding environment. Other parameters like “velocity”, “number of stops” and “time spent in the shelter” are more likely evaluated as anxiety-related behaviours. In fact these parameters correlate with anxiety-related behaviour on the elevated plus maze (De Visser et al., 2006).

In our case the velocity is calculated by the software as the total “distance moved” over time, so we can not consider it as an indicator of stress related behaviour. In order to have behavioural informations, velocity should be calculated only in ‘movement’ episodes, thus excluding periods of non-movement. Other parameters are necessary in order to completely establish the basal animal behaviour.

No differences in locomotory activity (distance moved and velocity) are detected between QDs treated animals and controls at all the time points analysed ($p>0,05$ two ways ANOVA for repeated measures)(Fig. 33).

The animals show predominantly activity during the dark phase as compared with the light phase, with peaks of activity at the change of the light.

In literature only a few papers reported behavioural tests after nanoparticle exposure and none of them has been done after QDs treatment.

Sleep/wake period analysis

A pilot experiment shows that after 1 week after QDs 800 systemic exposure, there are no difference between treated and controls in the sleep/wake period (Fig. 34) ($p>0,05$ one way ANOVA). The data are obtained with Neuroscore® EEG analysis. At the same time the behaviour of the animals is recorded in PhenoTyper® cages with video synchronisation in order to confirm the EEG data. The software automatically assigns a vigilance stage to each epoch. The stages are Sleep and Slow Wave Sleep, Wake, and Active Wake. The frequency content of the EEG combined with animal activity and movement are used as the basis of the scoring criteria.

The trend of increase of sleep period of treated animals compared to controls can be considered a feature of sickness behaviour. Further experiments are required for en-lighting the data on sleep/wakefulness cycle.

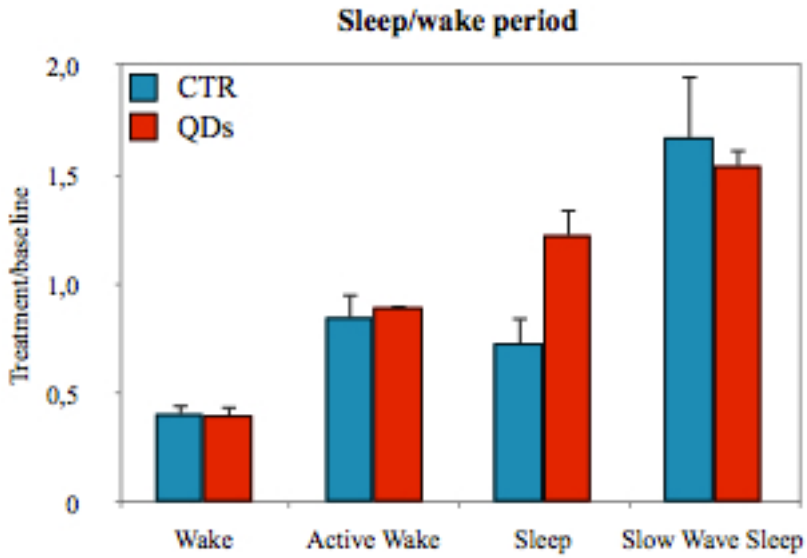

Fig. 34. Sleep/wake period assessed with Neuroscore® EEG analysis after 1 week after QDs800 treatment. Data represent average ±SEM.

The alteration of sleep/wake period has been reported in a few papers after NPs administration, and still very little is known. Gold NPs alter some genes, both in liver and spleen, that are related to the circadian rhythm, including D site albumin promoter binding protein, Period homolog 2 (Drosophila), Basic helix-loop- helix domain containing, class B3 and Neuronal PAS domain protein 2 (predicted), that is the liver homolog of CLOCK gene, expressed in the suprachiamatic nucleus in the brain. The gene encodes proteins regulating circadian rhythm (Balasubramanian et al., 2010).

The immune system also modulates sleep and wakefulness and some cytokines are involved in sleep regulation under physiological conditions (Imeri and Opp, 2009). Other type of PEGylated gold NPs increase the acute inflammatory response in the liver inducing the expression of adhesion molecules, chemokines and cytokines (IL1β, IL-6, IL-10, IL-12β, TNF-α) in the first 24h (Cho et al., 2009).

CONCLUSIONS

Our studies revealed that QDs nanoparticles accumulate in different organs for at least 3 weeks after a single i.v. injection. The reticuloendothelial system in liver and spleen is the major cleanup site of QDs nanoparticles via uptake by mononuclear phagocytes: Kupffer cells in liver and histiocytes in the spleen.

At lower concentration QDs enter the brain already after 24h from the injection. Interestingly, they are not stopped by microglia and sequestered in lysosomes, but they interact with different cellular structures (e.g. mitochondria, myelin sheath, chromatin, synapses). Their presence is evident around blood vessels in different brain areas, in epithelial cells, neurons and glial cells. It seems that the brain fails in the first instance in phagocyting activity, delaying the response as compared to liver and spleen. At 3 weeks the retention of QDs is only in the ependymal cells of the choroid plexus as a logical consequence of the function of the tissue.

At 3 weeks QDs impair object recognition test. This effect is probably caused by an alteration of hippocampal and cortical functions, which in turn can be due to the prolonged inflammatory response. As a matter of fact, we find an increasing expression of astrocytes and microglia cells in enthorinal and perirhinal cortices, dentate gyrus, areas CA1-CA3 of the limbic system after the treatment.

LTP, on the other hand, which is considered a model of learning and memory, fails to reproduce an impairment of hippocampal plasticity at 1 and 3 weeks after treatment.

We also assess if the prolonged exposure to QDs leads to a sickness behaviour syndrome, but no differences in circadian rhythm and basal activity are found between treated and controls animals.

Some nanomaterials have been studied in clinical trials or have already been approved by the U.S. Food and Drug Administration (FDA) for use in humans (McCarthy et al., 2005) and many proof-of-concept studies of nanomaterials in cell-culture and small-animal models for medical applications are under way (Resch-Genger et al., 2008). QDs are between them and recently they have been proposed for clinical use (Tab. 5). The Cornell Dots, for example, are nanoparticles similar to QDs, that in 2011 have been approved, by

the FDA for the first phase I clinical trial on five melanoma patients at Memorial Sloan-Kettering Cancer Center (MSKCC) in New Work City (http://www.sciencedaily.com/releases/2011/02/110205162831.htm).

Nanomaterial	Trade Name	Application	Target	Adverse Effects	Manufacturer	Current Status
Metallic						
Iron oxide	Feridex	MRI contrast	Liver	Back pain, vasodilatation	Bayer Schering	FDA approved
	Resovist	MRI contrast	Liver	None	Bayer Schering	FDA approved
	Combidex	MRI contrast	Lymph nodes	None	Advanced Magnetics	In phase 3 clinical trials
	NanoTherm	Cancer therapy	Various forms	Acute urinary retention	MagForce	In phase 3 clinical trials
Gold	Verigene	In vitro diagnostics	Genetic	Not applicable	Nanosphere	FDA approved
	Aurimmune	Cancer therapy	Various forms	Fever	CytImmune Sciences	In phase 2 clinical trials
Nanoshells	Auroshell	Cancer therapy	Head and neck	Under investigation	Nanospectra Biosciences	In phase 1 clinical trials
Semiconductor						
Quantum dot	Qdots, EviTags, semiconductor nanocrystals	Fluorescent contrast, in vitro diagnostics	Tumors, cells, tissues, and molecular sensing structures	Not applicable	Life Technologies, eBioscience, Nanoco, CrystalPlex, Cytodiagnostics	Research use only
Organic						
Protein	Abraxane	Cancer therapy	Breast	Cytopenia	Abraxis Bioscience	FDA approved
Liposome	Doxil/Caelyx	Cancer therapy	Various forms	Hand–foot syndrome, stomatitis	Ortho Biotech	FDA approved
Polymer	Oncaspar	Cancer therapy	Acute lymphoblastic leukemia	Urticaria, rash	Rhône-Poulenc Rorer	FDA approved
	CALAA-01	Cancer therapy	Various forms	Mild renal toxicity	Calando	In phase 2 clinical trials
Dendrimer	VivaGel	Microbicide	Cervicovaginal	Abdominal pain, dysuria	Starpharma	In phase 2 clinical trials
Micelle	Genexol-PM	Cancer therapy	Various forms	Peripheral sensory neuropathy, neutropenia	Samyang	For phase 4 clinical trials

Tab. 5. Nanomaterials in clinical use (Kim et al., 2010).

The results of this thesis indicate that the issue of QD toxicity is a serious obstacle to a full exploration of their *in vivo* usage in biomedical imaging.

New generation of fluorescent NPs without heavy metals and with coatings adapted for the excretion could be the alternative.

MATERIALS AND METHODS

Animals and treatment

Male Balb-c mice (6 weeks old) from Harlan-Nossan (Udine, Italy) are maintained on a 12h light/dark inverted schedule, 23 ± 1°C, with access to food and water *ad libitum*, and are habituated to the experimenters for two weeks prior to the procedures employed in the present study. Animals receive surgeries for implantation of subcutaneous transmitters for ECoG recording. The experiments receives authorisation from the Italian Ministry of Health, and are conducted following the principles of the NIH Guide for the Use and Care of Laboratory Animals, and the European Community Council (86/609/ EEC) directive. Mice are housed and used according to current European Community rules.

Experiments on mice are approved by the research committees from the University of Verona and Italian National Institute of Health.

At the start of the experiments the mice are approximately 12 weeks old. At 13 weeks old they receive one single treatment, via tail vein, of 10µl/g of 40pM QTracker® 800 QDs solution.

Serial sacrifices under (zolazepam and tiletamine anaesthesia) take place at baseline, 3h, 24h, 1 week, 2 weeks and 3 weeks after treatment. After anaesthesia animals are perfused for 5min with PBS at 4°C. Immediately organ samples are collected included brain, liver, lungs, spleen, kidneys.

At each time points we measure body weights and organ weights of each animals.

Tissue distribution analysis with Optical Imaging

Fluorescence of QDs both *in vivo* and *ex vivo* is investigated by using an exciting radiation in the 500–550 nm interval (DsRed/DsRed filters), and in the 810–875 nm range by using an exciting radiation in the 710–760 nm region (ICG/ ICG filters).

Visible and NIR fluorescence images of small living animals are acquired using an optical imager (IVIS 200, Caliper, Alameda, USA) equipped with a CCD camera cooled at 90° C. Images are acquired with: exposure time 1⁄4 1 s, binning 1⁄4 8 and aperture stop f 1⁄4 2.

Anesthetized (Isofluorane 2%) mice are put in prone position on the heated stage of the instrument. Animal treatments are approved by the Institutional Ethical Committee (CIR-

SAL) according to the regulations of the Italian Ministry of Health and to the European Communities Council (86/609/EEC) directive. Images are acquired before and after (continuously for 3 h) tail vein injection. Three hours after injection the animals are perfused with PBS. The extracted organs for each group are acquired with the following parameters: exposure time 1⁄4 1 s, binning 1⁄4 8 and f/1.

Tissue distribution study with ICP-MS

After PBS perfusion, organs are collected and weighted. Selenium (^{82}Se), tellurium (^{125}Te), Zinc (^{66}Zn) and cadmium (^{114}Cd) concentration are measured in each organ with ICP-MS XSERIES 2 system (ThermoFisher Scientific). 40-100mg of tissue are mineralised by Microwave mineralisator MARS XPRESS (CEM) with 1,5 mL nitric acid 13% and a thermal program of 5min 100°C, 5min 120°C and 5 min 180°C. The mineralised samples are diluted with milliQ water and analysed with ICP-MS instrument.

Tissue distribution study with confocal microscopy

At 3 weeks after i.v. injection of QDs, mice (n=5) are transcardially perfused with PBS and 4% paraformaldehyde. Brain, liver, spleen are immediately dissected and 60 μm-thick frozen sections are prepared. 120 μm-thick sections are prepared vibrating slicer (VT1200S, Leica) for confocal microscopy. Immunofluorescence images are captured and the spectral profiles of QDs on tissue sections are measured using a Zeiss LSM 710 Confocal Laser Scanning Microscope (CLSM) (Carl Zeiss, Germany). The NPs are excited by a laser at 405 nm and visualised with 20x objective lens (water immersed, confocal aperture 1) in the range 700-760 nm. Z-stacks and lambda scan of each sample are recorded using the ZEN 2010 software (Carl Zeiss, Germany). The images are analysed using Image J (v1.41, NIH).

Tissue distribution study with transmission electron microscopy

Samples are fixed in 2% glutaraldehyde in Sorensen buffer ph7,4 for 2h, post-fixed in1% osmium tetraoxide (OsO4) in aqueous solution for 2h, dehydrated in graded concentrations of acetone and embedded in Epon-Araldite mixture (Electron microscopy Sciences, Fort Washington, PA, USA). The semi-thin section (1μm thickness) are examined by light microscopy and stained with toluidine blue. The ultra-thin sections are cut at 70nm thickness and placed on Cu/Rh grids with Ultracut E (Reichert, Wien, Austria), and ob-

served using an electron microscope Morgagni 268D Philips (Zeiss, Oberkocken, Germany).

Immunohistochemistry and Immunofluorescence

Immunohistochemistry and immunofluorescence stainings are performed on 4% paraformaldehyde fixed tissues, on frozen sections (60 μm-thick), *n*=4, four consecutive sections per area of interest, per animal.

Immunohistochemistry is performed on sections which are incubated for 10min in 10% methanol with 3% H_2O_2. After blocking with 5% normal horse serum and 0.25% Triton-X in 10 mM PBS for 60 min at room temperature, sections are incubated with anti-Iba-1 antibody (rabbit polyclonal, 1:1000, Wako Chem, Japan) at 4°C 48h and then incubated with donkey anti-rabbit biotinylated secondary (1:400; Jackson, USA) at room temperature for 2h. The immunoreaction is detected using a Vectastain *Elite* ABC kit (Vector, Burlingame, CA, USA) and then visualized with 3.3′-diaminobenzidine tetrahydrocloride (DAKO) with Nickel sulphate for 5–10 min. Finally, sections are dehydrated with ethanol and mounted with Entellan® Mounting Medium (Merk Chemicals, Germany).

For immunofluorescence we use the mouse anti-PEG (AGP4) antibody, (dilution 1:200), a gift from dr Steve Roffler. PEG staining is performed on 60 μm-thick sections. The staining is performed using the methodology indicated on the KIT VECTOR M.O.M. (Vector, Burlingame, CA, USA) which permits to detect mouse primary antibodies on mouse tissue. Sections are incubated for 1h with mouse anti mouse PEG (AGP4) antibody, (dilution 1:200) a gift from Steve Roffler (Institute of Biomedical Sciences, Academia Sinica, Taiwan). The visualisation of the positivity is obtained by the use a secondary biotin goat anti mouse Cy5 (Invitrogen). For immunohistochemistry the visualisation is obtained with 3.3′-diaminobenzidine tetrahydrocloride (DAKO).

GFAP staining is performed before PEG staining. Sections are incubated for 48h at 4°C with rabbit anti GFAP (Abcam, Cambridge, UK) diluted 1:1000 in TBS. Secondary goat anti rabbit Alex 488 (Invitrogen) is incubated for 45min at room temperature (1:1000). Sections are mounted with Fluoromount™ Acqueous Mounting Medium (Sigma-Aldrich, US) and observed with confocal laser scanning microscope (510 Meta CLSM, Carl Zeiss, Jena, Germany).

Cell counting

The number of Iba-1^{+} cells are counted in 4 sections per animal (4 animals per group) using regions of interest (ROI), in both hemispheres beginning at bregma −1.28mm. The ROI is delimited by a squared frame placed in the analysed areas. Two ROI at 20x magnification are placed in the somatosensory cortex (S1Tr), two at 40x magnification on the hippocampus and CA1 area, while one ROI at 20x magnification is placed on LEnt and PRh area. In the somatosensory cortex the ROI are placed in the II-VI layers.

The Fig. 35 shows the ROI in CA1, DG, PPr, LEnt and S1Tr that are counted.

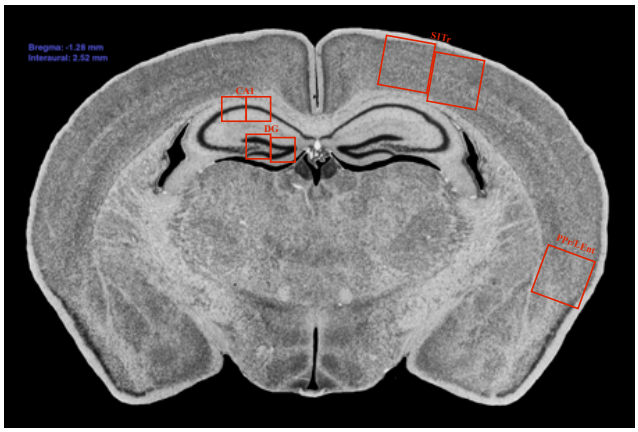

Fig. 35. Representative coronal section. The squares show the areas where the counting is performed

Western Blot

Hippocampal samples are homogenised on ice in 100µL RIPA buffer (50 mM Tris, 150mM NaCl, 1 mM EDTA, 1% Triton X-100, 1% sodium deoxycholate, 0.1% SDS, pH 7.4) with 10% protease inhibitor (Sigma P8340) using a Kontes Pellet Pestle, incubated on ice for 1 hour, centrifuged for 20 min at 4°C at 14000 rpm, and supernatant recovered. Protein concentrations are determined using BCA protein assay (Thermo Scientific) and a Bio-Rad xMark microplate spectrophotometer .

For Western blot, 10µg protein is separated by SDS-PAGE, and transferred to Immobilon-FL 0.45µm PVDF membrane (Millipore) using a Bio-Rad Trans-Blot SD semi-dry transfer cell. Membranes are blocked for 1 hour and incubated in primary antibody overnight at 4°C for anti-GFAP or for 1 hour at room temperature for anti-β-actin. Membranes are washed before being incubated in HRP-conjugated secondary for 1 hour at room temperature, washed again and HRP signal detected using Amersham ECL Plus Western Blotting Detection Reagent (GE Healthcare) and developed using Amersham Hyperfilm ECL chemiluminescent film (GE Healthcare). After developing, membranes are washed, and

stripped by incubating in stripping buffer (62.5 mM Tris, 2% SDS, 100 mM β-mercaptoethanol, pH 6.8) for 20 minutes at 37°C with agitation, washed again and either re-probed or air dried. Membrane washes are performed in Tris-buffered saline with 0.05% Tween-20 (TBST), and blocking steps and antibody dilutions and incubations are performed in 2% skim milk powder in TBST. Rabbit anti-GFAP polyclonal antibody (Abcam) was used at 1/10000 dilution, with donkey anti-rabbit secondary (Millipore) also at 1/ 10000. Mouse Anti-β-actin monoclonal antibody (Abcam) was used at 1/1000 dilution, with goat anti-rabbit secondary (Millipore) also at 1/1000.

Western blot images are scanned using an Epson Perfection U700 Photo scanner, and quantified using Image J software.

Citokines and chemokines quantification

Blood samples are collected after anaesthesia and before perfusion from the ophthalmic artery. The blood is allowed to clot at room temperature for 30 minutes before centrifugation at 1,800 g at 4°C for 10 minutes. Proteases inhibitor cocktail (SigmaAldrich) is add in order to preserve the proteins in the serum.

Brain samples are collected by dislocation and rapid collection of the brain. Brains are homogenised with TrisHCl 0,1M, NaCl 0,75M, Tween20 0,05% and protease inhibitor. The samples are centrifuged at 11000rpm for 20min at 4°C and stored at -20°C.

Citokines and chemokines are quantified by Luminex technology (Bio-Rad). All kits and reagents are obtained from Millipore (Billerica, MA, US). The cytokines evaluated are: interferon-gamma (IFN-γ), tumour necrosis factor-alpha (TNF-α), interleukin-1beta (IL-1β), T helper 17 (Th17), interleukin 12 p70 (IL12p70) and interleukin 12 p40 (IL12p40). Quantification is performed at CRIBI, Padova University.

Novel Object Recognition test

Ten different objects (in triplets) made of plastic, wood or glass that differ in terms of height, colour, shape and surface texture are used. The objects are fixed to the floor of the arena with tape to ensure that the mice can not displace them. The objects have no known ethological significance for the mice, and have never been paired with a reinforcer. Pilot studies ensured that mice of the Balb-c genetic background strain could discriminate between the objects, and there is no *per se* preference for one of these objects.

Novel object recognition test consists in one training trial of 10 minutes where the animals are exposed to two identical objects, followed by a test trial. In the test trial the animals are exposed two objects: one identical to the previous ones (familiar object) and one new object (novel object). The presentations of the objects in both training and test trials is performed as follows. The animal is confined in the end of the cage by the use of a mobile separator made of paper. The separator allowed to place the objects in the correct position in the cage without be seen by the animal. The objects are placed in a symmetrical position in the cage at the same distance from the walls and 7 cm from the other. Once the training trial is finished the objects are removed from the cage and the animals is left undisturbed for the delay time (1 h). Successively, the test trial of 5 minutes occurs. The position of novel object was randomly changed between animals. The test is performed between 9 am and 4 pm, during the dark phase. By the use of Ethovision XT by Noldus, a computerised tracking system, we measure the exploratory behaviour. The test is performed in the Phenotyper® cages used as animal home cages 22,5(l)x31(w)x45(h)cm. Each mouse is tested repeatedly at all time points. Each animal received only one object recognition test per day with at least 3 days rest between tests.

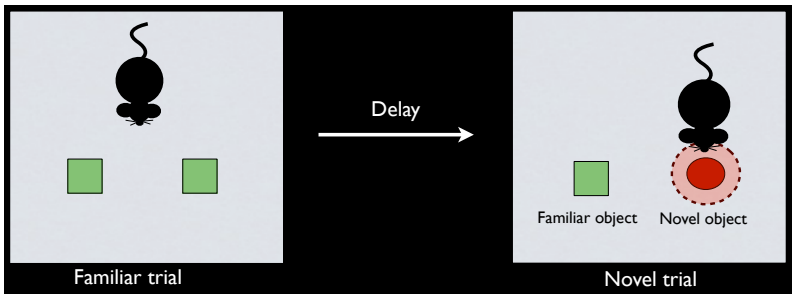

Fig. 36. Schematic representation of novel object recognition test.

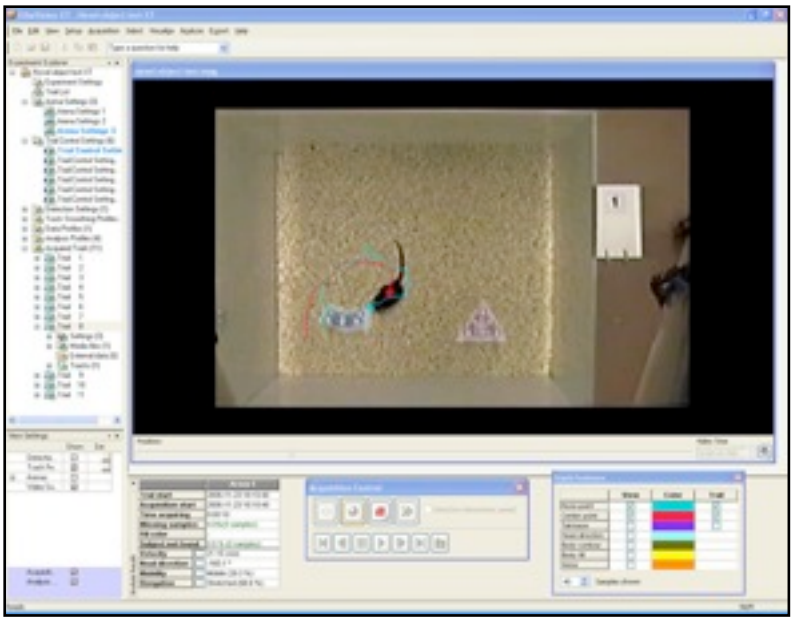

Fig. 37. An example of NOR analysis with EthoVision XT software. The software can discriminate the nose (blue dot) and the centre (red dot) of the animal and can record the duration and frequency of nose entrance in the object area, previously identified. In this example the object areas are the pink and the celestas drawn areas around the right and left objects

For each mouse, the time spent exploring the objects (in seconds) during the test trial is scored off-line from videotapes. Exploration of an object is assumed when the mouse approaches an object, and has physical contact with it, either with its whiskers, snout or forepaws. Vicinity to an object, at a distance less than 2 cm, is not considered as exploratory behaviour. For each retention delay, the proportion of time exploring the novel object, relative to the total time spent exploring both objects, is taken as a measure of object recognition (known as discrimination ratio, $t_{novel}/(t_{novel}+t_{familiar})$). Discrimination ratio values higher than 0.5 suggest a preference for the novel object, values close to=0.5 would suggest no recognition, while values well below 0.5 suggest a preference for the familiar object.

The animals are thus tested for the motor coordination by Rota-Rod (Ugo Basile, Varese, Italy), while motor strength is assessed by the Grip Strength Meter (Ugo Basile).

Rotarod test

Locomotor coordination and balance are measured by placing mice on an accelerating, 3-cm-diameter, rotating drum (Ugo Basile, Comerio, Italy) for two trials with a minimum 2 min interval between trials. The rotarod started at 4 rpm and increased to 40 rpm over a 5 min period. Pre-training is performed the day before baseline and consisted in two rides for 1 minute each at a constant velocity.

Fig. 38. Rotarod

Grip Strength Meter test

In a separate assessment of forelimb strength, a mouse is suspended by the tail and lowered until it grasped the loop of a mouse grip-strength meter (Ugo Basile). The mouse is then gently pulled away from the loop and the maximum grip force exerted by the mouse before losing its grip is recorded.

Ten trials are made per animal per time point and the average of these readings represents the animal's forelimb grip force at that particular time.

Fig. 39. Grip Strenght Meter system

Basal activity

Animals activity is automatically recorded with video-tracking in specially designed cages (PhenoTyper®, Noldus Information Technology, Wageningen, The Netherlands). The cages are divided into two rooms with a white plastic sheet to a final arena of 45x21x60cm per animal. Each cage contains a top-unit with built-in hardware for video-tracking, i.e. a digital infrared-sensitive video camera and infrared lights. These provides constant and even illumination of the cage. An infrared filter placed in front of the camera prevent the interference with room illumination. This method allows behavioural recording in both

dark and light periods. EthoVision XT (Noldus Information Technology, Wageningen, The Netherlands) is used as video-tracking software (Fig. 40).

Four home cages are connected to a single PC. The video images of these cages are converted into a single video image by a Quad unit. Nine home cages in total, each divided into two rooms are used in this experiment.

The cages are made of transparent Perspex walls with an white plastic floor covered with sawdust. Each cage contained a single animal. All cages were provided with bedding material (sawdust) and paper shreds (Enviro Dri®, TecniLab) as environmental enrichment A feeding station and a water bottle are attached to the outside of the cage wall.

Observations of home cage behaviour activity are recorded for 4 consecutive weeks (one week of baseline and 3 weeks after treatment). Video tracking is performed at a rate of 25000sample/sec. All parameters are calculated in 1-h bins and subsequently lumped into 12-h fragments to distinguish between dark and light periods. For circadian rhythmicity no lumping is performed, instead hourly values at each time point (baseline, 24h, 1, 2, 3 weeks) are used.

'Distance moved' total (distance travelled by the animal in the cage in one hour) is used as parameters for the analysis.

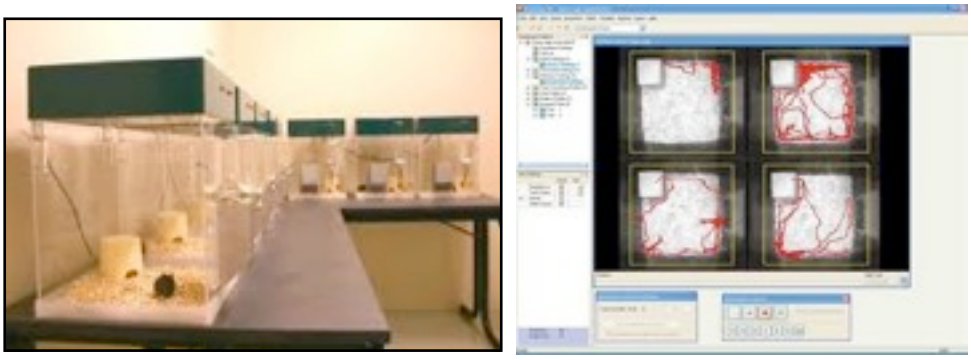

Fig. 40. Phenotypers cages for animal activity recording and analysis. On the right an example of Ethovision XT analysis.

Surgeries

After 1 week from animals arrival the surgeries are started. Mice were implanted with the telemetry transmitters TA11ETA-F10 (Data Science International, DSI PhysioTel transmitters, Arden Hills, MN, U.S.A).

Radio-telemetry is a technique that allows us to monitor and analyse electroencephalograms, locomotor activity and temperature in conscious and freely moving animals: these

devices continuously sense, process and transmit information from the animal to a data storing system.

Prior to the surgery all animals received Medetomidine (Domitor 0.05 mg/kg s.c) as sedative 5 min before the anesthetic Tiletamina+Zolazepam (Zoletil 20 mg/kg i.p); after anaesthesia (before the beginning of the surgery) the analgesic Carprofen (Rimadyl 5 mg/kg s.c), and prophylactic antibiotic Amoxicilina (Clamoxyl 150 mg/kg s.c) were done.

During the surgery the animal is shaved laterally and on the head. Incision is made on the lateral of the abdomen where the transmitter will be placed. Catheters containing two electrodes are passed subcutaneously from the abdomen up to an incision made over the skull, passing close to the scapula. The electrodes are then placed in the cortical zone and fixed with tissue glue and dental cement. Once the suture closed, the animal was awakened from anaesthesia with Atipamezole (Antisedan 5 mg/kg s.c.). Four weeks of recovery follow the surgeries.

Electrocorticogram recording

The electrocorticogram (ECoG) recording has been done using telemetric technology (Dataquest® A.R.T. Data Acquisition 3.0 for telemetry systems, Data Sciences International, Arden Hills, MN, USA). We use probes implanted subcutaneously on the back, with subcutaneous electrodes leading to the sub-dura mater above the parietal cortex. ECoG are recorded 24h/day from baseline to week three. All data are analysed with NeuroScore® (Data Sciences International) data system.

Long term potential (LTP) recording

LTP recordings are performed similar to Selig et al. (1995).

The hippocampal slice preparation

To obtain hippocampal slices, a mouse is anaesthetised with isofluorane (4%) and decapitated. Its brain is quickly removed from skull and placed in ice-cold artificial cerebrospinal fluid (ACSF) containing NaCl 126 mM, KCl 2.5 mM, $CaCl_2$ 2.4 mM, $MgCl_2$ 1.2 mM, NaH_2PO_4 1.2 mM, $NaHCO_3$ 24 mM and glucose 11 mM, bubbled with 95% O_2 and 5% CO_2. The brain is hemisected, cut into 400 μm horizontal slices containing the hippocampus on a vibrating slicer (VT1200S, Leica) and then transferred to a holding chamber to be equilibrated at 33ºC for at least 2 h.

Experimental set up

A pair of bipolar tungsten stimulating electrode is positioned in the *stratum radiatum* of the CA1 area (Schaffer collateral), approximately 300-400 µm from the recording site and ~200 µm from the CA1 pyramidal cell layer, at a depth of 100-200 µm. To record field excitatory postsynaptic potentials (fEPSP), the recording electrode, filled with ACSF, is positioned in the *stratum radiatum* at a similar distance from the pyramidal cell layer in the CA1 (Fig. 41). After establishing a stimulus-response profile of fEPSP by applying an increasing stimulus voltage every 15s (5V, 10V, 20V, 35V, 50V) until the maximum response is reached, a stable baseline fEPSP is then recorded for 30 mins (stimulated every 60 s) at a constant stimulus intensity that yielded a half-maximal fEPSP amplitude. To induce LTP, tetanic stimulations are delivered using the same stimulation intensity as for baseline. In the 3-week group, two tetanic stimulations are applied with a frequency of 100 Hz for 1 s, separated by 10 s interval, while in the 1-week group 4 tetanic stimulations of 1 s with an interval of 20 s are performed. Then the normal baseline recording settings resumed for a further 90 mins post-LTP induction. The fEPSPs are quantified by measuring the peak amplitudes for each episode and plotted against time.

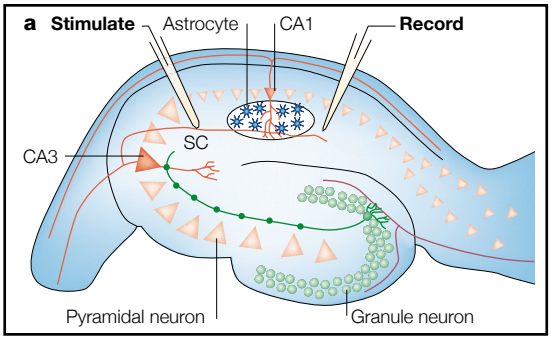

Fig. 41. Schematic representation of LTP recording.

Statistical analysis

Two ways ANOVA for repeated measures analysis of variance is used to examine novel object recognition test (N=8), rotarod (N=8), grip strengh meter test (N=8), distance moved during NOR test (N=8) and home cage activity (N=8).

Student's *t*-test is used to compare microglia cell counting (N=4, 4 sections per animal), Western Blot (N=5) and LTP (N=5).

Paired Student's *t*-test is used to compare Optical imaging data (N=3).

Two ways ANOVA is used to compare cytokines quantification ($N_{control}$=2; N_{QDs}=3) and ICP-MS data.

One way ANOVA is used to compare sleep/wake period scoring (N=3),

Statistical significance is assessed using an alpha level of 0,05. Statistical analyses are conducted using GraphPad Prism 5 for Mac (La Jolla, CA, USA).

APPENDIX - QDs Biodistribution and effects

QDs composition	[QD] used	Cells, tissue, organ, animals used	Exposure time	Biological fate	Observed toxicity	References
InP/ZnS Dendron coated	Emission wavelength: 710nm Dose: 1 nmol/animal	Intravenous injection in BALB-c mice	30, 60, 120 minutes	- Near-infrared emission, high stability in biological media, suitable size	- QD710-Dendron lacks significant toxicity at the doses tested	Gao et al., 2012
				- One day following administration, approximately 60% of QD710-Dendron was eliminated from the body based on the ICP-MS results. Organ/tissue accumulation was found to be highest in the liver, spleen, and kidney. Renal and hepatobiliary clearance.		
CdSe/ZnS Amino (PEG) anti-HER2ab (imaging of breast cancer) (Invitrogen) and CdSe/ZnS	Emission wavelength 525nm. Dose: 500nM	Wistar rats injected intravenously twice in the tail vein, once on day 0 and once on day 15	8 weeks	- Both QDs accumulated in the liver, kidney and spleen.	- The biochemistry panel assay showed nonsignificant changes in the anti-HER2ab-QDs treated group but these changes were significant in QDs treated group. No tissue damage, inflammation, lesions, and QDs deposition were found in histology and TEM images of the anti-HER2ab-QDs treated group. Apoptosis in liver and kidney was not found in the anti-HER2ab-QDs treated group. Animals treated with nonconjugated QDs showed comet formation and apoptosis. Cadmium deposition was confirmed in the QDs treated group compared with the anti-HER2ab-QDs treated group	Tiwari et al., 2011
aqueous synthesised QDs (aqQDs)		Injected in mice		- aqQDs are initially accumulated in liver after short-time (0.5-4 h) post-injection, and then are increasingly absorbed by kidney during long-time (15-80 days) blood circulation. Moreover, obviously size-dependent biodistribution is observed: aqQDs with larger sizes are more quickly accumulated in the spleen	- Histological and biochemical analysis, and body weight measurement demonstrate that there is no overt toxicity of aqQDs in mice even at long-time exposure time	Sui et al., 2011
CdTe/CdSe/ZnS carboxylated (COOH) and amino (NH_2) polyethylene glycol (PEG)-(Invitrogen)	250 µl of QDs (40 nM)	J774.A1 'murine macrophage-like' cells	10, 30, 60 and 120 min	- COOH and NH_2 (PEG) QDs, as well as 20 nm and 200 nm polystyrene beads were located within lysosomes and the mitochondria of macrophages after 2 h. Elemental transmission electron microscopy confirmed both COOH and NH_2 (PEG) QDs to be located within membrane-bound compartments at this time point.	- Toxicity was not assessed in this study.	Clift et al., 2011
CdSe/ZnS COOH (negative charge)	18 nm. Emission wavelength 655nm	Monocytes CD14+ isolated from porcine blood and differentiated into dendritic cells (DCs) with GM-CSF and IL-4	24h	- Monocytes showed cellular uptake of QDs, while lymphocytes did not. Monocyte differentiation into DCs increased the cellular uptake by sixfold when dosed with 2 nM of QDs.	- Viability assays, including 96AQ, CCK-8, alamar blue and ApoTox, exhibited minimal toxicity in DCs dosed with QDs at 24 h. Glutathione levels showed a significant decrease with 10 nM of QDS. QDs exposure was associated with a decrease in CD80/CD86 expression after LPS stimulation, suggesting suppression with DC maturation.	Zang et al., 2011
				- Transmission electron microscopy depicted QDs in the cytoplasmic vacuoles of DCs. Twelve endocytic inhibitors demonstrated QDs endocytosis in DCs, which was recognised by clathrin and scavenger receptors and regulated by F-actin and phospholipase C.		
				- DC maturation with lipopolysaccharide (LPS) caused an increase in QDs uptake compared with DCs without LPS stimulation.		
QDs(705) and $CdCl_2$	705nm	Intravenous injection in mice		- QD705 were detected in the brain during early exposure.Liver and spleen demonstrated a constant Cd concentration for 28 days after QD705 injection that the authors attributed to intact QD705 stored in mononuclear phagocytes. The kidneys showed a time-dependent accumulation of Cd in the QD705-exposed animals. By day 28, Cd in the kidneys from QD705 was 3-fold that of $CdCl_2$. QD705 have a longer kinetics in distribution and metabolism than $CdCl_2$.	QD705 showed a longer plasma and body retention than $CdCl_2$	Yeh et al., 2011
CdTe/CdSe encapsulated in poly(lactic-co-glycolic acid) (PLGA)	Size: 135.0-162.3 nm Dose: 20 µM	Intravenous injection in mice	1 h, 24 h, 48 h and 72 h	- QDs-loaded PLGA nanoparticles showed stability, high cellular uptake and long circulation time in vivo	- Cytotoxicity (MTT assay) of QDs-loaded PLGA nanospheres was comparable with that of empty PLGA nanospheres at least for 48 h treatment	Kim et al., 2011
	5, 40, 100 and 160 µM	KB cells	48h			

Table X. Biological fate of QDs

QDs composition	[QD] used	Cells, tissue, organ, animals used	Exposure time	Biological fate	Observed toxicity	References
CdSe QDs	20 nM $CdCl_2$, 5 nM, 10 nM and 20 nM QDs	murine hepatoma cells, Hepa 1–6, and monocyte-macrophage, J774A.1 cells	24 h and 48 h	- QDs distributed into various organs upon the in vivo administration. Liver appeared to be the predominant site for the QD accumulation.	- QDs promoted oxidative stress in vivo and in vitro	Liu et al., 2011
	Acute exposure: 200 nM $CdCl_2$ (292.8 ng/kg body weight), 20 nM (30.6 ng/kg body weight) and 200 nM (305.6 ng/kg body weight) CdSe QDs. Chronic exposure: 20 nM $CdCl_2$ (29.3 ng/kg body weight), 5 nM (7.6 ng/kg body weight) and 10 nM (15.3 ng/ kg body weight) QDs for 6 wks,	Intraperitoneal injection in mice	24 hrs after the final injection		- QDs induced dramatic hepatic toxicity in vivo and in vitro, which was much greater than that induced by cadmium ions at a similar or even a higher dose.	
CdTeSe/CdZnS QDs	20pmol	Female balb/c mice injected subcutaneously in the distal part of the right anterior paw	5, 15, 30, and 60 min; 4, 24, 48, 96 h and 10 days	QDs remain trapped in these LNs during several days. Liver is the organ of the reticuloendothelial system with the higher QD concentrations after s.c. injection. This accumulation is much lower than that observed after QD i.v. injection. During 10 days of observation, QDs were not cleared from the body neither by urine nor faeces (data not shown), suggesting that QDs are sequestered in vivo	- Increased inflammation	Pic et al., 2010
CdSe/ZnSe Mercaptopropionic acid (MPA) and Gum arabic (GA)/tri-n-octylphosphine oxide (TOPO)	1 nM MPA-coated QDs, 0.373 nM GA/TOPO-QDs, 0.746 nM GA/TOPO-QDs, 10 μM $CdCl_2$, and 50 μM $CdCl_2$	BALB/3T3 fibroblast cells	24h	- MPA-coated QDs were distributed inside the cytoplasmic region of cells. In contrast, GA/TOPO-coated QDs were not found inside cells.	- MPA-coated QDs were highly cyto-compatible, whereas GA/TOPO-coated QDs were toxic to the cells. Cells treated with GA/TOPO-coated QDs showed altered morphology, decreased viability, significant concentrations of intracellular free cadmium, detectable reactive oxygen species (ROS) formation, depolymerised cytoskeleton, and irregular-shaped nuclei.	Mahto et al., 2010
CdTe/CdS 3-mercaptopropionic acid (MPA) or polyethylene glycol (PEG) or SiO2	MPA-coated QDs (532), QDs(599), and QDs(656). TEM measured sizes: 1.67 ± 0.29 nm, 2.59 ± 0.43 and 3.21 ± 0.32 nm respectively. After coating with PEG or SiO2 shells, the QDs (656) increased in size to 4.20 ± 0.86 and 4.09 ± 1.02 nm, respectively. Doses: 350ul containing 20, 50, 86, or 125 mg Cd.	Intravenous injection in Kun Ming pregnant mice. The pregnant mice gave birth 1–5 days post-injection.	24h	QDs may be transferred from female mice to their foetuses across the placental barrier. Smaller QDs are more easily transferred than larger QDs and the number of QDs transferred increases with increasing dosage. Capping with an inorganic silica shell or organic polyethylene glycol reduces QD transfer but does not eliminate it	Toxicity was not assessed in this study.	Chu et al., 2010
CdTeSe/ZnS NH2 PEG (Initrogen)	40 nM	J774.A1 murine 'macrophage-like' cell	2h	- Elemental co-localization analysis of two elements present in the QDs (sulfur and cadmium) was performed on putative intracellular QDs with electron spectroscopic imaging (ESI). Both elements were shown on a single particle level and QDs were confirmed to be located inside intracellular vesicles. ESI analysis showed that not all nano-sized structures, initially identified as QDs, were confirmed.	Toxicity was not assessed in this study.	Brandenberger et al., 2010

Table X. Biological fate of QDs

QDs composition	[QD] used	Cells, tissue, organ, animals used	Exposure time	Biological fate	Observed toxicity	References
CdSe/ZnS - captopropil	13.5 (636nm)	Intraperitoneally in male ICR mice	6h	- QD-cap were delivered through systemic blood circulation. Mass balance studies of organs revealed: liver (2,25%), spleen (1,57%), kidney (0,718%) and brain (0,101%)	Toxicity was not assessed in this study.	Kato et al., 2010
				- Although QD-cap were predominantly located inside the blood vessels in liver, kidney and brain, a few were distributed in the brain parenchyma.		
				- The mass balance studies in the brain areas: brainstem (29,4%), thalamus (38,76%), Basal ganglia (2,64%), Hippocampus (1,98%), Cortex (21,36%), Olfactory bulbs (3,2%), Cerebellum (2,66%)		
CdTe QDs	1mmol/L, 10ul	nasal; once in ICR mice	30m	Located in the olfactory bulbs	Toxicity was not assessed in this study.	Yin et al., 2010
CdSeTe non targeted (Invitrogen) QDs705	40pmol	Intravenous injection in ICR mice	1 day, 1, 2, 4, 16 weeks	- After 4 weeks QDs accumulated in liver, kidney in a minor quantity in the spleen. No Cd was detected in urine and plasma, while CdCl2 mostly accumulated in in kidney, spleen and urine.	- The molar ratio of Cd/Te and the Metallothionein-1 (MT-1) expression demonstrated that the Cd/Se/Te complex is not stable or biologically inert. The increased MT protein was induced in the PCT epithelial cells of the kidneys indicating that QD705 was broken down in the kidneys with the release of free Cd which induced MT production in the renal epithelial cell.	Lin et al., 2009
CdCl2				- After 16 weeks Cd concentration was still high in the liver but increased the amount in the kidney		
Methoxy-PEG-5000 CdTe QDs	40pmol	i.v.; once in male ICR mice		- Persisted in the spleen, liver, and kidneys for at least 28 days. Partially eliminated after 6 months	- Mitochondrial alterations in renal tubular epithelial cells	Lin et al., 2008
CdSe QDs coated with silica	5nmol/mouse	i.v.; once in ICR male mice		- Mainly in the liver, kidneys, spleen and lungs. 33.3% and 23.8% of QDs in feaces and urine.	Toxicity was not assessed in this study.	Chen et al., 2008
AFP-Ab (Aplha fetoprotein monoclonal antibody CdsSe QDs	1,44-3600pmol/ mouse	i.v.; once in Balb-c male mice		- At the time point of 24 h, the QD–AFP-Ab probes were mainly distributed in the liver, spleen, and kidneys	- No animal died in the test group and no difference in body weight	Chen et al., 2008

Table X. Biological fate of QDs

QDs composition	[QD] used	Cells, tissue, organ, animals used	Exposure time	Biological fate	Observed toxicity	References
Carboxyl- and amine- CdSe QDs		i.v.; once in male Balb-c mice		- QDs were mainly found in the lungs, liver, and blood.	- Marked vascular thrombosis for carboxyl-QDs at high dose	Geys et al., 2008
fat- CdSe QDs		orally; Wistar rats		- QDs were degraded in the digestive tract. QDs with fat were more stable and degraded more slowly than bare ones.	Toxicity was not assessed in this study.	Karabanovas et al., 2008
Carboxylic acid group CdSeQDs	40pmol	s.c.; one in female fox mice		- Located in axillary lymph nods. Most of the injected QDs remained at the injec-tion site.	Toxicity was not assessed in this study.	Robe et al., 2008
Commercial PEGylated QD 545, QD 655, QD 705	QD-PEG CdSe/ ZnS core diameter (3-8nm); particle diameter (20-50m)	PC12 cells and primary cortical cultures. 30nM	24h	- PEGylated QD gave stronger signal compared to non PEGylated QD. In primary neuronal culture the uptake was higher in glia cell than neurons (<0,5% neurons relative to glia)	The biocompatibility as assessed by Alman Blue and cell counting was not significantly different from naive control PC12 cells, except when the cells were treated with non PEGylated QD 595.	Maysinger et al., 2007
Non commercial non PEGylated CdTe QDs and cerium oxide				-From cortical culture: no detection of QD in the mitochondria. Detection of QDs in lysosomes.		
Commercial PEGylated QD 545, QD 655, QD 705	QD-PEG CdSe/ ZnS core diameter (3-8nm); particle diameter (20-50m)	Subcutaneously in mice	1 h, 24 h, 72 h, 7 days	- The majority of the injected QDs accumulated within the Iba-1 positive microglia cells.	The astrocytes density was higher at 24h after administration in animals receiving QD705 as compared to control, receiving saline. There was no marked difference after 7 days. No detectable damage to either neurons or glia.	
Non commercial non PEGylated CdTe QDs and cerium oxide				- Fluorescent activated cell sorting and confocal microscopy showed that internalisation of QDs do not cause marked cell damage within one week.		
InAs/ZnSe-DHLA-PEG	8.7 nm	Injected both subcutaneously and intravenously (in both mice and rats)	Approximately 5 min	- QD were specifically engineered to have small diameters.	Toxicity was not assessed in this study.	Zimmer et al., 2006
				- When injected subcutaneously, QD migrated to sentinel lymph nodes, as observed previously with larger QD, but also migrated further into the lymphatic system.		
				- QD injected intravenously were shown to extravasate from the vasculature (first demonstration of this point in the literature).		
CdSe/ZnS-MAA-targeting peptides PEG	(maximal emission spectra at both 550 and 625 nm). In absence of peptide: 3.5 nm (green) or 5.5 nm (red). Diameter with peptide not reported, but size was approx. 190 kDa.	Intravenous injection into the tail vein (mice)	5–20 min	- QD were specifically targeted to the circulatory systems of normal lungs and tumours using peptides.	Toxicity was not assessed in this study.	Akerman et al., 2002
				- QD also accumulated in the liver and spleen, regardless of the peptide used for targeting.		
				- Adding PEG to the QD was shown to partially inhibit the nonspecific uptake of QD into the liver and spleen (suggesting the involvement of RE cells).		

Table X*X*. Biological fate and effects of QDs

QDs composition	[QD] used	Cell, tissue, organ, animal tested	Exposure time	Observed toxicity	References
Carboxyl-QDs and amine-QDs	data not shown in the abstract	data not shown in the abstract	data not shown in the abstract	- Amine-modified QDs, but not carboxyl-QDs, were strongly associated with the vessel wall of postcapillary venules and amplified ischemia-reperfusion-elicited leukocyte transmigration. Strong association of amine-QDs with microvessel walls was also present in the postischemic myocardium.	Rehberg et al., 2012
				- Electron microscopy and FACS analyses revealed that amine-modified QDs, but not carboxyl-QDs, were associated with endogenous microparticles. At microvessel walls, these aggregates were attached to endothelial cells.	
CdSe	invertebrate freshwater model, Hydra vulgaris			- Sub-lethal doses of QDs caused time and dose dependent morphological damages more severe than Cd(2+) ions at the same concentrations, impaired both reproductive and regenerative capability, activated biochemical and molecular responses. Low QD doses, apparently in the absence of morphological damages, caused early changes in the expression of general stress responsive and apoptotic genes	Ambrosone et al., 2012
$CdS/Cd(OH)_{(2)}$	(0.52mgCd/m(3))	Wistar rats head-nose exposed	6h/day on 5 days	- $CdS/Cd(OH)_{(2)}$ QD caused local neutrophil inflammation in the lungs that partially regressed after the 3-week recovery period. There was no evidence that QD were translocated to the central nervous system nor that a systemic acute phase response occurred	Ma-Hock et al., 2012
CdTe		mitochondria isolated from rat livers		- QDs affected the mitochondrial membrane properties, bioenergetics and induced mitochondrial permeability transition (MPT)	Li et al., 2011
CdSe/ZnS octylamine-poly (acrylic acid) (OPA) modified	545nm and 605nm	human skin cells	24h	- QD545 and QD605 show low cytotoxic response in HaCaT keratinocyte cells with TC50 values of 818.2 nM and 162.0 nM, respectively. Pretreatment with silibinin, an antioxidant molecule with membrane stabilising properties, significantly reduced QD-induced cell death in A375 and A375-S2 cells.	Zeng et al. 2011
Aqueous synthesised QDs (aqQDs): CdTe, CdTe/CdS core-shell structured and CdTe/CdS/ZnS core-shell-shell structured aqQDs and $CdCl_2$	37nM - 600nM	HEK293 cells	10h	- CdTe/CdS/ZnS core-shell-shell structured QDs are nearly nontoxic to cells further confirmed the role of released cadmium ions on cytotoxicity, and the effective protection of the ZnS shell. However, intracellular level of Cd^{2+} ions cannot be the only reason since the comparison with $CdCl_2$-treated cells suggests there are other factors contributed to the cytotoxicity of aqQDs. The studies on genome-wide gene expression profiling and subcellular localisation of aqQDs with synchrotron-based scanning transmission X-ray microscopy (STXM) suggested that the cytotoxicity of CdTe QDs not only comes from the release of Cd^{2+} ions but also intracellular distribution of QD nanoparticles in cells and the associated nanoscale effects	Chen et al., 2011
CdSe mercaptoacetic acid (MAA) - and CdSe doped with 1% cobalt ions of similar size	QDs Size: 5.0 ± 0.2 nm. Doses: 500, 1000, and 2000 mg/kg	per os in mice	2 and 7 days of treatment	- After two days of treatment, the high dose of doped MAA-QDs was significantly able to induce DNA damage, formation of micronuclei (MNs), and generation of DNA adduct (8-hydroxy-2-deoxyguanosine, 8-OHdG). However, increasing DNA damage and the frequency of MNs formation as well as the generation of DNA adducts were observed with both the undoped MAA-QDs (2000 mg/kg) and doped MAA-QDs (1000 and 2000 mg/kg) after seven days of treatment	Khalil et al., 2011
CdSe short-chain thioglycolic acid (TGA)	15 µg/ml, 30 µg/ml and 45 µg/ml	NIH/3T3 cells	12 and 24 h	- The expression patterns of miRNAs were altered by CdTe QDs in cells with apoptosis-like death with time- and dose-dependent tendencies. The differential expression of miRNAs are induced by CdTe QDs at the processing of miRNA biogenesis, which is an adaptive process of cells to external stimuli.	Li et al., 2011
				- As a regulator in miRNA biogenesis, p53 is involved in the transcription and processing of pri-miRNA. With no significant changes in the mRNA levels of p53, the increase in overall p53 protein levels and its post-translational modification by phosphorylation at Ser-15 are induced by CdTe QD treatment.	
CdTe mercaptosuccinic acid (MSA)	0.1-100µg/mL	human umbilical vein endothelial cells (HUVECs)		- Dose-dependently decreased the cell viability of HUVECs, indicating CdTe QDs induced significant endothelial toxicity	Yan et al., 2011
				- 10µg/mL CdTe QDs elicited significant oxidative stress, mitochondrial network fragmentation as well as disruption of mitochondrial membrane potential ($\Delta\psi$(m)); whereas ROS scavenger could protect HUVECs from QDs-induced mitochondrial dysfunction. Moreover, upon 24h exposure to 10µg/mL CdTe QDs, the apoptotic HUVECs dramatically increased by 402.01%, accompanied with alternative expression of apoptosis proteins, which were upregulation of Bax, downregulation of Bcl-2, release of mitochondrial cytochrome c and cleavage of caspase-9/caspase-3.	
ZnS and CdS QDs	1 and 10microM	human endothelial cells (EA hy926)	3, 4 and 6 days	The ZnS QDs with all four distinct types of surface conditions were nontoxic at all concentrations for at least 6 days. The CdS QDs with (3-mercaptopropyl) trimethoxysilane (MPS)-replacement plus silica capping were less cytotoxic than those with 3-mercaptopropionic acid (MPA) capping and those with MPS-replacement capping.	Li et al., 2011
				The CdS QDs were nontoxic only at 1 microM, and showed significant cytotoxicity at 10 microM after 3 days. Comparing the results of ZnS and CdS QDs with the same particle size, surface condition and concentration, it is indicated that the cytotoxicity of CdS QDs and the lack of it in ZnS QDs	
CdTe QDs	2 and 200 µM	living T. cruzi protozoa	72 h and 7 days	after 72 h, a 200 µM cadmium telluride (CdTe) QD solution induced important morphological alterations in T. cruzi, such as DNA damage, plasma membrane blebbing and mitochondrial swelling. No damage to the plasma membrane when incubated with 200 µM CdTe QDs for up to 72 h, giving no evidence of classical necrosis. Parasites incubated with 2 µM CdTe QDs still proliferated after seven days.	Vieira et al., 2011
				A low concentration of CdTe QDs (2 µM) is optimal for bioimaging, whereas a high concentration (200 µM CdTe) could be toxic to cells	

Table X*X*. Biological fate and effects of QDs

QDs composition	[QD] used	Cell, tissue, organ, animal tested	Exposure time	Observed toxicity	References
CdSe/ZnS- NH2 (positive), -COOH (negative), -PEG (neutral)	QDs (565) and QDs (655). QD565 was spherical, with an outside diameter of 4.6 nm, and QD655 was ellipsoid (6 nm ×12 nm). In vitro doses: 5, 10, and 20 nM	Bovine cornea	24 h and 48h	- QDs penetrated and were retained within the cornea for a relatively long period while the epithelium is injured. QDs affected corneal stromal cell viability up to a significant magnitude of 50%, under a relatively low concentration (20 nM) and short duration (48 h).	Kuo et al., 2011
	1mM	Injection into the eyes of mice	26 days	- QDs were proven to accumulate within the cornea in vivo for a much longer duration than that (26 days)	
CdSe/ZnS PEG, BSA, polymer (negative charged)	Size: 2-6nm. Doses: 15, 5, 2,5 nmol.	Systemic administration in Sprague Dawley rats.	1, 3, 10, 23, 84 days and surface chemistry study : 1, 3, 5, 7, 15, 30	Even at high doses (15 nmol), QDs do not cause significant toxicity in Sprague–Dawley rats over the course of this long- term study. Chronically dosed rats, which received a total of 60 nmol of QDs over 4 weeks, did not experience QD toxicity.	Hauck et al., 2010
CdSe QDs	1, 10, 50 microg/ml	Human umbilical vein endothelial cells	12h	- Formation of yH2AX foci, indicative of DNA damage, in a dose-dependent manner. Moreover, QD treatment clearly induced the generation of reactive oxygen species (ROS). Pre-treatment with N-acetyl-cysteine (NAC), a ROS scavenger, could inhibit the induction of ROS by QDs, as well as the formation of yH2AX foci.	Zhang et al., 2010
CdTe QDs	Emission wavelength: Green-QDs 535nm (size: 2.04 nm); Red-QDs 654 nm (size: 3.79nm)			- It is a study on toxic interaction of CdTe QDs with human serum albumin (HSA). The size of the nanoparticles affected the affinity for HSA and the increasing size of QDs enhanced the affinity for HSA.	Xiao et al., 2010
CdTe gelatinised and non-gelatinised Thioglycolic acid (TGA)		pheochromocytoma 12 (PC12) cells	72h	- Cell viability, DNA quantification and proliferation were affected by the presence of the QDs at various concentrations and incubation times. Cell response was found to not only be concentration dependant but also influenced by the surface environment of the QDs. Gelatine capping on the surface acts as a barrier towards the leaking of toxic atoms, thus reducing the negative impact of the QDs	
CdTe, CdTe/SiO (2) and Mn-doped ZnSe		in vitro study		- CdTe/SiO(2) NPs led to much less DNA damage when compared with CdTe QDs, as a silica overcoating layer could isolate the QDs from the external environment. Mn:ZnSe d-dots as a new class of non-cadmium doped QDs demonstrated almost no damage for DNA molecules	Wang et al., 2010
CdSe QDs	2-3nm diameter	Intrahippocampal injection in DG in Wistar rats of 0,5nM and 10nM solutions	120 minutes after injection	- QDs, no matter whether they are modified or not, could enhance basal synaptic transmission and impair short- and long-term synaptic plasticity in rat hippocampal DG area, including I/O functions, PPF and LTP.	Tang et al., 2009
CdSe/ZnS streptavidin (Molecular probe)	15-20nm (565nm emission peak)				
CdTe QDs	137,5ug	i.t.; once in female ApoE-/- female mice		inflammation, genotoxicity	Jacobsen et al., 2009
CdSe	0–500 nM	oocyte	24h	- CdSe-core QDs have cytotoxic effects on mouse blastocysts and are associated with defects in subsequent development	Hsieh et al., 2009
CdSe/ZnS		oocytes		- CdSe-core QDs induced a significant reduction in the rates of oocyte maturation, fertilisation, and in vitro embryo development, but not ZnS-coated CdSe QDs. Treatment of oocytes with 500 nM CdSe-core QDs during in vitro maturation (IVM) led to increased resorption of postimplantation embryos and decreased placental and foetal weights.	
CdSe/ZnS Carboxyl and CdSe/ZnS Amine	9 nmol/mL	Intravenous injection in male Balb-c High dose (720-3,600 pmol/mouse) and low dose (1,44-144pml/mouse)	1h, 4h, 24h	At doses of 3,600 and 720 pmol/mouse, QDs caused marked vascular thrombosis in the pulmonary circulation, especially with carboxyl-QDs, most likely by activating the coagulation cascade via contact activation. They saw an effect of surface charge for all the parameters tested. QDs were mainly found in lung, liver, and blood. Thrombotic complications were abolished, and P-selectin was not affected by pretreatment of the animals with heparin. In vitro, carboxyl-QDs and amine-QDs enhanced adenosine-5´-diphosphate–induced platelet aggregation.	Geys et al., 2008
		Human and murine platelet-rich plasma (PRP)		- Death after injection of high dose of carboxyl-QDs, no death with amino-QDs	
CdTe QDs	2ug/kg	i.v.; once; male rats		- Few signs of functional toxicity or clinical changes	Zhang et al., 2007
CdSe/ZnS and CdSe mercaptopropionic acid	2 - 10nM	MDA-MB-435S Breast Cancer Cells	18h	- Poisoning of NRK cells due to the release of Cd2+ ions starts at concentrations of 0.65 ± 0.12 μM and 5.9 ± 1.3 μM of surface Cd atoms for mercaptopropionic acid coated CdSe and CdSe/ZnS particles, respectively.	Kirchner et al., 2005
		NRK fibroblast	2 days		
		Two cell lines (RBL and CHO)	2 days	- No morphological changes of the cells were identified, although uptake of the nanocrystals by the cells was clearly verified by fluorescence microscopy. Patch-clamp recordings revealed no changes of ion channel function and characteristic electrophysiological properties of the cells between QDs incubated cells and controls.	

Table X*X*. Biological fate and effects of QDs

REFERENCES

Abbott, N. J., Rönnbäck, L., & Hansson, E. (2006). Astrocyte-endothelial interactions at the blood-brain barrier. Nature reviews. Neuroscience, 7(1), 41-53. doi:10.1038/nrn1824

About The Project on Emerging Nanotechnologies. (n.d.). Retrieved January 23, 2012, from http://www.nanotechproject.org/about/mission/

Abraham, W. C., Mason-Parker, S. E., Williams, J., & Dragunow, M. (1995). Analysis of the decremental nature of LTP in the dentate gyrus. Brain research. Molecular brain research, 30(2), 367-72.

Adams, L., & Davis, S. D. (2008). The Internal Anatomy of Home Range. American Society of Mammalogists.

Aderem, A., & Underhill, D. M. (1999). Mechanisms of phagocytosis in macrophages. Annual review of immunology, 17, 593-623. Annual Reviews 4139 El Camino Way, P.O. Box 10139, Palo Alto, CA 94303-0139, USA. doi:10.1146/annurev.immunol.17.1.593

Agrawal, A., Zhang, C., Byassee, T., Tripp, R. A., & Nie, S. (2006). Counting single native biomolecules and intact viruses with color-coded nanoparticles. Analytical chemistry, 78(4), 1061-70. American Chemical Society. doi:10.1021/ac051801t

Akerman, M. E., Chan, W. C. W., Laakkonen, P., Bhatia, S. N., & Ruoslahti, E. (2002). Nanocrystal targeting in vivo. Proceedings of the National Academy of Sciences of the United States of America, 99(20), 12617-21. doi:10.1073/pnas.152463399

Alivisatos, A. P. (1996). Semiconductor Clusters, Nanocrystals, and Quantum Dots. Science, 271(5251), 933-937. doi:10.1126/science.271.5251.933

Alivisatos, A P., Gu, W., & Larabell, C. (2005). Quantum dots as cellular probes. Annual review of biomedical engineering, 7, 55-76. doi:10.1146/annurev.bioeng.7.060804.100432

Ambrosone, A., Mattera, L., Marchesano, V., Quarta, A., Susha, A. S., Tino, A., Rogach, A. L., et al. (2012). Mechanisms underlying toxicity induced by CdTe quantum dots determined in an invertebrate model organism. Biomaterials, 33(7), 1991-2000. doi:10.1016/j.biomaterials.2011.11.041

Anas, A., Okuda, T., Kawashima, N., Nakayama, K., Itoh, T., Ishikawa, M., & Biju, V. (2009). Clathrin-mediated endocytosis of quantum dot-peptide conjugates in living cells. ACS nano, 3(8), 2419-29. doi:10.1021/nn900663r

Antonini, J. M., Sriram, K., Benkovic, S. A., Roberts, J. R., Stone, S., Chen, B. T., Schwegler-Berry, D., et al. (2009). Mild steel welding fume causes manganese accumulation and subtle neuroinflammatory changes but not overt neuronal damage in discrete

brain regions of rats after short-term inhalation exposure. Neurotoxicology, 30(6), 915-25. doi:10.1016/j.neuro.2009.09.006

Aouizerat, B. E., Dodd, M., Lee, K., West, C., Paul, S. M., Cooper, B. A., Wara, W., et al. (2009). Preliminary evidence of a genetic association between tumor necrosis factor alpha and the severity of sleep disturbance and morning fatigue. Biological research for nursing, 11(1), 27-41. SAGE Publications. doi:10.1177/1099800409333871

Aschner, M. (2009). Chapter 8 - Nanoparticles: Transport across the olfactory epithelium and application to the assessment of brain function in health and disease. Progress in brain research, 180, 141-52. doi:10.1016/S0079-6123(08)80008-8

Auerbach, J. M., & Segal, M. (1997). Peroxide modulation of slow onset potentiation in rat hippocampus. The Journal of neuroscience : the official journal of the Society for Neuroscience, 17(22), 8695-701.

Augustine, G. J., Santamaria, F., & Tanaka, K. (2003). Local calcium signaling in neurons. Neuron, 40(2), 331-46.

Bagalkot, V., Zhang, L., Levy-Nissenbaum, E., Jon, S., Kantoff, P. W., Langer, R., & Farokhzad, O. C. (2007). Quantum dot-aptamer conjugates for synchronous cancer imaging, therapy, and sensing of drug delivery based on bi-fluorescence resonance energy transfer. Nano letters, 7(10), 3065-70. American Chemical Society. doi:10.1021/nl071546n

Bakalova, R., Ohba, H., Zhelev, Z., Ishikawa, M., & Baba, Y. (2004). Quantum dots as photosensitizers? Nature biotechnology, 22(11), 1360-1. doi:10.1038/nbt1104-1360

Bakalova, R., Zhelev, Z., Aoki, I., Masamoto, K., Mileva, M., Obata, T., Higuchi, M., et al. (2008). Multimodal silica-shelled quantum dots: direct intracellular delivery, photosensitization, toxic, and microcirculation effects. Bioconjugate chemistry, 19(6), 1135-42. doi:10.1021/bc700431c

Bakalova, R., Zhelev, Z., Ohba, H., & Baba, Y. (2005). Quantum dot-conjugated hybridization probes for preliminary screening of siRNA sequences. Journal of the American Chemical Society, 127(32), 11328-35. American Chemical Society. doi:10.1021/ja051089h

Balasubramanian, S. K., Jittiwat, J., Manikandan, J., Ong, C.-N., Yu, L. E., & Ong, W.-Y. (2010). Biodistribution of gold nanoparticles and gene expression changes in the liver and spleen after intravenous administration in rats. Biomaterials, 31(8), 2034-42. doi:10.1016/j.biomaterials.2009.11.079

Ballou, B., Ernst, L. A., Andreko, S., Harper, T., Fitzpatrick, J. A. J., Waggoner, A. S., & Bruchez, M. P. (2007). Sentinel lymph node imaging using quantum dots in mouse tumor models. Bioconjugate chemistry, 18(2), 389-96. American Chemical Society. doi:10.1021/bc060261j

Ballou, B., Ernst, L. A., Andreko, S., Harper, T., Fitzpatrick, J. A. J., Waggoner, A. S., & Bruchez, M. P. (2007). Sentinel lymph node imaging using quantum dots in mouse

tumor models. Bioconjugate chemistry, 18(2), 389-96. American Chemical Society. doi:10.1021/bc060261j

Barroso, M. M. (2011). Quantum dots in cell biology. The journal of histochemistry and cytochemistry : official journal of the Histochemistry Society, 59(3), 237-51. SAGE Publications. doi:10.1369/0022155411398487

Bassi, G. S., Kanashiro, A., Santin, F. M., de Souza, G. E. P., Nobre, M. J., & Coimbra, N. C. (2011). Lipopolysaccharide-Induced Sickness Behaviour Evaluated in Different Models of Anxiety and Innate Fear in Rats. Basic & clinical pharmacology & toxicology. doi:10.1111/j.1742-7843.2011.00824.x

Bawendi, M. G., Carroll, P. J., Wilson, W. L., & Brus, L. E. (1992). Luminescence properties of CdSe quantum crystallites: Resonance between interior and surface localized states. The Journal of Chemical Physics, 96(2), 946. doi:10.1063/1.462114

Beattie, E. C., Stellwagen, D., Morishita, W., Bresnahan, J. C., Ha, B. K., Von Zastrow, M., Beattie, M. S., et al. (2002). Control of synaptic strength by glial TNFalpha. Science (New York, N.Y.), 295(5563), 2282-5. doi:10.1126/science.1067859

Becue, A., Moret, S., Champod, C., & Margot, P. (2009). Use of quantum dots in aqueous solution to detect blood fingermarks on non-porous surfaces. Forensic science international, 191(1-3), 36-41. doi:10.1016/j.forsciint.2009.06.005

Belarbi, K., Jopson, T., Tweedie, D., Arellano, C., Luo, W., Greig, N. H., & Rosi, S. (2012). TNF-alpha protein synthesis inhibitor restores neuronal function and reverses cognitive deficits induced by chronic neuroinflammation. Journal of Neuroinflammation, 9(1), 23. doi:10.1186/1742-2094-9-23

Belarbi, K., Jopson, T., Tweedie, D., Arellano, C., Luo, W., Greig, N. H., & Rosi, S. (2012). TNF-alpha protein synthesis inhibitor restores neuronal function and reverses cognitive deficits induced by chronic neuroinflammation. Journal of Neuroinflammation, 9(1), 23. doi:10.1186/1742-2094-9-23

Bergeret, F. S., Yeyati, A. L., & Martin-Rodero, A. (2007). Josephson effect through a quantum dot array. Physical Review B, 76(17), 9.

Berridge, M. J. (1998). Neuronal calcium signaling. Neuron, 21(1), 13-26.

Bhaskar, S., Tian, F., Stoeger, T., Kreyling, W., de la Fuente, J. M., GrazÃº, V., Borm, P., et al. (2010). Multifunctional Nanocarriers for diagnostics, drug delivery and targeted treatment across blood-brain barrier: perspectives on tracking and neuroimaging. Particle and fibre toxicology, 7, 3. doi:10.1186/1743-8977-7-3

Bliss, T. V., & Lomo, T. (1973). Long-lasting potentiation of synaptic transmission in the dentate area of the anaesthetized rabbit following stimulation of the perforant path. The Journal of physiology, 232(2), 331-56.

Bottrill, M., & Green, M. (2011). Some aspects of quantum dot toxicity. Chemical communications (Cambridge, England), 47(25), 7039-50. doi:10.1039/c1cc10692a

Bouldin, J. L., Ingle, T. M., Sengupta, A., Alexander, R., Hannigan, R. E., & Buchanan, R. A. (2008). Aqueous toxicity and food chain transfer of Quantum DOTs in freshwater algae and Ceriodaphnia dubia. Environmental toxicology and chemistry / SETAC, 27(9), 1958-63.

Boussif, O., Lezoualc'h, F., Zanta, M. A., Mergny, M. D., Scherman, D., Demeneix, B., & Behr, J. P. (1995). A versatile vector for gene and oligonucleotide transfer into cells in culture and in vivo: polyethylenimine. Proceedings of the National Academy of Sciences of the United States of America, 92(16), 7297-301.

Brandenberger, C., Clift, M. J. D., Vanhecke, D., MÃ¼hlfeld, C., Stone, V., Gehr, P., & Rothen-Rutishauser, B. (2010). Intracellular imaging of nanoparticles: is it an elemental mistake to believe what you see? Particle and fibre toxicology, 7, 15. doi:10.1186/1743-8977-7-15

Broadbent, N. J., Squire, L. R., & Clark, R. E. (2004). Spatial memory, recognition memory, and the hippocampus. Proceedings of the National Academy of Sciences of the United States of America, 101(40), 14515-20. doi:10.1073/pnas.0406344101

Brooks, S. P., Pask, T., Jones, L., & Dunnett, S. B. (2005). Behavioural profiles of inbred mouse strains used as transgenic backgrounds. II: cognitive tests. Genes, brain, and behavior, 4(5), 307-17. doi:10.1111/j.1601-183X.2004.00109.x

Brown, D M, Donaldson, K., Borm, P. J., Schins, R. P., Dehnhardt, M., Gilmour, P., Jimenez, L. A., et al. (2004). Calcium and ROS-mediated activation of transcription factors and TNF-alpha cytokine gene expression in macrophages exposed to ultrafine particles. American journal of physiology. Lung cellular and molecular physiology, 286(2), L344-53. doi:10.1152/ajplung.00139.2003

Bruchez Jr., M. (1998). Semiconductor Nanocrystals as Fluorescent Biological Labels. Science, 281(5385), 2013-2016. doi:10.1126/science.281.5385.2013

Bruchez, M. P. (2005). Turning all the lights on: quantum dots in cellular assays. Current opinion in chemical biology, 9(5), 533-7. doi:10.1016/j.cbpa.2005.08.019

Bruchez, M., Moronne, M., Gin, P., Weiss, S., & Alivisatos, A. P. (1998). Semiconductor nanocrystals as fluorescent biological labels. Science (New York, N.Y.), 281(5385), 2013-6.

Buzea, C., Pacheco, I. I., & Robbie, K. (2007). Nanomaterials and nanoparticles: sources and toxicity. Biointerphases, 2(4), MR17-71.

Cai, W., Chen, K., Li, Z.-B., Gambhir, S. S., & Chen, X. (2007). Dual-function probe for PET and near-infrared fluorescence imaging of tumor vasculature. Journal of nuclear medicine : official publication, Society of Nuclear Medicine, 48(11), 1862-70. Society of Nuclear Medicine. doi:10.2967/jnumed.107.043216

Calvo, P., Gouritin, B., Chacun, H., Desmaële, D., D'Angelo, J., Noel, J. P., Georgin, D., et al. (2001). Long-circulating PEGylated polycyanoacrylate nanoparticles as new drug carrier for brain delivery. Pharmaceutical research, 18(8), 1157-66.

Chan, P., Yuen, T., Ruf, F., Gonzalez-Maeso, J., & Sealfon, S. C. (2005). Method for multiplex cellular detection of mRNAs using quantum dot fluorescent in situ hybridization. Nucleic acids research, 33(18), e161. doi:10.1093/nar/gni162

Chan, W. C. (1998). Quantum Dot Bioconjugates for Ultrasensitive Nonisotopic Detection. Science, 281(5385), 2016-2018. doi:10.1126/science.281.5385.2016

Chan, W.H., Shiao, N.-H., & Lu, P.-Z. (2006). CdSe quantum dots induce apoptosis in human neuroblastoma cells via mitochondrial-dependent pathways and inhibition of survival signals. Toxicology letters, 167(3), 191-200. doi:10.1016/j.toxlet.2006.09.007

Chang, S.-quan, Dai, Y.-dong, Kang, B., Han, W., Mao, L., & Chen, D. (2009). UV-enhanced cytotoxicity of thiol-capped CdTe quantum dots in human pancreatic carcinoma cells. Toxicology letters, 188(2), 104-11. doi:10.1016/j.toxlet.2009.03.013

Chen, H., Titushkin, I., Stroscio, M., & Cho, M. (2007). Altered membrane dynamics of quantum dot-conjugated integrins during osteogenic differentiation of human bone marrow derived progenitor cells. Biophysical journal, 92(4), 1399-408. doi:10.1529/biophysj.106.094896

Chen, Lei, Yokel, R. A., Hennig, B., & Toborek, M. (2008). Manufactured aluminum oxide nanoparticles decrease expression of tight junction proteins in brain vasculature. Journal of neuroimmune pharmacology : the official journal of the Society on NeuroImmune Pharmacology, 3(4), 286-95. doi:10.1007/s11481-008-9131-5

Chibli, H., Carlini, L., Park, S., Dimitrijevic, N. M., & Nadeau, J. L. (2011). Cytotoxicity of InP/ZnS quantum dots related to reactive oxygen species generation. Nanoscale, 3(6), 2552-9. doi:10.1039/c1nr10131e

Cho, K., Wang, X., Nie, S., Chen, Z. G., & Shin, D. M. (2008). Therapeutic nanoparticles for drug delivery in cancer. Clinical cancer research : an official journal of the American Association for Cancer Research, 14(5), 1310-6. doi:10.1158/1078-0432.CCR-07-1441

Cho, S. J., Maysinger, D., Jain, M., Röder, B., Hackbarth, S., & Winnik, F. M. (2007). Long-term exposure to CdTe quantum dots causes functional impairments in live cells. Langmuir : the ACS journal of surfaces and colloids, 23(4), 1974-80. doi:10.1021/la060093j

Choi, A. O., Cho, S. J., Desbarats, J., Lovrić, J., & Maysinger, D. (2007). Quantum dot-induced cell death involves Fas upregulation and lipid peroxidation in human neuroblastoma cells. Journal of nanobiotechnology, 5, 1. doi:10.1186/1477-3155-5-1

Choi, H. S., Liu, W., Misra, P., Tanaka, E., Zimmer, J. P., Itty Ipe, B., Bawendi, M. G., et al. (2007). Renal clearance of quantum dots. Nature biotechnology, 25(10), 1165-70. doi:10.1038/nbt1340

Christopherson, K. S, Ullian, E. M., Stokes, C. C. A., Mullowney, C. E., Hell, J. W., Agah, A., Lawler, J., et al. (2005). Thrombospondins are astrocyte-secreted proteins that promote CNS synaptogenesis. Cell, 120(3), 421-33. doi:10.1016/j.cell.2004.12.020

Chu, M., Wu, Q., Yang, H., Yuan, R., Hou, S., Yang, Y., Zou, Y., et al. (2010). Transfer of quantum dots from pregnant mice to pups across the placental barrier. Small (Weinheim an der Bergstrasse, Germany), 6(5), 670-8. doi:10.1002/smll.200902049

Clift, M. J. D., Brandenberger, C., Rothen-Rutishauser, B., Brown, D. M., & Stone, V. (2011). The uptake and intracellular fate of a series of different surface coated quantum dots in vitro. Toxicology, 286(1-3), 58-68. doi:10.1016/j.tox.2011.05.006

Clift, M. J. D., Rothen-Rutishauser, B., Brown, D. M., Duffin, R., Donaldson, K., Proudfoot, L., Guy, K., et al. (2008). The impact of different nanoparticle surface chemistry and size on uptake and toxicity in a murine macrophage cell line. Toxicology and applied pharmacology, 232(3), 418-27. doi:10.1016/j.taap.2008.06.009

Colvin, V. L. (2003). The potential environmental impact of engineered nanomaterials. Nature biotechnology, 21(10), 1166-70. doi:10.1038/nbt875

Dabbousi, B. O., Rodriguez-Viejo, J., Mikulec, F. V., Heine, J. R., Mattoussi, H., Ober, R., Jensen, K. F., et al. (1997). (CdSe)ZnS Coreâ'Shell Quantum Dots: Synthesis and Characterization of a Size Series of Highly Luminescent Nanocrystallites. The Journal of Physical Chemistry B, 101(46), 9463-9475. American Chemical Society. doi:10.1021/jp971091y

Dahan, M., Lévi, S., Luccardini, C., Rostaing, P., Riveau, B., & Triller, A. (2003). Diffusion dynamics of glycine receptors revealed by single-quantum dot tracking. Science (New York, N.Y.), 302(5644), 442-5. doi:10.1126/science.1088525

Daneshvar, H., Nelms, J., Muhammad, O., Jackson, H., Tkach, J., Davros, W., Peterson, T., et al. (2008). Imaging characteristics of zinc sulfide shell, cadmium telluride core quantum dots. Nanomedicine (London, England), 3(1), 21-9. doi:10.2217/17435889.3.1.21

Dantzer, R., Bluthé, R. M., Layé, S., Bret-Dibat, J. L., Parnet, P., & Kelley, K. W. (1998). Cytokines and sickness behavior. Annals of the New York Academy of Sciences, 840, 586-90.

Das, G. K., Chan, P. P. Y., Teo, A., Loo, J. S. C., Anderson, J. M., & Tan, T. T. Y. (2010). In vitro cytotoxicity evaluation of biomedical nanoparticles and their extracts. Journal of biomedical materials research. Part A, 93(1), 337-46. doi:10.1002/jbm.a.32533

Davalos, D., Grutzendler, J., Yang, G., Kim, J. V., Zuo, Y., Jung, S., Littman, D. R., et al. (2005). ATP mediates rapid microglial response to local brain injury in vivo. Nature neuroscience, 8(6), 752-8. doi:10.1038/nn1472

De Jong, W. H., & Borm, P. J. A. (2008). Drug delivery and nanoparticles:applications and hazards. International journal of nanomedicine, 3(2), 133-49.

Decuzzi, P., & Ferrari, M. (2007). The role of specific and non-specific interactions in receptor-mediated endocytosis of nanoparticles. Biomaterials, 28(18), 2915-22. doi:10.1016/j.biomaterials.2007.02.013

Decuzzi, P., & Ferrari, M. (2007). The role of specific and non-specific interactions in receptor-mediated endocytosis of nanoparticles. Biomaterials, 28(18), 2915-22. doi:10.1016/j.biomaterials.2007.02.013

Dellu, F., Contarino, A., Simon, H., Koob, G. F., & Gold, L. H. (2000). Genetic differences in response to novelty and spatial memory using a two-trial recognition task in mice. Neurobiology of learning and memory, 73(1), 31-48. doi:10.1006/nlme.1999.3919

Dere, E., Huston, J. P., & De Souza Silva, M. A. (2007). The pharmacology, neuroanatomy and neurogenetics of one-trial object recognition in rodents. Neuroscience and biobehavioral reviews, 31(5), 673-704. doi:10.1016/j.neubiorev.2007.01.005

Derfus, A. M., Chen, A. A., Min, D.-H., Ruoslahti, E., & Bhatia, S. N. (2007). Targeted quantum dot conjugates for siRNA delivery. Bioconjugate chemistry, 18(5), 1391-6. American Chemical Society. doi:10.1021/bc060367e

Derfus, A. M., Chan, W. C. W., & Bhatia, S. N. (2004). Intracellular Delivery of Quantum Dots for Live Cell Labeling and Organelle Tracking. Advanced Materials, 16(12), 961-966. doi:10.1002/adma.200306111

Diamond, D., Dunwiddie, T., & Rose, G. (1988). Characteristics of hippocampal primed burst potentiation in vitro and in the awake rat. J. Neurosci., 8(11), 4079-4088.

Ditto, A. J., Shah, P. N., & Yun, Y. H. (2009). Non-viral gene delivery using nanoparticles. Expert opinion on drug delivery, 6(11), 1149-60. Informa UK Ltd London, UK. doi:10.1517/17425240903241796

Duan, H., & Nie, S. (2007). Cell-penetrating quantum dots based on multivalent and endosome-disrupting surface coatings. Journal of the American Chemical Society, 129(11), 3333-8. American Chemical Society. doi:10.1021/ja068158s

Dubertret, B., Skourides, P., Norris, D. J., Noireaux, V., Brivanlou, A. H., & Libchaber, A. (2002). In vivo imaging of quantum dots encapsulated in phospholipid micelles. Science (New York, N.Y.), 298(5599), 1759-62. doi:10.1126/science.1077194

Dubertret, Benoit, Skourides, P., Norris, D. J., Noireaux, V., Brivanlou, A. H., & Libchaber, A. (2002). In vivo imaging of quantum dots encapsulated in phospholipid micelles. Science (New York, N.Y.), 298(5599), 1759-62. doi:10.1126/science.1077194

Dumas, E. M., Ozenne, V., Mielke, R. E., & Nadeau, J. L. (2009). Toxicity of CdTe quantum dots in bacterial strains. IEEE transactions on nanobioscience, 8(1), 58-64. doi:10.1109/TNB.2009.2017313

D'Mello, C., & Swain, M. G. (2011). Liver-brain inflammation axis. American journal of physiology. Gastrointestinal and liver physiology, 301(5), G749-61. doi:10.1152/ajpgi.00184.2011

D'Mello, C., Le, T., & Swain, M. G. (2009). Cerebral microglia recruit monocytes into the brain in response to tumor necrosis factoralpha signaling during peripheral organ inflammation. The Journal of neuroscience : the official journal of the Society for Neuroscience, 29(7), 2089-102. Society for Neuroscience. doi:10.1523/JNEUROSCI.3567-08.2009

Echarte, M. M., Bruno, L., Arndt-Jovin, D. J., Jovin, T. M., & Pietrasanta, L. I. (2007). Quantitative single particle tracking of NGF-receptor complexes: transport is bidirectional but biased by longer retrograde run lengths. FEBS letters, 581(16), 2905-13. doi:10.1016/j.febslet.2007.05.041

Edmund, A. R., Kambalapally, S., Wilson, T. A., & Nicolosi, R. J. (2011). Encapsulation of cadmium selenide quantum dots using a self-assembling nanoemulsion (SANE) reduces their in vitro toxicity. Toxicology in vitro : an international journal published in association with BIBRA, 25(1), 185-90. doi:10.1016/j.tiv.2010.10.017

Efros, A. L., & Rosen, M. (2000). THE E LECTRONIC S TRUCTURE OF SEMICONDUCTOR N ANOCRYSTALS 1. Annual Review of Materials Science, 30(1), 475-521. Annual Reviews 4139 El Camino Way, P.O. Box 10139, Palo Alto, CA 94303-0139, USA. doi:10.1146/annurev.matsci.30.1.475

Ekimov, A. I., & Onushchenko, A. A. (1981). Quantum size effect in three-dimensional microscopic semiconductor crystals. Journal of Experimental and Theoretical Physics Letters, 34.

Ekimov, A. I., & Onushchenko, A. A. (1981). Quantum size effect in three-dimensional microscopic semiconductor crystals. Journal of Experimental and Theoretical Physics Letters, 34.

Ema, M., Kobayashi, N., Naya, M., Hanai, S., & Nakanishi, J. (2010). Reproductive and developmental toxicity studies of manufactured nanomaterials. Reproductive toxicology (Elmsford, N.Y.), 30(3), 343-52. doi:10.1016/j.reprotox.2010.06.002

Ennaceur, A, & Delacour, J. (1988). A new one-trial test for neurobiological studies of memory in rats. 1: Behavioral data. Behavioural brain research, 31(1), 47-59.

Ennaceur, A, Neave, N., & Aggleton, J. P. (1997). Spontaneous object recognition and object location memory in rats: the effects of lesions in the cingulate cortices, the medial prefrontal cortex, the cingulum bundle and the fornix. Experimental brain research. Experimentelle Hirnforschung. Experimentation cerebrale, 113(3), 509-19.

Ennaceur, Abdelkader, Neave, N., & Aggleton, J. P. (1996). Neurotoxic lesions of the perirhinal cortex do not mimic the behavioural effects of fornix transection in the rat. Behavioural Brain Research, 80(1-2), 9-25. doi:10.1016/0166-4328(96)00006-X

Erathodiyil, N., & Ying, J. Y. (2011). Functionalization of Inorganic Nanoparticles for Bioimaging Applications. Accounts of chemical research, 44(10), 925-35. doi:10.1021/ar2000327

Fenart, L., Casanova, A., Dehouck, B., Duhem, C., Slupek, S., Cecchelli, R., & Betbeder, D. (1999). Evaluation of effect of charge and lipid coating on ability of 60-nm nanoparticles to cross an in vitro model of the blood-brain barrier. The Journal of pharmacology and experimental therapeutics, 291(3), 1017-22.

Ferrara, D. E., Weiss, D., Carnell, P. H., Vito, R. P., Vega, D., Gao, X., Nie, S., et al. (2006). Quantitative 3D fluorescence technique for the analysis of en face preparations of arterial walls using quantum dot nanocrystals and two-photon excitation laser scanning microscopy. American journal of physiology. Regulatory, integrative and comparative physiology, 290(1), R114-23. doi:10.1152/ajpregu.00449.2005

Feynman, R. P. (1960). There is Plenty of Room at the Bottom. Engineering and Science. California Institute of Technology.

Fischer, H. C., Liu, L., Pang, K. S., & Chan, W. C. W. (2006). Pharmacokinetics of Nanoscale Quantum Dots: In Vivo Distribution, Sequestration, and Clearance in the Rat. Advanced Functional Materials, 16(10), 1299-1305. doi:10.1002/adfm.200500529

Fortéa, J. O. Y., De La Llave, E., Regnault, B., Coppée, J.-Y., Milon, G., Lang, T., & Prina, E. (2009). Transcriptional signatures of BALB/c mouse macrophages housing multiplying Leishmania amazonensis amastigotes. BMC Genomics, 10, 119. BioMed Central.

Fourgeaud, L., & Boulanger, L. M. (2010). Role of immune molecules in the establishment and plasticity of glutamatergic synapses. The European journal of neuroscience, 32(2), 207-17. doi:10.1111/j.1460-9568.2010.07342.x

Fournier-Bidoz, S., Jennings, T. L., Klostranec, J. M., Fung, W., Rhee, A., Li, D., & Chan, W. C. W. (2008). Facile and rapid one-step mass preparation of quantum-dot barcodes. Angewandte Chemie (International ed. in English), 47(30), 5577-81. doi:10.1002/anie.200800409

Frangioni, J. V. (2006). Self-illuminating quantum dots light the way. Nature biotechnology, 24(3), 326-8. Nature Publishing Group. doi:10.1038/nbt0306-326

Frank, M. G., Barrientos, R. M., Watkins, L. R., & Maier, S. F. (2010). Aging sensitizes rapidly isolated hippocampal microglia to LPS ex vivo. Journal of neuroimmunology, 226(1-2), 181-4. doi:10.1016/j.jneuroim.2010.05.022

Gagnaire, B., Adam-Guillermin, C., Bouron, A., & Lestaevel, P. (2011). The effects of radionuclides on animal behavior. Reviews of environmental contamination and toxicology, 210, 35-58. doi:10.1007/978-1-4419-7615-4_2

Gagné, F, Auclair, J., Turcotte, P., Fournier, M., Gagnon, C., Sauvé, S., & Blaise, C. (2008). Ecotoxicity of CdTe quantum dots to freshwater mussels: impacts on immune system, oxidative stress and genotoxicity. Aquatic toxicology (Amsterdam, Netherlands), 86(3), 333-40. doi:10.1016/j.aquatox.2007.11.013

Ganea, K., Liebl, C., Sterlemann, V., Müller, M. B., & Schmidt, M. V. (2007). Pharmacological validation of a novel home cage activity counter in mice. Journal of neuroscience methods, 162(1-2), 180-6. doi:10.1016/j.jneumeth.2007.01.008

Gao, J., Chen, K., Luong, R., Bouley, D., Mao, H., Qiao, T., Gambhir, S. S., et al. (2011). A Novel Clinically Translatable Fluorescent Nanoparticle for Targeted Molecular Imaging of Tumors in Living Subjects. Nano letters, 12(1), 281-6. doi:10.1021/nl203526f

Gao, Xiaohu, & Nie, S. (2003). Molecular profiling of single cells and tissue specimens with quantum dots. Trends in biotechnology, 21(9), 371-3.

Gao, Xiaohu, Cui, Y., Levenson, R. M., Chung, L. W. K., & Nie, S. (2004). In vivo cancer targeting and imaging with semiconductor quantum dots. Nature biotechnology, 22(8), 969-76. Nature Publishing Group. doi:10.1038/nbt994

Gao, Xiaohu, Cui, Y., Levenson, R. M., Chung, L. W. K., & Nie, S. (2004). In vivo cancer targeting and imaging with semiconductor quantum dots. Nature biotechnology, 22(8), 969-76. doi:10.1038/nbt994

Gaponik, N., Talapin, D. V., Rogach, A. L., Hoppe, K., Shevchenko, E. V., Kornowski, A., Eychmuller, A., et al. (2002). Thiol-Capping of CdTe Nanocrystals: An Alternative to Organometallic Synthetic Routes. The Journal of Physical Chemistry B, 106(29), 7177-7185. American Chemical Society. doi:10.1021/jp025541k

Geiser, M., Rothen-Rutishauser, B., Kapp, N., SchÃ¼rch, S., Kreyling, W., Schulz, H., Semmler, M., et al. (2005). Ultrafine particles cross cellular membranes by nonphagocytic mechanisms in lungs and in cultured cells. Environmental health perspectives, 113(11), 1555-60.

Gerlai, R. (2003). Memory enhancement: the progress and our fears. Genes, brain, and behavior, 2(4), 187-8; discussion 189-90.

Geys, J., De Vos, R., Nemery, B., & Hoet, P. H. M. (2009). In vitro translocation of quantum dots and influence of oxidative stress. American journal of physiology. Lung cellular and molecular physiology, 297(5), L903-11. doi:10.1152/ajplung.00029.2009

Geys, J., Nemmar, A., Verbeken, E., Smolders, E., Ratoi, M., Hoylaerts, M. F., Nemery, B., et al. (2008). Acute toxicity and prothrombotic effects of quantum dots: impact of surface charge. Environmental health perspectives, 116(12), 1607-13. doi:10.1289/ehp.11566

Ghaderi, S., Ramesh, B., & Seifalian, A. M. (2011). Fluorescence nanoparticles â€œquantum dotsâ as drug delivery system and their toxicity: a review. Journal of drug targeting, 19(7), 475-86. doi:10.3109/1061186X.2010.526227

Golde, T. E., & Miller, V. M. (2009). Proteinopathy-induced neuronal senescence: a hypothesis for brain failure in Alzheimer's and other neurodegenerative diseases. Alzheimer's research & therapy, 1(2), 5. doi:10.1186/alzrt5

Gomes, F. C., Paulin, D., & Moura Neto, V. (1999). Glial fibrillary acidic protein (GFAP): modulation by growth factors and its implication in astrocyte differentiation. Brazilian journal of medical and biological research = Revista brasileira de pesquisas medicas e biologicas / Sociedade Brasileira de Biofisica ... [et al.], 32(5), 619-31.

Goulding, E. H., Schenk, A. K., Juneja, P., MacKay, A. W., Wade, J. M., & Tecott, L. H. (2008). A robust automated system elucidates mouse home cage behavioral structure. Proceedings of the National Academy of Sciences of the United States of America, 105(52), 20575-82. doi:10.1073/pnas.0809053106

Graeber, M. B. (2010). Changing face of microglia. Science (New York, N.Y.), 330(6005), 783-8. doi:10.1126/science.1190929

Graeber, M. B., Li, W., & Rodriguez, M. (2011). Role of microglia in CNS inflammation. FEBS letters, 585(23), 3798-805. doi:10.1016/j.febslet.2011.08.033

Gramowski, A., Flossdorf, J., Bhattacharya, K., Jonas, L., Lantow, M., Rahman, Q., Schiffmann, D., et al. (2010). Nanoparticles induce changes of the electrical activity of neuronal networks on microelectrode array neurochips. Environmental health perspectives, 118(10), 1363-9. doi:10.1289/ehp.0901661

Grigorescu, A. E., & Hagen, C. W. (2009). Resists for sub-20-nm electron beam lithography with a focus on HSQ: state of the art. Nanotechnology, 20(29), 292001. doi:10.1088/0957-4484/20/29/292001

Guo, W., Li, J. J., Wang, Y. A., & Peng, X. (2003). Conjugation Chemistry and Bioapplications of Semiconductor Box Nanocrystals Prepared via Dendrimer Bridging. Chemistry of Materials, 15(16), 3125-3133. American Chemical Society. doi:10.1021/cm034341y

Hanaki, K.-ichi, Momo, A., Oku, T., Komoto, A., Maenosono, S., Yamaguchi, Y., & Yamamoto, K. (2003). Semiconductor quantum dot/albumin complex is a long-life and highly photostable endosome marker. Biochemical and biophysical research communications, 302(3), 496-501.

Hardebo, J. E., & Kåhrström, J. (1985). Endothelial negative surface charge areas and blood-brain barrier function. Acta physiologica Scandinavica, 125(3), 495-9.

Hardman, R. (2006). A toxicologic review of quantum dots: toxicity depends on physicochemical and environmental factors. Environmental health perspectives, 114(2), 165-72.

Harma, H., Soukka, T., & Lovgren, T. (2001). Europium Nanoparticles and Time-resolved Fluorescence for Ultrasensitive Detection of Prostate-specific Antigen. Clin. Chem., 47(3), 561-568.

Hauck, T. S., Anderson, R. E., Fischer, H. C., Newbigging, S., & Chan, W. C. W. (2010). In vivo quantum-dot toxicity assessment. Small (Weinheim an der Bergstrasse, Germany), 6(1), 138-44. doi:10.1002/smll.200900626

Henry, C. J., Huang, Y., Wynne, A., Hanke, M., Himler, J., Bailey, M. T., Sheridan, J. F., et al. (2008). Minocycline attenuates lipopolysaccharide (LPS)-induced neuroinflammation, sickness behavior, and anhedonia. Journal of neuroinflammation, 5, 15. doi:10.1186/1742-2094-5-15

Heppner, G. H., & Miller, B. E. (1983). Tumor heterogeneity: biological implications and therapeutic consequences. CANCER AND METASTASIS REVIEW, 2(1), 5-23. Springer Netherlands. doi:10.1007/BF00046903

Hernandez-Guillamon, M., Solé, M., Delgado, P., Garciá-Bonilla, L., Giralt, D., Boada, C., Penalba, A., et al. (2012). VAP-1/SSAO plasma activity and brain expression in human hemorrhagic stroke. Cerebrovascular diseases (Basel, Switzerland), 33(1), 55-63. doi:10.1159/000333370

Hilderbrand, S. A., & Weissleder, R. (2010). Near-infrared fluorescence: application to in vivo molecular imaging. Current opinion in chemical biology, 14(1), 71-9. doi:10.1016/j.cbpa.2009.09.029

Histologie du systeme nerveux de l'homme & des vertebres. (1909). Retrieved from http://openlibrary.org/books/OL14734754M/Histologie_du_systeme_nerveux_de_l'homme_des_vertebres

Ho, C.C., Chang, H., Tsai, H.-T., Tsai, M.-H., Yang, C.-S., Ling, Y.-C., & Lin, P. (2011). Quantum dot 705, a cadmium-based nanoparticle, induces persistent inflammation and granuloma formation in the mouse lung. Nanotoxicology. Informa UK, Ltd. London. doi:10.3109/17435390.2011.635814

Holsapple, M. P., Farland, W. H., Landry, T. D., Monteiro-Riviere, N. A., Carter, J. M., Walker, N. J., & Thomas, K. V. (2005). Research strategies for safety evaluation of nanomaterials, part II: toxicological and safety evaluation of nanomaterials, current challenges and data needs. Toxicological sciences : an official journal of the Society of Toxicology, 88(1), 12-7. doi:10.1093/toxsci/kfi293

Hopkins, S. J. (2007). Central nervous system recognition of peripheral inflammation: a neural, hormonal collaboration. Acta bio-medica : Atenei Parmensis, 78 Suppl 1, 231-47.

Hopwood, D., Spiers, E. M., Ross, P. E., Anderson, J. T., McCullough, J. B., & Murray, F. E. (1995). Endocytosis of fluorescent microspheres by human oesophageal epithelial cells: comparison between normal and inflamed tissue. Gut, 37(5), 598-602.

Hsieh, M.-S., Shiao, N.-H., & Chan, W.-H. (2009). Cytotoxic effects of CdSe quantum dots on maturation of mouse oocytes, fertilization, and fetal development. International journal of molecular sciences, 10(5), 2122-35. doi:10.3390/ijms10052122

Hu, H. (2000). Exposure to metals. Primary care, 27(4), 983-96.

Hu, R., Gong, X., Duan, Y., Li, N., Che, Y., Cui, Y., Zhou, M., et al. (2010). Neurotoxicological effects and the impairment of spatial recognition memory in mice caused by

exposure to TiO2 nanoparticles. Biomaterials, 31(31), 8043-50. doi:10.1016/j.biomaterials.2010.07.011

Hu, Rui, Yong, K.-T., Roy, I., Ding, H., Law, W.C., Cai, H., Zhang, X., et al. (2010). Functionalized near-infrared quantum dots for in vivo tumor vasculature imaging. Nanotechnology, 21(14), 145105. doi:10.1088/0957-4484/21/14/145105

Huang, C.F., Hsu, C.-J., Liu, S.-H., & Lin-Shiau, S.-Y. (2008). Neurotoxicological mechanism of methylmercury induced by low-dose and long-term exposure in mice: oxidative stress and down-regulated Na+/K(+)-ATPase involved. Toxicology letters, 176(3), 188-97. doi:10.1016/j.toxlet.2007.11.004

Imeri, L., & Opp, M. R. (2009). How (and why) the immune system makes us sleep. Nature reviews. Neuroscience, 10(3), 199-210. doi:10.1038/nrn2576

Ingle, T. M., Alexander, R., Bouldin, J., & Buchanan, R. A. (2008). Absorption of semiconductor nanocrystals by the aquatic invertebrate Ceriodaphnia dubia. Bulletin of environmental contamination and toxicology, 81(3), 249-52. doi:10.1007/s00128-008-9481-y

Inoue, K., Takano, H., Yanagisawa, R., Ichinose, T., Shimada, A., & Yoshikawa, T. (2005). Pulmonary exposure to diesel exhaust particles induces airway inflammation and cytokine expression in NC/Nga mice. Archives of toxicology, 79(10), 595-9. doi:10.1007/s00204-005-0668-2

Ipe, B. I., Lehnig, M., & Niemeyer, C. M. (2005). On the generation of free radical species from quantum dots. Small (Weinheim an der Bergstrasse, Germany), 1(7), 706-9. doi:10.1002/smll.200500105

Jacobsen, N. R., Møller, P., Jensen, K. A., Vogel, U., Ladefoged, O., Loft, S., & Wallin, H. (2009). Lung inflammation and genotoxicity following pulmonary exposure to nanoparticles in ApoE-/- mice. Particle and fibre toxicology, 6, 2. doi:10.1186/1743-8977-6-2

Jain, K. K. (2003). Nanodiagnostics: application of nanotechnology in molecular diagnostics. Expert review of molecular diagnostics, 3(2), 153-61. doi:10.1586/14737159.3.2.153

Jain, K. K. (2005). Nanotechnology in clinical laboratory diagnostics. Clinica chimica acta; international journal of clinical chemistry, 358(1-2), 37-54. doi:10.1016/j.cccn.2005.03.014

Jain, R K. (1999). Transport of molecules, particles, and cells in solid tumors. Annual review of biomedical engineering, 1, 241-63. Annual Reviews 4139 El Camino Way, P.O. Box 10139, Palo Alto, CA 94303-0139, USA. doi:10.1146/annurev.bioeng.1.1.241

Jaiswal, J. K., Goldman, E. R., Mattoussi, H., & Simon, S. M. (2004). Use of quantum dots for live cell imaging. Nature methods, 1(1), 73-8. Nature Publishing Group. doi:10.1038/nmeth1004-73

Jakobs, S., Subramaniam, V., Schönle, A., Jovin, T. M., & Hell, S. W. (2000). EFGP and DsRed expressing cultures of Escherichia coli imaged by confocal, two-photon and fluorescence lifetime microscopy. FEBS letters, 479(3), 131-5.

Jayagopal, A., Russ, P. K., & Haselton, F. R. (2007). Surface engineering of quantum dots for in vivo vascular imaging. Bioconjugate chemistry, 18(5), 1424-33. American Chemical Society. doi:10.1021/bc070020r

Jeng, H. A., & Swanson, J. (2006). Toxicity of metal oxide nanoparticles in mammalian cells. Journal of environmental science and health. Part A, Toxic/hazardous substances & environmental engineering, 41(12), 2699-711. doi:10.1080/10934520600966177

Jenkins, S. J., Ruckerl, D., Cook, P. C., Jones, L. H., Finkelman, F. D., van Rooijen, N., MacDonald, A. S., et al. (2011). Local macrophage proliferation, rather than recruitment from the blood, is a signature of TH2 inflammation. Science (New York, N.Y.), 332(6035), 1284-8. doi:10.1126/science.1204351

Ji, K.A., Eu, M. Y., Kang, S.-H., Gwag, B. J., Jou, I., & Joe, E.-H. (2008). Differential neutrophil infiltration contributes to regional differences in brain inflammation in the substantia nigra pars compacta and cortex. Glia, 56(10), 1039-47. doi:10.1002/glia.20677

Ji, K.A., Eu, M. Y., Kang, S.-H., Gwag, B. J., Jou, I., & Joe, E.-H. (2008). Differential neutrophil infiltration contributes to regional differences in brain inflammation in the substantia nigra pars compacta and cortex. Glia, 56(10), 1039-47.

Jiang, Zhengran, Li, R., Todd, N. W., Stass, S. A., & Jiang, F. (2007). Detecting genomic aberrations by fluorescence in situ hybridization with quantum dots-labeled probes. Journal of nanoscience and nanotechnology, 7(12), 4254-9.

Juzenas, P., Chen, W., Sun, Y.-P., Coelho, M. A. N., Generalov, R., Generalova, N., & Christensen, I. L. (2008). Quantum dots and nanoparticles for photodynamic and radiation therapies of cancer. Advanced drug delivery reviews, 60(15), 1600-14. doi:10.1016/j.addr.2008.08.004

Kaji, N., Tokeshi, M., & Baba, Y. (2007). Single-molecule measurements with a single quantum dot. Chemical record (New York, N.Y.), 7(5), 295-304. doi:10.1002/tcr.20128

Karabanovas, V., Zakarevicius, E., Sukackaite, A., Streckyte, G., & Rotomskis, R. (2008). Examination of the stability of hydrophobic (CdSe)ZnS quantum dots in the digestive tract of rats. Photochemical & photobiological sciences : Official journal of the European Photochemistry Association and the European Society for Photobiology, 7(6), 725-9. doi:10.1039/b707920f

Kas, M. J. H., & Van Ree, J. M. (2004). Dissecting complex behaviours in the post-genomic era. Trends in neurosciences, 27(7), 366-9. doi:10.1016/j.tins.2004.04.011

Kato, S., Itoh, K., Yaoi, T., Tozawa, T., Yoshikawa, Y., Yasui, H., Kanamura, N., et al. (2010). Organ distribution of quantum dots after intraperitoneal administration, with special reference to area-specific distribution in the brain. Nanotechnology, 21(33), 335103. doi:10.1088/0957-4484/21/33/335103

Kaul, Z., Yaguchi, T., Kaul, S. C., Hirano, T., Wadhwa, R., & Taira, K. (2003). Mortalin imaging in normal and cancer cells with quantum dot immuno-conjugates. Cell research, 13(6), 503-7. doi:10.1038/sj.cr.7290194

Khalil, W. K. B., Girgis, E., Emam, A. N., Mohamed, M. B., & Rao, K. V. (2011). Genotoxicity evaluation of nanomaterials: dna damage, micronuclei, and 8-hydroxy-2-deoxyguanosine induced by magnetic doped CdSe quantum dots in male mice. Chemical research in toxicology, 24(5), 640-50. doi:10.1021/tx2000015

Kim, B. Y. S., Rytka, J. T., & Chan, W. C. W. (2010). Nanomedicine — New England Journal of Medicine, 363, 2434-43.

Kim, D. H., & Rossi, J. J. (2007). Strategies for silencing human disease using RNA interference. Nature reviews. Genetics, 8(3), 173-84. Nature Publishing Group. doi:10.1038/nrg2006

Kim, G. W., Gasche, Y., Grzeschik, S., Copin, J.-C., Maier, C. M., & Chan, P. H. (2003). Neurodegeneration in striatum induced by the mitochondrial toxin 3-nitropropionic acid: role of matrix metalloproteinase-9 in early blood-brain barrier disruption? The Journal of neuroscience : the official journal of the Society for Neuroscience, 23(25), 8733-42.

Kim, J. S., Cho, K. J., Tran, T. H., Nurunnabi, M., Moon, T. H., Hong, S. M., & Lee, Y.-kyu. (2011). In vivo NIR imaging with CdTe/CdSe quantum dots entrapped in PLGA nanospheres. Journal of colloid and interface science, 353(2), 363-71. doi:10.1016/j.jcis.2010.08.053

Kim, S., & Bawendi, M. G. (2003). Oligomeric ligands for luminescent and stable nanocrystal quantum dots. Journal of the American Chemical Society, 125(48), 14652-3. American Chemical Society. doi:10.1021/ja0368094

Kim, S., & Bawendi, M. G. (2003). Oligomeric ligands for luminescent and stable nanocrystal quantum dots. Journal of the American Chemical Society, 125(48), 14652-3. doi:10.1021/ja0368094

Kim, S., Lim, Y. T., Soltesz, E. G., De Grand, A. M., Lee, J., Nakayama, A., Parker, J. A., et al. (2004). Near-infrared fluorescent type II quantum dots for sentinel lymph node mapping. Nature biotechnology, 22(1), 93-7. doi:10.1038/nbt920

Kim, S., Lim, Y. T., Soltesz, E. G., De Grand, A. M., Lee, J., Nakayama, A., Parker, J. A., et al. (2004). Near-infrared fluorescent type II quantum dots for sentinel lymph node mapping. Nature biotechnology, 22(1), 93-7. Nature Publishing Group. doi:10.1038/nbt920

King-Heiden, T. C., Wiecinski, P. N., Mangham, A. N., Metz, K. M., Nesbit, D., Pedersen, J. A., Hamers, R. J., et al. (2009). Quantum dot nanotoxicity assessment using the zebrafish embryo. Environmental science & technology, 43(5), 1605-11.

Kipp, M., Norkute, A., Johann, S., Lorenz, L., Braun, A., Hieble, A., Gingele, S., et al. (2008). Brain-region-specific astroglial responses in vitro after LPS exposure. Journal of molecular neuroscience : MN, 35(2), 235-43. Humana Press Inc. doi:10.1007/s12031-008-9057-7

Kirchner, C., Liedl, T., Kudera, S., Pellegrino, T., Muñoz Javier, A., Gaub, H. E., Sölzle, S., et al. (2005). Cytotoxicity of colloidal CdSe and CdSe/ZnS nanoparticles. Nano letters, 5(2), 331-8. doi:10.1021/nl047996m

Kniesel, U., & Wolburg, H. (2000). Tight Junctions of the Bloodâ“Brain Barrier. Cellular and Molecular Neurobiology (Vol. 20, pp. 57-76). Springer Netherlands. doi:10.1023/A:1006995910836

Kobzik, L. (1995). Lung macrophage uptake of unopsonized environmental particulates. Role of scavenger-type receptors. Journal of immunology (Baltimore, Md. : 1950), 155(1), 367-76.

Koeppel, F., Jaiswal, J. K., & Simon, S. M. (2007). Quantum dot-based sensor for improved detection of apoptotic cells. Nanomedicine (London, England), 2(1), 71-8. Future Medicine Ltd London, UK. doi:10.2217/17435889.2.1.71

Kondo, S., Kohsaka, S., & Okabe, S. (2011). Long-term changes of spine dynamics and microglia after transient peripheral immune response triggered by LPS in vivo. Molecular brain, 4(1), 27. doi:10.1186/1756-6606-4-27

Koziara, J M, Lockman, P. R., Allen, D. D., & Mumper, R. J. (n.d.). The blood-brain barrier and brain drug delivery. Journal of nanoscience and nanotechnology, 6(9-10), 2712-35.

Kreuter, J. (1994). Drug targeting with nanoparticles. European journal of drug metabolism and pharmacokinetics, 19(3), 253-6.

Kreuter, J, Alyautdin, R. N., Kharkevich, D. A., & Ivanov, A. A. (1995). Passage of peptides through the blood-brain barrier with colloidal polymer particles (nanoparticles). Brain research, 674(1), 171-4.

Kreuter, J., Shamenkov, D., Petrov, V., Ramge, P., Cychutek, K., Koch-Brandt, C., & Alyautdin, R. (2002). Apolipoprotein-mediated transport of nanoparticle-bound drugs across the blood-brain barrier. Journal of drug targeting, 10(4), 317-25. doi:10.1080/10611860290031877

Kreutzberg, G. W. (1996). Microglia: a sensor for pathological events in the CNS. Trends in neurosciences, 19(8), 312-8.

Kurtoglu, M. E., Longenbach, T., Reddington, P., & Gogotsi, Y. (2011). Effect of Calcination Temperature and Environment on Photocatalytic and Mechanical Properties of

Ultrathin Sol-Gel Titanium Dioxide Films. Journal of the American Ceramic Society, 94(4), 1101-1108. doi:10.1111/j.1551-2916.2010.04218.x

Ladeby, R., Wirenfeldt, M., Garcia-Ovejero, D., Fenger, C., Dissing-Olesen, L., Dalmau, I., & Finsen, B. (2005). Microglial cell population dynamics in the injured adult central nervous system. Brain research. Brain research reviews, 48(2), 196-206. doi:10.1016/j.brainresrev.2004.12.009

Lai, C. Y., Trewyn, B. G., Jeftinija, D. M., Jeftinija, K., Xu, S., Jeftinija, S., & Lin, V. S.-Y. (2003). A mesoporous silica nanosphere-based carrier system with chemically removable CdS nanoparticle caps for stimuli-responsive controlled release of neurotransmitters and drug molecules. Journal of the American Chemical Society, 125(15), 4451-9. doi:10.1021/ja028650l

Lai, S. K., Hida, K., Man, S. T., Chen, C., Machamer, C., Schroer, T. A., & Hanes, J. (2007). Privileged delivery of polymer nanoparticles to the perinuclear region of live cells via a non-clathrin, non-degradative pathway. Biomaterials, 28(18), 2876-84. doi:10.1016/j.biomaterials.2007.02.021

Lalancette-Hébert, M., Moquin, A., Choi, A. O., Kriz, J., & Maysinger, D. (2010). Lipopolysaccharide-QD micelles induce marked induction of TLR2 and lipid droplet accumulation in olfactory bulb microglia. Molecular pharmaceutics, 7(4), 1183-94. doi:10.1021/mp1000372

Landrigan, P. J., Whitworth, R. H., Baloh, R. W., Staehling, N. W., Barthel, W. F., & Rosenblum, B. F. (1975). Neuropsychological dysfunction in children with chronic low-level lead absorption. Lancet, 1(7909), 708-12.

Larson, D. R., Zipfel, W. R., Williams, R. M., Clark, S. W., Bruchez, M. P., Wise, F. W., & Webb, W. W. (2003). Water-soluble quantum dots for multiphoton fluorescence imaging in vivo. Science (New York, N.Y.), 300(5624), 1434-6. American Association for the Advancement of Science. doi:10.1126/science.1083780

Le Gac, S., Vermes, I., & van den Berg, A. (2006). Quantum dots based probes conjugated to annexin V for photostable apoptosis detection and imaging. Nano letters, 6(9), 1863-9. American Chemical Society. doi:10.1021/nl060694v

Leatherdale, C. A., Woo, W.-K., Mikulec, F. V., & Bawendi, M. G. (2002). On the Absorption Cross Section of CdSe Nanocrystal Quantum Dots. The Journal of Physical Chemistry B, 106(31), 7619-7622. American Chemical Society. doi:10.1021/jp025698c

Lee, C. M., Jang, D., Cheong, S.-J., Kim, E.-M., Jeong, M.-H., Kim, S.-H., Kim, D. W., et al. (2010). Surface engineering of quantum dots for in vivo imaging. Nanotechnology, 21(28), 285102. doi:10.1088/0957-4484/21/28/285102

Lee, J., Ji, K., Kim, J., Park, C., Lim, K. H., Yoon, T. H., & Choi, K. (2010). Acute toxicity of two CdSe/ZnSe quantum dots with different surface coating in Daphnia magna under various light conditions. Environmental toxicology, 25(6), 593-600. doi:10.1002/tox.20520

Lee, Jiyoun, Ji, K., Kim, J., Park, C., Lim, K. H., Yoon, T. H., & Choi, K. (2010). Acute toxicity of two CdSe/ZnSe quantum dots with different surface coating in Daphnia magna under various light conditions. Environmental toxicology, 25(6), 593-600. doi:10.1002/tox.20520

Leigh, K., Bouldin, J., & Buchanan, R. (2012). Effects of exposure to semiconductor nanoparticles on aquatic organisms. Journal of toxicology, 2012, 397657. doi:10.1155/2012/397657

Lewin, M., Carlesso, N., Tung, C. H., Tang, X. W., Cory, D., Scadden, D. T., & Weissleder, R. (2000). Tat peptide-derivatized magnetic nanoparticles allow in vivo tracking and recovery of progenitor cells. Nature biotechnology, 18(4), 410-4. doi:10.1038/74464

Li, H., Li, M., Shih, W. Y., Lelkes, P. I., & Shih, W.-H. (2011). Cytotoxicity tests of water soluble ZnS and CdS quantum dots. Journal of nanoscience and nanotechnology, 11(4), 3543-51.

Li, J., Zhang, Y., Xiao, Q., Tian, F., Liu, X., Li, R., Zhao, G., et al. (2011). Mitochondria as target of Quantum dots toxicity. Journal of hazardous materials, 194, 440-4. doi:10.1016/j.jhazmat.2011.07.113

Li, Shuchun, Wang, Y., Wang, H., Bai, Y., Liang, G., Wang, Y., Huang, N., et al. (2011). MicroRNAs as participants in cytotoxicity of CdTe quantum dots in NIH/3T3 cells. Biomaterials, 32(15), 3807-14. doi:10.1016/j.biomaterials.2011.01.074

Li, W., Chen, C., Ye, C., Wei, T., Zhao, Y., Lao, F., Chen, Z., et al. (2008). The translocation of fullerenic nanoparticles into lysosome via the pathway of clathrin-mediated endocytosis. Nanotechnology, 19(14), 145102. doi:10.1088/0957-4484/19/14/145102

Liang, Ru-Qiang, Li, W., Li, Y., Tan, C.-yan, Li, J.-X., Jin, Y.-X., & Ruan, K.-C. (2005). An oligonucleotide microarray for microRNA expression analysis based on labeling RNA with quantum dot and nanogold probe. Nucleic acids research, 33(2), e17. doi:10.1093/nar/gni019

Liang, X.J., Meng, H., Wang, Y., He, H., Meng, J., Lu, J., Wang, P. C., et al. (2010). Metallofullerene nanoparticles circumvent tumor resistance to cisplatin by reactivating endocytosis. Proceedings of the National Academy of Sciences of the United States of America, 107(16), 7449-54. doi:10.1073/pnas.0909707107

Lidke, D. S., Nagy, P., Heintzmann, R., Arndt-Jovin, D. J., Post, J. N., Grecco, H. E., Jares-Erijman, E. A., et al. (2004). Quantum dot ligands provide new insights into erbB/HER receptor-mediated signal transduction. Nature biotechnology, 22(2), 198-203. Nature Publishing Group. doi:10.1038/nbt929

Lim, Y. T., Kim, S., Nakayama, A., Stott, N. E., Bawendi, M. G., & Frangioni, J. V. (2003). Selection of quantum dot wavelengths for biomedical assays and imaging. Molecular imaging, 2(1), 50-64.

Lin, C.H., Chang, L. W., Chang, H., Yang, M.-H., Yang, C.-S., Lai, W.-H., Chang, W.-H., et al. (2009). The chemical fate of the Cd/Se/Te-based quantum dot 705 in the biolo-

gical system: toxicity implications. Nanotechnology, 20(21), 215101. doi:10.1088/0957-4484/20/21/215101

Lin, C.H., Chang, L. W., Chang, H., Yang, M.-H., Yang, C.-S., Lai, W.-H., Chang, W.H., et al. (2009). The chemical fate of the Cd/Se/Te-based quantum dot 705 in the biological system: toxicity implications. Nanotechnology, 20(21), 215101. doi:10.1088/0957-4484/20/21/215101

Lin, P., Chen, J.-W., Chang, L. W., Wu, J.-P., Redding, L., Chang, H., Yeh, T.-K., et al. (2008). Computational and ultrastructural toxicology of a nanoparticle, Quantum Dot 705, in mice. Environmental science & technology, 42(16), 6264-70.

Liu, B., & Hong, J.-S. (2003). Role of microglia in inflammation-mediated neurodegenerative diseases: mechanisms and strategies for therapeutic intervention. The Journal of pharmacology and experimental therapeutics, 304(1), 1-7. doi:10.1124/jpet.102.035048

Liu, J., Lau, S. K., Varma, V. A., Moffitt, R. A., Caldwell, M., Liu, T., Young, A. N., et al. (2010). Molecular mapping of tumor heterogeneity on clinical tissue specimens with multiplexed quantum dots. ACS nano, 4(5), 2755-65. doi:10.1021/nn100213v

Liu, W., Zhang, S., Wang, L., Qu, C., Zhang, C., Hong, L., Yuan, L., et al. (2011). CdSe quantum dot (QD)-induced morphological and functional impairments to liver in mice. PloS one, 6(9), e24406. doi:10.1371/journal.pone.0024406

Liu, Z., Cai, W., He, L., Nakayama, N., Chen, K., Sun, X., Chen, X., et al. (2007). In vivo biodistribution and highly efficient tumour targeting of carbon nanotubes in mice. Nature nanotechnology, 2(1), 47-52. Nature Publishing Group. doi:10.1038/nnano.2006.170

Lockman, Paul R, Koziara, J. M., Mumper, R. J., & Allen, D. D. (2004). Nanoparticle surface charges alter blood-brain barrier integrity and permeability. Journal of drug targeting, 12(9-10), 635-41. doi:10.1080/10611860400015936

Lockman, Paul R, Oyewumi, M. O., Koziara, J. M., Roder, K. E., Mumper, R. J., & Allen, D. D. (2003). Brain uptake of thiamine-coated nanoparticles. Journal of Controlled Release, 93(3), 271-282. doi:10.1016/j.jconrel.2003.08.006

Lockman, Paul R, Oyewumi, M. O., Koziara, J. M., Roder, K. E., Mumper, R. J., & Allen, D. D. (2003). Brain uptake of thiamine-coated nanoparticles. Journal of Controlled Release, 93(3), 271-282. doi:10.1016/j.jconrel.2003.08.006

Lok, J., Gupta, P., Guo, S., Kim, W. J., Whalen, M. J., van Leyen, K., & Lo, E. H. (2007). Cell-cell signaling in the neurovascular unit. Neurochemical research, 32(12), 2032-45. doi:10.1007/s11064-007-9342-9

Long, H., Shi, T., Borm, P. J., Määttää, J., Husgafvel-Pursiainen, K., Savolainen, K., & Krombach, F. (2004). ROS-mediated TNF-alpha and MIP-2 gene expression in alveolar macrophages exposed to pine dust. Particle and fibre toxicology, 1(1), 3. doi:10.1186/1743-8977-1-3

Lovrić, J., Bazzi, H. S., Cuie, Y., Fortin, G. R. A., Winnik, F. M., & Maysinger, D. (2005). Differences in subcellular distribution and toxicity of green and red emitting CdTe quantum dots. Journal of molecular medicine (Berlin, Germany), 83(5), 377-85. doi:10.1007/s00109-004-0629-x

Lovrić, J., Cho, S. J., Winnik, F. M., & Maysinger, D. (2005). Unmodified cadmium telluride quantum dots induce reactive oxygen species formation leading to multiple organelle damage and cell death. Chemistry & biology, 12(11), 1227-34. doi:10.1016/j.chembiol.2005.09.008

Lukaszewska, I., & Radulska, A. (1994). Object recognition is not impaired in old rats. Acta neurobiologiae experimentalis, 54(2), 143-50.

Lynch, M A, Introduction, I., Erk, B., Potentiation, L.-term, Age, D., & Cognition, E. (2004). Long-Term Potentiation and Memory. Physiological Reviews, 87-136.

Lynch, M. A. (2002). Vitamins & Hormones Volume 64 (Vol. 64). Elsevier. doi:10.1016/S0083-6729(02)64006-3

Lynch, N. J., Willis, C. L., Nolan, C. C., Roscher, S., Fowler, M. J., Weihe, E., Ray, D. E., et al. (2004). Microglial activation and increased synthesis of complement component C1q precedes blood-brain barrier dysfunction in rats. Molecular immunology, 40(10), 709-16.

Ma-Hock, L., Brill, S., Wohlleben, W., Farias, P. M. A., Chaves, C. R., TenÃ³rio, D. P. L. A., Fontes, A., et al. (2011). Short term inhalation toxicity of a liquid aerosol of CdS/Cd(OH)(2) core shell quantum dots in male Wistar rats. Toxicology letters, 208(2), 115-24. doi:10.1016/j.toxlet.2011.10.011

Macphail, R. C., Peele, D. B., & Crofton, K. M. (1989). Motor Activity and Screening for Neurotoxicity. International Journal of Toxicology, 8(1), 117-125. doi:10.3109/10915818909009098

Maestripieri, D., Schino, G., Aureli, F., & Troisi, A. (1992). A modest proposal: displacement activities as an indicator of emotions in primates. Animal Behaviour, 44(5), 967-979. doi:10.1016/S0003-3472(05)80592-5

Mahto, S. K., Park, C., Yoon, T. H., & Rhee, S. W. (2010). Assessment of cytocompatibility of surface-modified CdSe/ZnSe quantum dots for BALB/3T3 fibroblast cells. Toxicology in vitro : an international journal published in association with BIBRA, 24(4), 1070-7. doi:10.1016/j.tiv.2010.03.017

Male, K. B., Lachance, B., Hrapovic, S., Sunahara, G., & Luong, J. H. T. (2008). Assessment of cytotoxicity of quantum dots and gold nanoparticles using cell-based impedance spectroscopy. Analytical chemistry, 80(14), 5487-93. doi:10.1021/ac8004555

Mancini, M. C., Kairdolf, B. A., Smith, A. M., & Nie, S. (2008). Oxidative quenching and degradation of polymer-encapsulated quantum dots: new insights into the long-term fate and toxicity of nanocrystals in vivo. Journal of the American Chemical Society, 130(33), 10836-7. doi:10.1021/ja8040477

Marques, C. P., Cheeran, M. C.J., Palmquist, J. M., Hu, S., & Lokensgard, J. R. (2008). Microglia are the major cellular source of inducible nitric oxide synthase during experimental herpes encephalitis. Journal of neurovirology, 14(3), 229-38. doi:10.1080/13550280802093927

Matsuno, A., Mizutani, A., Okinaga, H., Takano, K., Yamada, S., Yamada, S. M., Nakaguchi, H., et al. (2011). Molecular morphology of pituitary cells, from conventional immunohistochemistry to fluorescein imaging. Molecules (Basel, Switzerland), 16(5), 3618-35. doi:10.3390/molecules16053618

Mattheakis, L. C., Dias, J. M., Choi, Y.-J., Gong, J., Bruchez, M. P., Liu, J., & Wang, E. (2004). Optical coding of mammalian cells using semiconductor quantum dots. Analytical biochemistry, 327(2), 200-8. doi:10.1016/j.ab.2004.01.031

Mattoussi, Hedi, Mauro, J. M., Goldman, E. R., Anderson, G. P., Sundar, V. C., Mikulec, F. V., & Bawendi, M. G. (2000). Self-Assembly of CdSeâ'ZnS Quantum Dot Bioconjugates Using an Engineered Recombinant Protein. Journal of the American Chemical Society, 122(49), 12142-12150. American Chemical Society. doi:10.1021/ja002535y

Maysinger, D., Behrendt, M., Lalancette-HÃ©bert, M., & Kriz, J. (2007). Real-time imaging of astrocyte response to quantum dots: in vivo screening model system for biocompatibility of nanoparticles. Nano letters, 7(8), 2513-20. doi:10.1021/nl071611t

McCall, M. A., Gregg, R. G., Behringer, R. R., Brenner, M., Delaney, C. L., Galbreath, E. J., Zhang, C. L., et al. (1996). Targeted deletion in astrocyte intermediate filament (Gfap) alters neuronal physiology. Proceedings of the National Academy of Sciences of the United States of America, 93(13), 6361-6.

Medintz, I. L., Clapp, A. R., Mattoussi, H., Goldman, E. R., Fisher, B., & Mauro, J. M. (2003). Self-assembled nanoscale biosensors based on quantum dot FRET donors. Nature materials, 2(9), 630-8. doi:10.1038/nmat961

Medintz, I. L., Mattoussi, H., & Clapp, A. R. (2008). Potential clinical applications of quantum dots. International journal of nanomedicine, 3(2), 151-67.

Michalet, X., Pinaud, F. F., Bentolila, L. A., Tsay, J. M., Doose, S., Li, J. J., Sundaresan, G., et al. (2005). Quantum dots for live cells, in vivo imaging, and diagnostics. Science (New York, N.Y.), 307(5709), 538-44. doi:10.1126/science.1104274

Minami, S. S., Sun, B., Popat, K., Kauppinen, T., Pleiss, M., Zhou, Y., Ward, M. E., et al. (2012). Selective targeting of microglia by quantum dots. Journal of neuroinflammation, 9(1), 22. doi:10.1186/1742-2094-9-22

Mohs, A. M., Duan, H., Kairdolf, B. A., Smith, A. M., & Nie, S. (2009). Proton-Resistant Quantum Dots: Stability in Gastrointestinal Fluids and Implications for Oral Delivery of Nanoparticle Agents. Nano research, 2(6), 500-508. doi:10.1007/s12274-009-9046-3

Moreno, C., Vivas, O., Lamprea, N. P., Lamprea, M. R., Múnera, A., & Troncoso, J. (2010). Vibrissal paralysis unveils a preference for textural rather than positional no-

velty in the one-trial object recognition task in rats. Behavioural brain research, 211(2), 229-35. doi:10.1016/j.bbr.2010.03.044

Morris, M. C., Depollier, J., Mery, J., Heitz, F., & Divita, G. (2001). A peptide carrier for the delivery of biologically active proteins into mammalian cells. Nature biotechnology, 19(12), 1173-6. Nature Publishing Group. doi:10.1038/nbt1201-1173

Morris, R. G., Anderson, E., Lynch, G. S., & Baudry, M. (1986). Selective impairment of learning and blockade of long-term potentiation by an N-methyl-D-aspartate receptor antagonist, AP5. Nature, 319(6056), 774-6. doi:10.1038/319774a0

Mortensen, L. J., OberdÃ¶rster, G., Pentland, A. P., & Delouise, L. A. (2008). In vivo skin penetration of quantum dot nanoparticles in the murine model: the effect of UVR. Nano letters, 8(9), 2779-87. doi:10.1021/nl801323y

Mulder, W. J. M., Koole, R., Brandwijk, R. J., Storm, G., Chin, P. T. K., Strijkers, G. J., de Mello DonegÃ¡, C., et al. (2006). Quantum dots with a paramagnetic coating as a bimodal molecular imaging probe. Nano letters, 6(1), 1-6. American Chemical Society. doi:10.1021/nl051935m

Mumby, D. G., Glenn, M. J., Nesbitt, C., & Kyriazis, D. A. (2002). Dissociation in retrograde memory for object discriminations and object recognition in rats with perirhinal cortex damage. Behavioural Brain Research, 132(2), 215-226. doi:10.1016/S0166-4328(01)00444-2

Murphy, D. D., & Segal, M. (1997). Morphological plasticity of dendritic spines in central neurons is mediated by activation of cAMP response element binding protein. Proceedings of the National Academy of Sciences of the United States of America, 94(4), 1482-7.

Murray, C. A., McGahon, B., McBennett, S., & Lynch, M. A. (n.d.). Interleukin-1 beta inhibits glutamate release in hippocampus of young, but not aged, rats. Neurobiology of aging, 18(3), 343-8.

Murray, C., & Lynch, M. (1998). Evidence that increased hippocampal expression of the cytokine interleukin-1 beta is a common trigger for age- and stress-induced impairments in long-term potentiation. Journal of Neuroscience, 18(8), 2974-2981.

Na, R., Stender, I.-M., Ma, L., & Wulf, H. C. (2000). Autofluorescence spectrum of skin: component bands and body site variations. Skin Research and Technology, 6(3), 112-117. doi:10.1034/j.1600-0846.2000.006003112.x

Naber, P. A., Caballero-Bleda, M., Jorritsma-Byham, B., & Witter, M. P. (1997). Parallel input to the hippocampal memory system through peri- and postrhinal cortices. Neuroreport, 8(11), 2617-21.

Nabiev, I., Mitchell, S., Davies, A., Williams, Y., Kelleher, D., Moore, R., GunâTMko, Y. K., et al. (2007). Nonfunctionalized nanocrystals can exploit a cellâTMs active transport machinery delivering them to specific nuclear and cytoplasmic compartments. Nano letters, 7(11), 3452-61. doi:10.1021/nl0719832

Nadeau, J. L, Clarke, S. J., Hollmann, C. A., & Bahcheli, D. M. (2006). Quantum dot-FRET systems for imaging of neuronal action potentials. Conference proceedings : ... Annual International Conference of the IEEE Engineering in Medicine and Biology Society. IEEE Engineering in Medicine and Biology Society. Conference, 1, 855-8. doi:10.1109/IEMBS.2006.259551

Nagy, Z., Peters, H., & Hüttner, I. (1983). Charge-related alterations of the cerebral endothelium. Laboratory investigation; a journal of technical methods and pathology, 49(6), 662-71.

Nano & Me - Nano Products - Nano in Computing & Electronics. (n.d.). Retrieved January 23, 2012, from http://www.nanoandme.org/nano-products/computing-and-electronics/

Nano & Me - Nano Products - Nano in Transport. (n.d.). Retrieved January 23, 2012, from http://www.nanoandme.org/nano-products/transport/

Nanotechnology. (n.d.). Retrieved from http://www.americanelements.com/nanotech.htm

Nanotechnology. (n.d.). Retrieved January 23, 2012, from http://www.americanelements.com/nanotech.htm

Nanotoxicology: An Emerging Discipline Evolving from Studies of Ultrafine Particles. (2005).Environmental Health Perspectives, 113(7). Retrieved from http://ehp03.niehs.nih.gov/article/info:doi/10.1289/ehp.7339

Nel, A. E., MÃ¤dler, L., Velegol, D., Xia, T., Hoek, E. M. V., Somasundaran, P., Klaessig, F., et al. (2009). Understanding biophysicochemical interactions at the nano-bio interface. Nature materials, 8(7), 543-57. doi:10.1038/nmat2442

Nel, A., Xia, T., MÃ¤dler, L., & Li, N. (2006). Toxic potential of materials at the nanolevel. Science (New York, N.Y.), 311(5761), 622-7. doi:10.1126/science.1114397

Nel, A., Xia, T., MÃ¤dler, L., & Li, N. (2006). Toxic potential of materials at the nanolevel. Science (New York, N.Y.), 311(5761), 622-7. doi:10.1126/science.1114397

Nemmar, A. (2002). Ultrafine Particles Affect Experimental Thrombosis in an In Vivo Hamster Model. American Journal of Respiratory and Critical Care Medicine, 166(7), 998-1004. American Thoracic Society. doi:10.1164/rccm.200110-026OC

Ness, J. M., Akhtar, R. S., Latham, C. B., & Roth, K. A. (2003). Combined Tyramide Signal Amplification and Quantum Dots for Sensitive and Photostable Immunofluorescence Detection. Journal of Histochemistry & Cytochemistry, 51(8), 981-987. SAGE Publications. doi:10.1177/002215540305100801

Neu, M., Fischer, D., & Kissel, T. (2005). Recent advances in rational gene transfer vector design based on poly(ethylene imine) and its derivatives. The journal of gene medicine, 7(8), 992-1009. doi:10.1002/jgm.773

Neves, G., Cooke, S. F., & Bliss, T. V. P. (2008). Synaptic plasticity, memory and the hippocampus: a neural network approach to causality. Nature reviews. Neuroscience, 9(1), 65-75. Nature Publishing Group. doi:10.1038/nrn2303

Newman, E. A. (2003). New roles for astrocytes: Regulation of synaptic transmission. Trends in Neurosciences, 26(10), 536-542. doi:10.1016/S0166-2236(03)00237-6

Newsholme, P., Haber, E. P., Hirabara, S. M., Rebelato, E. L. O., Procopio, J., Morgan, D., Oliveira-Emilio, H. C., et al. (2007). Diabetes associated cell stress and dysfunction: role of mitochondrial and non-mitochondrial ROS production and activity. The Journal of physiology, 583(Pt 1), 9-24. doi:10.1113/jphysiol.2007.135871

Nimmerjahn, A., Kirchhoff, F., & Helmchen, F. (2005). Resting microglial cells are highly dynamic surveillants of brain parenchyma in vivo. Science (New York, N.Y.), 308(5726), 1314-8. doi:10.1126/science.1110647

Nishikawa, T., Iwakiri, N., Kaneko, Y., Taguchi, A., Fukushima, K., Mori, H., Morone, N., et al. (2009). Nitric oxide release in human aortic endothelial cells mediated by delivery of amphiphilic polysiloxane nanoparticles to caveolae. Biomacromolecules, 10(8), 2074-85. doi:10.1021/bm900128x

Nolan, Y., Minogue, A., Vereker, E., Bolton, A. E., Campbell, V. A., & Lynch, M. A. (2002). Attenuation of LPS-induced changes in synaptic activity in rat hippocampus by VasogenâTMs Immune Modulation Therapy. Neuroimmunomodulation, 10(1), 40-6.

Norman, G., & Eacott, M. J. (2005). Dissociable effects of lesions to the perirhinal cortex and the postrhinal cortex on memory for context and objects in rats. Behavioral neuroscience, 119(2), 557-66. doi:10.1037/0735-7044.119.2.557

Norris, D. J., & Bawendi, M. G. (1995). Structure in the lowest absorption feature of CdSe quantum dots. The Journal of Chemical Physics, 103(13), 5260. doi:10.1063/1.470561

Northrop, N. A., Northrup, N. A., & Yamamoto, B. K. (2011). Neuroimmune pharmacology from a neuroscience perspective. Journal of neuroimmune pharmacology : the official journal of the Society on NeuroImmune Pharmacology, 6(1), 10-9. Springer New York. doi:10.1007/s11481-010-9239-2

Oberdörster, G., Ferin, J., & Lehnert, B. E. (1994). Correlation between particle size, in vivo particle persistence, and lung injury. Environmental health perspectives, 102 Suppl , 173-9.

Oberdörster, G., Maynard, A., Donaldson, K., Castranova, V., Fitzpatrick, J., Ausman, K., Carter, J., et al. (2005). Principles for characterizing the potential human health effects from exposure to nanomaterials: elements of a screening strategy. Particle and fibre toxicology, 2, 8. doi:10.1186/1743-8977-2-8

Oberdörster, G., Oberdörster, E., & Oberdörster, J. (2005). Nanotoxicology: an emerging discipline evolving from studies of ultrafine particles. Environmental health perspectives, 113(7), 823-39.

Oberdörster, G., Sharp, Z., Atudorei, V., Elder, A., Gelein, R., Lunts, A., Kreyling, W., et al. (2002). Extrapulmonary translocation of ultrafine carbon particles following whole-body inhalation exposure of rats. Journal of toxicology and environmental health. Part A, 65(20), 1531-43. doi:10.1080/00984100290071658

Ohnishi, S., Lomnes, S. J., Laurence, R. G., Gogbashian, A., Mariani, G., & Frangioni, J. V. (2005). Organic alternatives to quantum dots for intraoperative near-infrared fluorescent sentinel lymph node mapping. Molecular imaging, 4(3), 172-81.

Ohsawa, K., Imai, Y., Nakajima, K., & Kohsaka, S. (1997). Generation and characterization of a microglial cell line, MG5, derived from a p53-deficient mouse. Glia, 21(3), 285-98.

Oliet, S. H., Piet, R., & Poulain, D. A. (2001). Control of glutamate clearance and synaptic efficacy by glial coverage of neurons. Science (New York, N.Y.), 292(5518), 923-6. doi:10.1126/science.1059162

Olivier, J.-C. (2005). Drug transport to brain with targeted nanoparticles. NeuroRx : the journal of the American Society for Experimental NeuroTherapeutics, 2(1), 108-19. doi:10.1602/neurorx.2.1.108

Orndorff, R. L., Warnement, M. R., Mason, J. N., Blakely, R. D., & Rosenthal, S. J. (2008). Quantum dot ex vivo labeling of neuromuscular synapses. Nano letters, 8(3), 780-5. doi:10.1021/nl072460x

Osaki, F., Kanamori, T., Sando, S., Sera, T., & Aoyama, Y. (2004). A quantum dot conjugated sugar ball and its cellular uptake. On the size effects of endocytosis in the subviral region. Journal of the American Chemical Society, 126(21), 6520-1. American Chemical Society. doi:10.1021/ja048792a

Pack, D. W., Hoffman, A. S., Pun, S., & Stayton, P. S. (2005). Design and development of polymers for gene delivery. Nature reviews. Drug discovery, 4(7), 581-93. doi:10.1038/nrd1775

Palecanda, A., & Kobzik, L. (2000). Alveolar macrophage-environmental particle interaction: analysis by flow cytometry. Methods (San Diego, Calif.), 21(3), 241-7. doi:10.1006/meth.2000.1004

Panaro, M. A., & Cianciulli, A. (2012). Current opinions and perspectives on the pathogensis of parkinsonâ™s disease: overviewing the role of immune system. Current pharmaceutical design.

Park, J.-B. (2003). Phagocytosis induces superoxide formation and apoptosis in macrophages. Experimental & molecular medicine, 35(5), 325-35.

Pathak, S., Choi, S. K., Arnheim, N., & Thompson, M. E. (2001). Hydroxylated quantum dots as luminescent probes for in situ hybridization. Journal of the American Chemical Society, 123(17), 4103-4.

Patolsky, F., Gill, R., Weizmann, Y., Mokari, T., Banin, U., & Willner, I. (2003). Lighting-up the dynamics of telomerization and DNA replication by CdSe-ZnS quantum dots. Journal of the American Chemical Society, 125(46), 13918-9. American Chemical Society. doi:10.1021/ja035848c

Patolsky, F., Gill, R., Weizmann, Y., Mokari, T., Banin, U., & Willner, I. (2003). Lighting-up the dynamics of telomerization and DNA replication by CdSe-ZnS quantum dots. Journal of the American Chemical Society, 125(46), 13918-9. doi:10.1021/ja035848c

Pelley, J. L., Daar, A. S., & Saner, M. A. (2009). State of academic knowledge on toxicity and biological fate of quantum dots. Toxicological sciences : an official journal of the Society of Toxicology, 112(2), 276-96. doi:10.1093/toxsci/kfp188

Pellmar, T. C., & Lepinski, D. L. (1993). Gamma radiation (5-10 Gy) impairs neuronal function in the guinea pig hippocampus. Radiation research, 136(2), 255-61.

Pepperkok, R., Squire, A., Geley, S., & Bastiaens, P. I. (1999). Simultaneous detection of multiple green fluorescent proteins in live cells by fluorescence lifetime imaging microscopy. Current biology : CB, 9(5), 269-72.

Peralta-Videa, J. R., Zhao, L., Lopez-Moreno, M. L., de la Rosa, G., Hong, J., & Gardea-Torresdey, J. L. (2011). Nanomaterials and the environment: a review for the biennium 2008-2010. Journal of hazardous materials, 186(1), 1-15. doi:10.1016/j.jhazmat.2010.11.020

Perrault, S. D., Walkey, C., Jennings, T., Fischer, H. C., & Chan, W. C. W. (2009). Mediating tumor targeting efficiency of nanoparticles through design. Nano letters, 9(5), 1909-15. doi:10.1021/nl900031y

Persistent Tissue Kinetics and Redistribution of Nanoparticles, Quantum Dot 705, in Mice: ICP-MS Quantitative Assessment. (2007).Environmental Health Perspectives, 115(9).

Peters, A., Veronesi, B., Calderón-Garcidueñas, L., Gehr, P., Chen, L. C., Geiser, M., Reed, W., et al. (2006). Translocation and potential neurological effects of fine and ultrafine particles a critical update. Particle and fibre toxicology, 3(1), 13. doi:10.1186/1743-8977-3-13

Peyrot, C., Gagnon, C., Gagné, F., Willkinson, K. J., Turcotte, P., & Sauvé, S. (2009). Effects of cadmium telluride quantum dots on cadmium bioaccumulation and metallothionein production to the freshwater mussel, Elliptio complanata. Comparative biochemistry and physiology. Toxicology & pharmacology : CBP, 150(2), 246-51. doi:10.1016/j.cbpc.2009.05.002

Pic, E., Bezdetnaya, L., Guillemin, F., & Marchal, F. (2009). Quantification techniques and biodistribution of semiconductor quantum dots. Anti-cancer agents in medicinal chemistry, 9(3), 295-303.

Pic, E., Pons, T., Bezdetnaya, L., Leroux, A., Guillemin, F., Dubertret, B., & Marchal, F. (2010). Fluorescence imaging and whole-body biodistribution of near-infrared-emitting quantum dots after subcutaneous injection for regional lymph node mapping in mice. Molecular imaging and biology : MIB : the official publication of the Academy of Molecular Imaging, 12(4), 394-405. doi:10.1007/s11307-009-0288-y

Piccio, L., Rossi, B., Scarpini, E., Laudanna, C., Giagulli, C., Issekutz, A. C., Vestweber, D., et al. (2002). Molecular mechanisms involved in lymphocyte recruitment in inflamed brain microvessels: critical roles for P-selectin glycoprotein ligand-1 and heterotrimeric G(i)-linked receptors. Journal of immunology (Baltimore, Md. : 1950), 168(4), 1940-9. American Association of Immunologists.

Piet, Richard, Vargová, L., Syková, E., Poulain, D. A., & Oliet, S. H. R. (2004). Physiological contribution of the astrocytic environment of neurons to intersynaptic crosstalk. Proceedings of the National Academy of Sciences of the United States of America, 101(7), 2151-5. doi:10.1073/pnas.0308408100

Pinaud, F., King, D., Moore, H.-P., & Weiss, S. (2004). Bioactivation and cell targeting of semiconductor CdSe/ZnS nanocrystals with phytochelatin-related peptides. Journal of the American Chemical Society, 126(19), 6115-23. doi:10.1021/ja031691c

Pons, T., Pic, E., Lequeux, N., Cassette, E., Bezdetnaya, L., Guillemin, F., Marchal, F., et al. (2010). Cadmium-free CuInS2/ZnS quantum dots for sentinel lymph node imaging with reduced toxicity. ACS nano, 4(5), 2531-8. doi:10.1021/nn901421v

Pozzi-Mucelli, S., Boschi, F., Calderan, L., Sbarbati, A., & Osculati, F. (2009). Quantum Dots: Proteomics characterization of the impact on biological systems. Journal of Physics: Conference Series, 170(1), 012021. doi:10.1088/1742-6596/170/1/012021

Pradhan, N., & Peng, X. (2007). Efficient and color-tunable Mn-doped ZnSe nanocrystal emitters: control of optical performance via greener synthetic chemistry. Journal of the American Chemical Society, 129(11), 3339-47. American Chemical Society. doi:10.1021/ja068360v

Prasad, B. R., Nikolskaya, N., Connolly, D., Smith, T. J., Byrne, S. J., Gérard, V. A., Gun'ko, Y. K., et al. (2010). Long-term exposure of CdTe quantum dots on PC12 cellular activity and the determination of optimum non-toxic concentrations for biological use. Journal of nanobiotechnology, 8, 7. doi:10.1186/1477-3155-8-7

Pérez-Nievas, B. G., Madrigal, J. L. M., GarcÃ-a-Bueno, B., Zoppi, S., & Leza, J. C. (2010). Corticosterone basal levels and vulnerability to LPS-induced neuroinflammation in the rat brain. Brain research, 1315, 159-68.

Pérez-Nievas, B. G., Madrigal, J. L. M., GarcÃ-a-Bueno, B., Zoppi, S., & Leza, J. C. (2010). Corticosterone basal levels and vulnerability to LPS-induced neuroinflammation in the rat brain. Brain research, 1315, 159-68.

Qiu, Y., Liu, Y., Wang, L., Xu, L., Bai, R., Ji, Y., Wu, X., et al. (2010). Surface chemistry and aspect ratio mediated cellular uptake of Au nanorods. Biomaterials, 31(30), 7606-19. doi:10.1016/j.biomaterials.2010.06.051

Rai, A., Maurya, S. K., Khare, P., Srivastava, A., & Bandyopadhyay, S. (2010). Characterization of developmental neurotoxicity of As, Cd, and Pb mixture: synergistic action of metal mixture in glial and neuronal functions. Toxicological sciences : an official journal of the Society of Toxicology, 118(2), 586-601. doi:10.1093/toxsci/kfq266

Ramot, Y., Steiner, M., Morad, V., Leibovitch, S., Amouyal, N., Cesta, M. F., & Nyska, A. (2010). Pulmonary thrombosis in the mouse following intravenous administration of quantum dot-labeled mesenchymal cells. Informa UK LtdLondon, UK.

Rampazzo, E., Boschi, F., Bonacchi, S., Juris, R., Montalti, M., Zaccheroni, N., Prodi, L., et al. (2011). Multicolor core/shell silica nanoparticles for in vivo and ex vivo imaging. Nanoscale, 4(3), 824-830. The Royal Society of Chemistry. doi:10.1039/c1nr11401h

Ray, S., Chandra, H., & Srivastava, S. (2010). Nanotechniques in proteomics: current status, promises and challenges. Biosensors & bioelectronics, 25(11), 2389-401. doi:10.1016/j.bios.2010.04.010

Reiter, L. (2007). Use of Activity Measures in Behavioral Toxicology. National Institute of Environmental Health Sciences. National Institutes of Health. Department of Health, Education and Welfare.

Riehemann, K., Schneider, S. W., Luger, T. A., Godin, B., Ferrari, M., & Fuchs, H. (2009). Nanomedicine--challenge and perspectives. Angewandte Chemie (International ed. in English), 48(5), 872-97. doi:10.1002/anie.200802585

Robe, A., Pic, E., Lassalle, H.-P., Bezdetnaya, L., Guillemin, F., & Marchal, F. (2008). Quantum dots in axillary lymph node mapping: biodistribution study in healthy mice. BMC cancer, 8, 111. doi:10.1186/1471-2407-8-111

Rodgers, P. (2006). Nanoelectronics: Single file. Nature Nanotechnology. Nature Publishing Group. doi:10.1038/nnano.2006.5

Rogach, A. L. (2000). Optical Properties of Colloidal Synthesized II-VI Semiconductor Nanocrystals In: Optical Properties of Semiconductor Nanostructures. (M. L. Sadowski, M. Potemski, & M. Grynberg, Eds.) (Kluwer Aca., pp. 379-393). Dordrecht.

Rosi, N. L., Giljohann, D. A., Thaxton, C. S., Lytton-Jean, A. K. R., Han, M. S., & Mirkin, C. A. (2006). Oligonucleotide-modified gold nanoparticles for intracellular gene regulation. Science (New York, N.Y.), 312(5776), 1027-30. doi:10.1126/science.1125559

Rossetti R, Nakahara S and Brus, L. (1983). Quantum size effects in the redox potentials, resonance Raman spectra, and electron spectra of CdS crystallites in aqueous solution. Journal of chemical physics, 79, 1086.

Rostène, W., Kitabgi, P., & Parsadaniantz, S. M. (2007). Chemokines: a new class of neuromodulator? Nature reviews. Neuroscience, 8(11), 895-903. doi:10.1038/nrn2255

Rozenzhak, S. M., Kadakia, M. P., Caserta, T. M., Westbrook, T. R., Stone, M. O., & Naik, R. R. (2005). Cellular internalization and targeting of semiconductor quantum dots. Chemical communications (Cambridge, England), (17), 2217-9. The Royal Society of Chemistry. doi:10.1039/b418454h

Ryman-Rasmussen, J. P., Riviere, J. E., & Monteiro-Riviere, N. A. (2006). Penetration of intact skin by quantum dots with diverse physicochemical properties. Toxicological sciences : an official journal of the Society of Toxicology, 91(1), 159-65. doi:10.1093/toxsci/kfj122

Ryman-Rasmussen, J. P., Riviere, J. E., & Monteiro-Riviere, N. A. (2007). Surface coatings determine cytotoxicity and irritation potential of quantum dot nanoparticles in epidermal keratinocytes. The Journal of investigative dermatology, 127(1), 143-53. doi:10.1038/sj.jid.5700508

Ryman-Rasmussen, J. P., Riviere, J. E., & Monteiro-Riviere, N. A. (2007). Variables influencing interactions of untargeted quantum dot nanoparticles with skin cells and identification of biochemical modulators. Nano letters, 7(5), 1344-8. doi:10.1021/nl070375j

Rzigalinski, B. A., & Strobl, J. S. (2009). Cadmium-containing nanoparticles: perspectives on pharmacology and toxicology of quantum dots. Toxicology and applied pharmacology, 238(3), 280-8. doi:10.1016/j.taap.2009.04.010

Sahagun, G., Moore, S. A., & Hart, M. N. (1990). Permeability of neutral vs. anionic dextrans in cultured brain microvascular endothelium. The American journal of physiology, 259(1 Pt 2), H162-6.

Salminen, A., Kauppinen, A., Suuronen, T., Kaarniranta, K., & Ojala, J. (2009). ER stress in Alzheimerâ™s disease: a novel neuronal trigger for inflammation and Alzheimer's pathology. Journal of neuroinflammation, 6(1), 41. doi:10.1186/1742-2094-6-41

Samia, A. C. S., Dayal, S., & Burda, C. (n.d.). Quantum dot-based energy transfer: perspectives and potential for applications in photodynamic therapy. Photochemistry and photobiology, 82(3), 617-25. doi:10.1562/2005-05-11-IR-525

Santra, S., Yang, H., Holloway, P. H., Stanley, J. T., and, Mericle, R. A. (2005). Synthesis of Water-Dispersible Fluorescent, Radio-Opaque, and Paramagnetic CdS:Mn/ZnS Quantum Dots: A Multifunctional Probe for Bioimaging. American Chemical Society.

Shatz, C. J. (2009). MHC class I: an unexpected role in neuronal plasticity. Neuron, 64(1), 40-5. doi:10.1016/j.neuron.2009.09.044

Sheldon, M. H. (1968). The effect of electric shock on rat’s choice between familiar and unfamiliar maze arms: a replication. The Quarterly journal of experimental psychology, 20(4), 400-4. doi:10.1080/14640746808400182

Shin, J. A., Lee, E. J., Seo, S. M., Kim, H. S., Kang, J. L., & Park, E. M. (2010). Nanosized titanium dioxide enhanced inflammatory responses in the septic brain of mouse. Neuroscience, 165(2), 445-54. doi:10.1016/j.neuroscience.2009.10.057

Shiu, C., Barbier, E., Di Cello, F., Choi, H. J., & Stins, M. (2007). HIV-1 gp120 as well as alcohol affect blood-brain barrier permeability and stress fiber formation: involvement of reactive oxygen species. Alcoholism, clinical and experimental research, 31(1), 130-7. doi:10.1111/j.1530-0277.2006.00271.x

Simkó, M., & Mattsson, M.-O. (2010). Risks from accidental exposures to engineered nanoparticles and neurological health effects: a critical review. Particle and fibre toxicology, 7, 42. doi:10.1186/1743-8977-7-42

Singh, S., & Nalwa, H. S. (2007). Nanotechnology and health safety--toxicity and risk assessments of nanostructured materials on human health. Journal of nanoscience and nanotechnology, 7(9), 3048-70.

Sioutas, C., Delfino, R. J., & Singh, M. (2005). Exposure assessment for atmospheric ultrafine particles (UFPs) and implications in epidemiologic research. Environmental health perspectives, 113(8), 947-55.

Smith, A. M., & Nie, S. (2004). Chemical analysis and cellular imaging with quantum dots. The Analyst, 129(8), 672-7.

Smith, A. M., & Nie, S. (2004). Chemical analysis and cellular imaging with quantum dots. The Analyst, 129(8), 672. The Royal Society of Chemistry. doi:10.1039/b404498n

Smith, A. M., Dave, S., Nie, S., True, L., & Gao, X. (2006). Multicolor quantum dots for molecular diagnostics of cancer. Expert review of molecular diagnostics, 6(2), 231-44. doi:10.1586/14737159.6.2.231

Smith, A. M., Duan, H., Mohs, A. M., & Nie, S. (2008). Bioconjugated quantum dots for in vivo molecular and cellular imaging. Advanced drug delivery reviews, 60(11), 1226-40. doi:10.1016/j.addr.2008.03.015

Smith, A. M., Mancini, M. C., & Nie, S. (2009). Bioimaging: second window for in vivo imaging. Nature nanotechnology, 4(11), 710-1. Nature Publishing Group. doi:10.1038/nnano.2009.326

Smith, J. W., Al-Khamees, O., Costall, B., Naylor, R. J., & Smythe, J. W. (n.d.). Chronic aspirin ingestion improves spatial learning in adult and aged rats. Pharmacology, biochemistry, and behavior, 71(1-2), 233-8.

So, M.K., Xu, C., Loening, A. M., Gambhir, S. S., & Rao, J. (2006). Self-illuminating quantum dot conjugates for in vivo imaging. Nature biotechnology, 24(3), 339-43. Nature Publishing Group. doi:10.1038/nbt1188

Soenen, S. J. H., & De Cuyper, M. (2010). Assessing iron oxide nanoparticle toxicity in vitro: current status and future prospects. Nanomedicine (London, England), 5(8), 1261-75. doi:10.2217/nnm.10.106

Soltesz, E. G., Kim, S., Laurence, R. G., DeGrand, A. M., Parungo, C. P., Dor, D. M., Cohn, L. H., et al. (2005). Intraoperative Sentinel Lymph Node Mapping of the Lung Using Near-Infrared Fluorescent Quantum Dots. Ann. Thorac. Surg., 79(1), 269-277.

Spruijt, B. M., & DeVisser, L. (2006). Advanced behavioural screening: automated home cage ethology. Drug Discovery Today: Technologies, 3(2), 231-237. doi:10.1016/j.ddtec.2006.06.010

Stern, S. T., Zolnik, B. S., McLeland, C. B., Clogston, J., Zheng, J., & McNeil, S. E. (2008). Induction of autophagy in porcine kidney cells by quantum dots: a common cellular response to nanomaterials? Toxicological sciences : an official journal of the Society of Toxicology, 106(1), 140-52. doi:10.1093/toxsci/kfn137

Streit, W. J, Walter, S. A., & Pennell, N. A. (1999). Reactive microgliosis. Progress in neurobiology, 57(6), 563-81.

Streit, W. J. (2002). Microglia as neuroprotective, immunocompetent cells of the CNS. Glia, 40(2), 133-9. doi:10.1002/glia.10154

Stroh, M., Zimmer, J. P., Duda, D. G., Levchenko, T. S., Cohen, K. S., Brown, E. B., Scadden, D. T., et al. (2005). Quantum dots spectrally distinguish multiple species within the tumor milieu in vivo. Nature medicine, 11(6), 678-82. doi:10.1038/nm1247

Su, Y., Peng, F., Jiang, Z., Zhong, Y., Lu, Y., Jiang, X., Huang, Q., et al. (2011). In vivo distribution, pharmacokinetics, and toxicity of aqueous synthesized cadmium-containing quantum dots. Biomaterials, 32(25), 5855-62. doi:10.1016/j.biomaterials.2011.04.063

Sugama, S., Takenouchi, T., Cho, B. P., Joh, T. H., Hashimoto, M., & Kitani, H. (2009). Possible roles of microglial cells for neurotoxicity in clinical neurodegenerative diseases and experimental animal models. Inflammation & allergy drug targets, 8(4), 277-84.

Sundara Rajan, S., & Vu, T. Q. (2006). Quantum dots monitor TrkA receptor dynamics in the interior of neural PC12 cells. Nano letters, 6(9), 2049-59. American Chemical Society. doi:10.1021/nl0612650

Swerdlow, R. H. (2007). Treating neurodegeneration by modifying mitochondria: potential solutions to a â€œcomplexâ problem. Antioxidants & redox signaling, 9(10), 1591-603. doi:10.1089/ars.2007.1676

Tada, H., Higuchi, H., Wanatabe, T. M., & Ohuchi, N. (2007). In vivo real-time tracking of single quantum dots conjugated with monoclonal anti-HER2 antibody in tumors of mice. Cancer research, 67(3), 1138-44. American Association for Cancer Research. doi:10.1158/0008-5472.CAN-06-1185

Takenaka, S., Karg, E., Roth, C., Schulz, H., Ziesenis, A., Heinzmann, U., Schramel, P., et al. (2001). Pulmonary and systemic distribution of inhaled ultrafine silver particles in rats. Environmental health perspectives, 109 Suppl , 547-51.

Tamaru, M., Yoneda, Y., Ogita, K., Shimizu, J., & Nagata, Y. (1991). Age-related decreases of the N-methyl-D-aspartate receptor complex in the rat cerebral cortex and hippocampus. Brain research, 542(1), 83-90.

Tanaka, T., Mangala, L. S., Vivas-Mejia, P. E., Nieves-Alicea, R., Mann, A. P., Mora, E., Han, H.-D., et al. (2010). Sustained small interfering RNA delivery by mesoporous silicon particles. Cancer research, 70(9), 3687-96. doi:10.1158/0008-5472.CAN-09-3931

Tang, M., Li, Z., Chen, L., Xing, T., Hu, Y., Yang, B., Ruan, D.-Y., et al. (2009). The effect of quantum dots on synaptic transmission and plasticity in the hippocampal dentate gyrus area of anesthetized rats. Biomaterials, 30(28), 4948-55. doi:10.1016/j.biomaterials.2009.06.012

Tang, M., Wang, M., Xing, T., Zeng, J., Wang, H., & Ruan, D.-Y. (2008). Mechanisms of unmodified CdSe quantum dot-induced elevation of cytoplasmic calcium levels in primary cultures of rat hippocampal neurons. Biomaterials, 29(33), 4383-91. doi:10.1016/j.biomaterials.2008.08.001

Tang, M., Xing, T., Zeng, J., Wang, H., Li, C., Yin, S., Yan, D., et al. (2008). Unmodified CdSe quantum dots induce elevation of cytoplasmic calcium levels and impairment of functional properties of sodium channels in rat primary cultured hippocampal neurons. Environmental health perspectives, 116(7), 915-22. doi:10.1289/ehp.11225

Tang, Xiangdong, & Sanford, L. D. (2005). Home cage activity and activity-based measures of anxiety in 129P3/J, 129X1/SvJ and C57BL/6J mice. Physiology & behavior, 84(1), 105-15. doi:10.1016/j.physbeh.2004.10.017

Tang, Xiangdong, & Sanford, L. D. (2005). Home cage activity and activity-based measures of anxiety in 129P3/J, 129X1/SvJ and C57BL/6J mice. Physiology & behavior, 84(1), 105-15. doi:10.1016/j.physbeh.2004.10.017

Tavares, A. J., Chong, L., Petryayeva, E., Algar, W. R., & Krull, U. J. (2011). Quantum dots as contrast agents for in vivo tumor imaging: progress and issues. Analytical and bioanalytical chemistry, 399(7), 2331-42. doi:10.1007/s00216-010-4010-3

Tecott, L. H., & Nestler, E. J. (2004). Neurobehavioral assessment in the information age. Nature neuroscience, 7(5), 462-6. Nature Publishing Group. doi:10.1038/nn1225

Tekle, C., Deurs, B. van, Sandvig, K., & Iversen, T.-G. (2008). Cellular trafficking of quantum dot-ligand bioconjugates and their induction of changes in normal routing of unconjugated ligands. Nano letters, 8(7), 1858-65. American Chemical Society. doi:10.1021/nl0803848

Terminology for nanomaterials. (2007). Publicly available specification 136. London: British Standards Institute. Retrieved from http://www.nanointeract.net/x/file/PAS%20136 .pdf.)

The Project on Emerging Nanotechnologies. (n.d.). Retrieved January 23, 2012, from http://www.nanotechproject.org/inventories/consumer/analysis_draft/

Theis, T., Parr, D., Binks, P., Ying, J., Drexler, K. E., Schepers, E., Mullis, K., et al. (2006). nanâ™o.tech.nol'o.gy n. Nature nanotechnology, 1(1), 8-10. Nature Publishing Group. doi:10.1038/nnano.2006.77

Theis, T., Parr, D., Binks, P., Ying, J., Drexler, K. E., Schepers, E., Mullis, K., et al. (2006). nanâ™o.tech.nol'o.gy n. Nature nanotechnology, 1(1), 8-10. Nature Publishing Group. doi:10.1038/nnano.2006.77

Thompson, W. L., Karpus, W. J., & Van Eldik, L. J. (2008). MCP-1-deficient mice show reduced neuroinflammatory responses and increased peripheral inflammatory responses to peripheral endotoxin insult. Journal of neuroinflammation, 5, 35. doi:10.1186/1742-2094-5-35

Thorne, R. G., & Nicholson, C. (2006). In vivo diffusion analysis with quantum dots and dextrans predicts the width of brain extracellular space. Proceedings of the National Academy of Sciences of the United States of America, 103(14), 5567-72. doi:10.1073/pnas.0509425103

Tino, A., Ambrosone, A., Mattera, L., Marchesano, V., Susha, A., Rogach, A., & Tortiglione, C. (2011). A new in vivo model system to assess the toxicity of semiconductor nanocrystals. International journal of biomaterials, 2011, 792854. doi:10.1155/2011/792854

Tiwari, D. K., Jin, T., & Behari, J. (2011). Bio-distribution and toxicity assessment of intravenously injected anti-HER2 antibody conjugated CdSe/ZnS quantum dots in Wistar rats. International journal of nanomedicine, 6, 463-75. doi:10.2147/IJN.S15124

Tiwari, S. B., & Amiji, M. M. (2006). A review of nanocarrier-based CNS delivery systems. Current drug delivery, 3(2), 219-32.

Tremblay, M.-Ã., & Majewska, A. K. (2011). A role for microglia in synaptic plasticity? Communicative & integrative biology, 4(2), 220-2. doi:10.4161/cib.4.2.14506

Trickler, W. J., Lantz, S. M., Murdock, R. C., Schrand, A. M., Robinson, B. L., Newport, G. D., Schlager, J. J., et al. (2010). Silver nanoparticle induced blood-brain barrier inflammation and increased permeability in primary rat brain microvessel endothelial cells. Toxicological sciences : an official journal of the Society of Toxicology, 118(1), 160-70. doi:10.1093/toxsci/kfq244

Trump, B. F., & Berezesky, I. K. (1995). Calcium-mediated cell injury and cell death. The FASEB journal : official publication of the Federation of American Societies for Experimental Biology, 9(2), 219-28.

Turrens, J. F. (2003). Mitochondrial formation of reactive oxygen species. The Journal of physiology, 552(Pt 2), 335-44. doi:10.1113/jphysiol.2003.049478

Ullian, E M, Sapperstein, S. K., Christopherson, K. S., & Barres, B. A. (2001). Control of synapse number by glia. Science (New York, N.Y.), 291(5504), 657-61. doi:10.1126/science.291.5504.657

Van Strien, N. M., Cappaert, N. L. M., & Witter, M. P. (2009). The anatomy of memory: an interactive overview of the parahippocampal-hippocampal network. Nature reviews. Neuroscience, 10(4), 272-82. Nature Publishing Group. doi:10.1038/nrn2614

Vereker, E, Oâ™Donnell, E., Lynch, A., Kelly, A., Nolan, Y., & Lynch, M. A. (2001). Evidence that interleukin-1beta and reactive oxygen species production play a pivotal role in stress-induced impairment of LTP in the rat dentate gyrus. The European journal of neuroscience, 14(11), 1809-19.

Vgontzas, A. N., Papanicolaou, D. A., Bixler, E. O., Kales, A., Tyson, K., & Chrousos, G. P. (1997). Elevation of plasma cytokines in disorders of excessive daytime sleepiness: role of sleep disturbance and obesity. The Journal of clinical endocrinology and metabolism, 82(5), 1313-6.

Vieira, C. S., Almeida, D. B., de Thomaz, A. A., Menna-Barreto, R. F. S., dos Santos-Mallet, J. R., Cesar, C. L., Gomes, S. A. O., et al. (2011). Studying nanotoxic effects of CdTe quantum dots in Trypanosoma cruzi. Memorias do Instituto Oswaldo Cruz, 106(2), 158-65.

Wade, J. M., Juneja, P., MacKay, A. W., Graham, J., Havel, P. J., Tecott, L. H., & Goulding, E. H. (2008). Synergistic impairment of glucose homeostasis in ob/ob mice lacking functional serotonin 2C receptors. Endocrinology, 149(3), 955-61. doi:10.1210/en.2007-0927

Wang, C., Gao, X., & Su, X. (2010). In vitro and in vivo imaging with quantum dots. Analytical and bioanalytical chemistry, 397(4), 1397-415. Springer Berlin / Heidelberg. doi:10.1007/s00216-010-3481-6

Wang, C., Gao, X., & Su, X. (2010). Study the damage of DNA molecules induced by three kinds of aqueous nanoparticles. Talanta, 80(3), 1228-33. doi:10.1016/j.talanta.2009.09.014

Wang, H.-Z., Wang, H.-Y., Liang, R.-Q., & Ruan, K.-C. (2004). Detection of Tumor Marker CA125 in Ovarian Carcinoma Using Quantum Dots. Acta Biochimica et Biophysica Sinica, 36(10), 681-686. doi:10.1093/abbs/36.10.681

Wang, J., Liu, Y., Jiao, F., Lao, F., Li, W., Gu, Y., Li, Y., et al. (2008). Time-dependent translocation and potential impairment on central nervous system by intranasally instilled TiO(2) nanoparticles. Toxicology, 254(1-2), 82-90. doi:10.1016/j.tox.2008.09.014

Wang, Lingling, Zheng, H., Long, Y., Gao, M., Hao, J., Du, J., Mao, X., et al. (2010). Rapid determination of the toxicity of quantum dots with luminous bacteria. Journal of hazardous materials, 177(1-3), 1134-7. doi:10.1016/j.jhazmat.2009.12.001

Wang, S., Jarrett, B. R., Kauzlarich, S. M., & Louie, A. Y. (2007). Core/shell quantum dots with high relaxivity and photoluminescence for multimodality imaging. Journal of the American Chemical Society, 129(13), 3848-56. American Chemical Society. doi:10.1021/ja065996d

Wang, Zhenjia, Tiruppathi, C., Minshall, R. D., & Malik, A. B. (2009). Size and dynamics of caveolae studied using nanoparticles in living endothelial cells. ACS nano, 3(12), 4110-6. doi:10.1021/nn9012274

Weissleder, R. (2001). A clearer vision for in vivo imaging. Nature biotechnology, 19(4), 316-7. Nature Publishing Group. doi:10.1038/86684

Wenzel, J., Lammert, G., Meyer, U., & Krug, M. (1991). The influence of long-term potentiation on the spatial relationship between astrocyte processes and potentiated synapses in the dentate gyrus neuropil of rat brain. Brain Research, 560(1-2), 122-131. doi:10.1016/0006-8993(91)91222-M

Willard, D. M., Carillo, L. L., Jung, J., & Van Orden, A. (2001). CdSeâ'ZnS Quantum Dots as Resonance Energy Transfer Donors in a Model Proteinâ'Protein Binding Assay. Nano Letters, 1(9), 469-474. American Chemical Society. doi:10.1021/nl015565n

Willard, D. M., Mutschler, T., Yu, M., Jung, J., & Van Orden, A. (2006). Directing energy flow through quantum dots: towards nanoscale sensing. Analytical and bioanalytical chemistry, 384(3), 564-71. Springer Berlin / Heidelberg. doi:10.1007/s00216-005-0250-z

Willis, C L, Brooks, T. A., & Davis, T. P. (2008). Chronic inflammatory pain and the neurovascular unit: a central role for glia in maintaining BBB integrity? Current pharmaceutical design, 14(16), 1625-43.

Win-Shwe, T.-T., Yamamoto, S., Fujitani, Y., Hirano, S., & Fujimaki, H. (2008). Spatial learning and memory function-related gene expression in the hippocampus of mouse exposed to nanoparticle-rich diesel exhaust. Neurotoxicology, 29(6), 940-7. doi:10.1016/j.neuro.2008.09.007

Winters, B. D., Saksida, L. M., & Bussey, T. J. (2008). Object recognition memory: neurobiological mechanisms of encoding, consolidation and retrieval. Neuroscience and biobehavioral reviews, 32(5), 1055-70. doi:10.1016/j.neubiorev.2008.04.004

Wu, Xingyong, Liu, H., Liu, J., Haley, K. N., Treadway, J. A., Larson, J. P., Ge, N., et al. (2003). Immunofluorescent labeling of cancer marker Her2 and other cellular targets with semiconductor quantum dots. Nature biotechnology, 21(1), 41-6. Nature Publishing Group. doi:10.1038/nbt764

Wu, Xingyong, Liu, H., Liu, J., Haley, K. N., Treadway, J. A., Larson, J. P., Ge, N., et al. (2003). Immunofluorescent labeling of cancer marker Her2 and other cellular targets with semiconductor quantum dots. Nature biotechnology, 21(1), 41-6. doi:10.1038/nbt764

Würbel, H. (2002). Behavioral phenotyping enhanced--beyond (environmental) standardization. Genes, brain, and behavior, 1(1), 3-8.

Xia, Z., Xing, Y., So, M.-K., Koh, A. L., Sinclair, R., & Rao, J. (2008). Multiplex detection of protease activity with quantum dot nanosensors prepared by intein-mediated speci-

fic bioconjugation. Analytical chemistry, 80(22), 8649-55. American Chemical Society. doi:10.1021/ac801562f

Xiao, J., Bai, Y., Wang, Y., Chen, J., & Wei, X. (2010). Systematic investigation of the influence of CdTe QDs size on the toxic interaction with human serum albumin by fluorescence quenching method. Spectrochimica acta. Part A, Molecular and biomolecular spectroscopy, 76(1), 93-7. doi:10.1016/j.saa.2010.02.028

Yan, L., Zheng, Y. B., Zhao, F., Li, S., Gao, X., Xu, B., Weiss, P. S., et al. (2012). Chemistry and physics of a single atomic layer: strategies and challenges for functionalization of graphene and graphene-based materials. Chemical Society reviews, 41(1), 97-114. The Royal Society of Chemistry. doi:10.1039/c1cs15193b

Yan, M., Zhang, Y., Xu, K., Fu, T., Qin, H., & Zheng, X. (2011). An in vitro study of vascular endothelial toxicity of CdTe quantum dots. Toxicology, 282(3), 94-103. doi:10.1016/j.tox.2011.01.015

Yang, C.-S., Tzou, B.-C., Liu, Y.-P., Tsai, M.-J., Shyue, S.-K., & Tzeng, S.-F. (2008). Inhibition of cadmium-induced oxidative injury in rat primary astrocytes by the addition of antioxidants and the reduction of intracellular calcium. Journal of cellular biochemistry, 103(3), 825-34. doi:10.1002/jcb.21452

Yang, Hu. (2010). Nanoparticle-mediated brain-specific drug delivery, imaging, and diagnosis. Pharmaceutical research, 27(9), 1759-71. doi:10.1007/s11095-010-0141-7

Yang, R. S. H., Chang, L. W., Wu, J.-P., Tsai, M.-H., Wang, H.-J., Kuo, Y.-C., Yeh, T.-K., et al. (2007). Persistent tissue kinetics and redistribution of nanoparticles, quantum dot 705, in mice: ICP-MS quantitative assessment. Environmental health perspectives, 115(9), 1339-43. doi:10.1289/ehp.10290

Yang, S. T., Wang, X., Wang, H., Lu, F., Luo, P. G., Cao, L., Meziani, M. J., et al. (2009). Carbon Dots as Nontoxic and High-Performance Fluorescence Imaging Agents. The journal of physical chemistry. C, Nanomaterials and interfaces, 113(42), 18110-18114. doi:10.1021/jp9085969

Yasunaga, I., Tanizawa, H., & Takino, Y. (1988). [Spontaneous heart failure in BALB/c mice]. Jikken dobutsu. Experimental animals, 37(2), 121-6.

Yeh, T. K., Wu, J.-P., Chang, L. W., Tsai, M.-H., Chang, W.-H., Tsai, H.-T., Yang, C. S., et al. (2011). Comparative tissue distributions of cadmium chloride and cadmium-based quantum dot 705 in mice: Safety implications and applications. Nanotoxicology, 5(1), 91-7. doi:10.3109/17435390.2010.502260

Yong, K. T., Roy, I., Ding, H., Bergey, E. J., & Prasad, P. N. (2009). Biocompatible near-infrared quantum dots as ultrasensitive probes for long-term in vivo imaging applications. Small (Weinheim an der Bergstrasse, Germany), 5(17), 1997-2004. doi:10.1002/smll.200900547

Yu, X., Chen, L., Li, K., Li, Y., Xiao, S., Luo, X., Liu, J., et al. (2007). Immunofluorescence detection with quantum dot bioconjugates for hepatoma in vivo. Journal of biomedical optics, 12(1), 014008. doi:10.1117/1.2437744

Zhang, L. W., & Monteiro-Riviere, N. A. (2009). Mechanisms of quantum dot nanoparticle cellular uptake. Toxicological sciences : an official journal of the Society of Toxicology, 110(1), 138-55. doi:10.1093/toxsci/kfp087

Zhang, L. W., BÃ¤umer, W., & Monteiro-Riviere, N. A. (2011). Cellular uptake mechanisms and toxicity of quantum dots in dendritic cells. Nanomedicine (London, England), 6(5), 777-91. doi:10.2217/nnm.11.73

Zhao, L., Liu, R., Zhao, X., Yang, B., Gao, C., Hao, X., & Wu, Y. (2009). New strategy for the evaluation of CdTe quantum dot toxicity targeted to bovine serum albumin. The Science of the total environment, 407(18), 5019-23. doi:10.1016/j.scitotenv.2009.05.052

Zhao, Y., Lin, K., Zhang, W., & Liu, L. (2010). Quantum dots enhance Cu2+ -induced hepatic L02 cells toxicity. Journal of environmental sciences (China), 22(12), 1987-92.

Zheng, D., Seferos, D. S., Giljohann, D. A., Patel, P. C., & Mirkin, C. A. (2009). Aptamer nano-flares for molecular detection in living cells. Nano letters, 9(9), 3258-61. American Chemical Society. doi:10.1021/nl901517b

Zheng, Hong, Chen, G., Song, F., DeLouise, L. A., & Lou, Z. (2011). The cytotoxicity of OPA-modified CdSe/ZnS core/shell quantum dots and its modulation by silibinin in human skin cells. Journal of biomedical nanotechnology, 7(5), 648-58.

Zhu, X.-X., Cao, Y.-C., Jin, X., Yang, J., Hua, X.-F., Wang, H.-Q., Liu, B., et al. (2008). Optical encoding of microbeads based on silica particle encapsulated quantum dots and its applications. Nanotechnology, 19(2), 025708. doi:10.1088/0957-4484/19/02/025708

Zimmer, J. P., Kim, S.-W., Ohnishi, S., Tanaka, E., Frangioni, J. V., & Bawendi, M. G. (2006). Size series of small indium arsenide-zinc selenide core-shell nanocrystals and their application to in vivo imaging. Journal of the American Chemical Society, 128(8), 2526-7. doi:10.1021/ja0579816

Ziv, Y., Ron, N., Butovsky, O., Landa, G., Sudai, E., Greenberg, N., Cohen, H., et al. (2006). Immune cells contribute to the maintenance of neurogenesis and spatial learning abilities in adulthood. Nature neuroscience, 9(2), 268-75. doi:10.1038/nn1629

Zotova, E., Holmes, C., Johnston, D., Neal, J. W., Nicoll, J. A. R., & Boche, D. (2011). Microglial alterations in human Alzheimer's disease following AÎ²42 immunization. Neuropathology and applied neurobiology, 37(5), 513-24. doi:10.1111/j.1365-2990.2010.01156.x